IWMI International Water Management Institute

igrac International Groundwater Resources Assessment Centre

USAID FROM THE AMERICAN PEOPLE

Hydrogeological Modelling for Ramotswa Transboundary Aquifer Area

December 2018

Submitted by:

Implemented by:

In partnership with:

This report was made possible by the support of the American people through the United States Agency for International Development (USAID). Its contents are the sole responsibility of IWMI, and do not necessarily reflect the views of USAID or the United States Government.

Contributors
Girma Y. Ebrahim (IWMI)
Manuel Magombeyi (IWMI)
Karen G. Villholth (IWMI)
Jonathan Lautze (IWMI)
Geert-Jan Nijsten (IGRAC)
Keetile Keodumetse (DWA, Botswana)
Piet Kenabatho (University of Botswana)
Naicker Sivashni (DWS, South Africa)
Phemelo Makoba (DWA, Botswana)
Sakhile Mndaweni (DWS, South Africa)
Moses Moehadu (WUC, Botswana)
Modreck Gomo (University of Free State, South Africa)
Bochengedu Somolekae (DWA-Botswana)
Charles Nkile (DWA-Botswana)

Acknowledgments
The contribution and support from the Department of Water and Sanitation (DWS) – South Africa, The Department of Water Affairs (DWA) - Botswana, Botswana Geoscience Institute (BGI) – Botswana, and the Water Utilities Corporation (WUC) – Botswana is acknowledge.

Executive Summary

Increasing demand to harness groundwater resource potential. In the face of increasing population, urbanization, climate change and unreliability of surface water supplies in arid and semi-arid regions, groundwater resources are being increasingly used. The relative reliability of groundwater for long-term supply and its potential to serve as a buffer against drought make groundwater a critical water source. Managed Aquifer Recharge (MAR) is an alternative water resource management option that is gaining attention as a way to increase the quantity of water that is stored underground when there is excess during wet periods for use during dry period. Strategic implementation of MAR can enhance the benefits derived from groundwater use. However, determining the feasibility of MAR involves careful assessment of: i) aquifer response to additional recharge, ii) capacity of the aquifer to store water, iii) optimally locating MAR infiltration/ injection and recovery systems.

Hydrogeological models can be used to contextualize the role and feasibility of MAR. Hydrogeological models can be used to gain a better understanding of the aquifer system such as recharge dynamics, groundwater-surface water interaction, the effect of groundwater pumping, and storage processes and overall water budget of the aquifer system. With respect to MAR, hydrogeological models enable us to determine the storage capacity of the aquifer, aquifer response to additional recharge, the best location of recharge and recovery systems, and recovery efficiency. More broadly, hydrogeological modelling can provide a practical indication of the contribution and impact of MAR in an aquifer system.

Report Objective. The objective of the present study is to develop a three-dimensional (3D) transient hydrogeological model for the Ramotswa Transboundary Aquifer. The model can be used to understand recharge, storage, flow processes, water use and its dynamics in in the area, as well as to develop a water budget that can help to understand water balance change over time. The developed transient model is then used to evaluate MAR potential in the study area.

Context. The Ramotswa Transboundary Aquifer area (TBAA) is located in a border region between Botswana and South Africa. It is densely populated on the Botswana side as it is close to the Capital Gaborone. It consists of peri-urban settlements relying on the aquifer for reticulated domestic supply. Due to recent floods and droughts and the increased stress on existing water resources, there is an expressed need from the two governments to evaluate the opportunities to boost the water security in the area by implementing MAR.

Approach. A transient 3D hydrogeological model was developed using MODFLOW 2005 in MODELMUSE modelling environment. The modelled area covers an area of 80 km^2 and encompasses Ramotswa town and wellfield area. The Equivalent Porous Media (EPM) approach was used for the modelling. The model is designed to operate on a monthly time scale. Eight year simulation, from 2008 to 2015, is presented. First, a steady state model was calibrated against average water level data observed in 17 observation wells during the period of 2000-2012. This period was selected for steady state calibration because there was no pumping in the aquifer in this period. Hence, this period was assumed to represent the steady state condition. The output from the calibrated steady state model was then used as initial condition for the transient model. Water level data only available for the period 2000-2012 and 2015-2017. Therefore, the transient model was calibrated using observed water level data from 17 observation wells measured from 2000-2008 and validated for the period 2009-2012. Water level data monitored in 11 observation wells in 2017 was used to assess model

performance. Water level data for the period of 2015-2016 were not used as they were not reliable. In order to understand recharge dynamics, independent recharge estimation was accomplished using the Water Table Fluctuation (WTF) method.

Results. In general, good agreement between observed and simulated water levels were obtained. The transient 3D hydrological model reproduced the observed water level dynamics. The residuals are randomly distributed across the study area. Results of the water budget analysis show that water budget in the study area is highly variable. Recharge rate (total recharge, diffuse from rainfall and focused from the river) during the simulation period ranges from 0.43 – 53.2 mm/a (a mean of 24.5 ± 14.4 mm/a, or, of 5.6 ± 1.3 % mean annual rainfall). Groundwater replenishment from focused recharge is associated with large uncertainty as a result of its dependence on the magnitude and frequency of river runoff and flooding. Evapotranspiration directly from the groundwater (GWET) is a significant component of the groundwater budget in the study area. GWET occurs along the river channel where depth to groundwater are shallow. The minimum depth in observation wells within 200 m of the river ranges from 0.88-2.61 m. The simulated GWET ranges from 14.7 – 40.0 mm/a (with a mean of 27.0 ± 6.8 mm/a), which is exceeding the recharge rate. Evapotranspiration from the groundwater mainly occurs along the river where the depth to groundwater is relatively shallow. Groundwater discharge to the river is the smallest component of the water budget with a mean of 2.4 ± 1.64 mm/a. Groundwater outflow from the model domain through the specified GHB is 1.9 ± 1.41 mm/a. Groundwater abstraction only occurs during the recent period [2015-2017], and it ranges from 0-25.37 mm/a (with a mean of 2.76 ± 6.80 mm/a). Change in groundwater storage is highly variable ranging from -31.4 – 15.7 mm/a (with a mean of -11.4 ± 11.3 mm/a). Negative mean storage change means groundwater depletion over time. Annual groundwater storage change are strongly correlated with annual rainfall (R^2=0.88). The annual storage change is a measure of the volume of water lost or gained in the basin during the year.

Summing Up. The transient 3D hydrogeological model is reasonably calibrated. The model can be used for feasibility assessment of MAR or to evaluate other groundwater management alternatives.

Table of Contents

List of Figures

List of Tables

Acronyms/Abbreviations

Amsl	Above Mean Sea Level
AET	actual evapotranspiration
BGI	Botswana Geoscience Institute
DEM	Digital Elevation Model.
DGPS	Differential Global Positioning System
DSM	Department of Survey and Mapping, Botswana
DWA	Department of Water Affairs (Botswana)
DWS	Department of Water and Sanitation (South Africa)
ET	Evapotranspiration
EPM	Equivalent Porous Medium
GCS	Geotechnical Consulting Services, Botswana
GIS	Geographic Information System
GNSS	Global Navigation Satellite Systems
GPS	Global Positioning System
GWET	Groundwater Evapotranspiration
IGRAC	International Groundwater Resources Assessment Centre
IWMI	International Water Management Institute
LULC	Land Use Land Cover
MAR	Managed Aquifer Recharge
Mbgl	metres below ground level
ModelMuse	Graphic user interface for MODFLOW-2005, MODFLOW-OWHM, and others
MODFLOW	Modular Three-Dimensional Finite-Difference Groundwater Flow Model
RTK	Real-Time Kinematic Surveying system using GNSS
RTN	Real-Time Network Surveying system using GNSS
RTBAA	Ramotswa Transboundary Aquifer Area (RTBAA).
SRTM	Shuttle Radar Topography Mission
SWL	Static Water Level
USDA	United States Department of Agriculture
USAID	United States Agency for International Development
USGS	U.S. Geological survey
WLE	Water, Land and Ecosystems
WUC	Water Utilities Corporation (Botswana)

1. Introduction

1.1 Background

In arid/semi-arid regions, surface water resources are generally scarce and unreliable, resulting in groundwater is being increasingly used as a critical source of water. The reliability of groundwater for long-term supply and its buffering capacity during drought periods make groundwater a critical water resource. However, in order to retain the buffer capacity of groundwater under increasing pressure and use, it is important to look at protecting and supporting its replenishment. Managed Aquifer Recharge (MAR) practices are increasingly being used as a means of increasing groundwater availability and improving the overall reliability of water supplies. Storing water in an aquifer during times of excess supply and recovering the same water for use when the demand is high is becoming an attractive water management option. Hydrogeological models can be used to assess the feasibility of MAR prior to conducting expensive field test. They provide a quantitative technique for analysing the effect of groundwater pumping, recharge dynamics, groundwater-surface water interaction, and can be used to develop a more reliable estimate of aquifer water budget with and without MAR. In particular with respect to MAR assessment, they provide important information such as storage capacity of the aquifer, the response of the aquifer to induced recharge, best location of recharge and recovery sites, and assessing the recovery efficiency (Mansouri and Mezouary, 2015; Woolfenden and Koczot, 2001). Hydrogeological models serves as essential tools: to develop a better understanding of the groundwater system through more reliable estimates of the water budgets, and variability in same, to explore different management options. Integrated modelling brings data together into a logical holistic picture on a quantitative basis, also supporting future data collection needs (Kinzelbach et al., 2003; Zhou and Li, 2011).

1.2 Objectives

The main goal of this report is to develop a hydrogeological mode for the Ramotswa Aquifer Transboundary aquifer to investigate the use and movement of groundwater, recharge, discharge and storage processes. The model can be used to assess the feasibility of MAR in the area.

The specific modeling objectives are:

- to develop a three-dimensional (3D) hydrogeological model that describes the movement of groundwater and current water budget, recharge, discharge and storage process,
- to obtain a better understanding of the interrelationship of the different hydrological process
- to describe the recharge and discharge process and their dynamics and variability in space and time
- to gain a better understanding how human activities (irrigation pumping) affect the hydrological response

In the long term, the model can also be used to assess groundwater management alternative and impact assessment modelling. These includes:

- As operational tool for wellfields. The model can be used as a management tool for wellfield operation to assess the implementation of any management alternatives
- To assess the impact of climate change and land use/land cover changes
- Contaminant transport and remediation (e.g. nitrate in the aquifer). Hydrogeological model development is the first step for contaminant transport modelling. The hydrogeological model calculates the velocity field required by contaminant transport modelling. The hydrogeological model can be easily linked with 3D contaminant transport model, e.g. MT3D or others

1.3 Scope of Work

In order to achieve the above objectives the overall scope of the hydrogeological modelling is divided into four activities:

1) Development of a conceptual model
2) Data collection, borehole elevation survey, groundwater level , soil infiltration test
3) Development and calibration on a steady state 3D hydrogeological model,
4) Development and calibration of a transient 3D hydrogeological model, this includes updating the steady state model calibration based on additional data and borehole elevation survey.

The first activity was contained in the previous hydrogeological modeling deliverable (March 2018). This report builds on that work to develop a transient 3D hydrogeological model. Description of activities 2 and 4, such as using the transient 3D hydrogeological model for MAR scenario assessment, soil infiltration test, water source availability, water quality issues, and evaluation of the geochemical implication of mixing of recharge water with native groundwater using Geochemical model are covered in the deliverable on Managed Aquifer Recharge (December 2018).

2. Study Area

2.1 The Ramotswa Transboundary Aquifer Area

Ramotswa Transboundary Aquifer Area (RTBAA). The Ramotswa Aquifer is located in the Upper Limpopo River Basin and is shared between South Africa and Botswana. The Ramotswa Aquifer corresponds to the Ramotswa dolomitic aquifer, whose surficial extent is mapped based on surface geology, but extends beyond this in the subsurface. The RTBAA is a slightly larger area than delineated by the surface geology, in order to partially account for the broader extent of the aquifer in the subsurface (Figure 1).

Ramotswa Aquifer Flight Area The flight area (area about 1,500 km^2) was commonly used as an encompassing boundary within which the aquifer was found. It was used to overcome ambiguities of a precise boundary for the aquifer in phase 1 of the RAMOTSWA project. Airborne geophysical surveys were conducted within this flight area in 2016 (Figure 1).

Gaborone Dam Catchment The Gaborone catchment area, located in the Upper Limpopo River Basin (Area ~4,318 km^2, Figure 1), reflects the immediate surface water boundaries within which the

Ramotswa Aquifer is located. Given the linkages between surface and groundwater, the catchment is a very relevant scale.

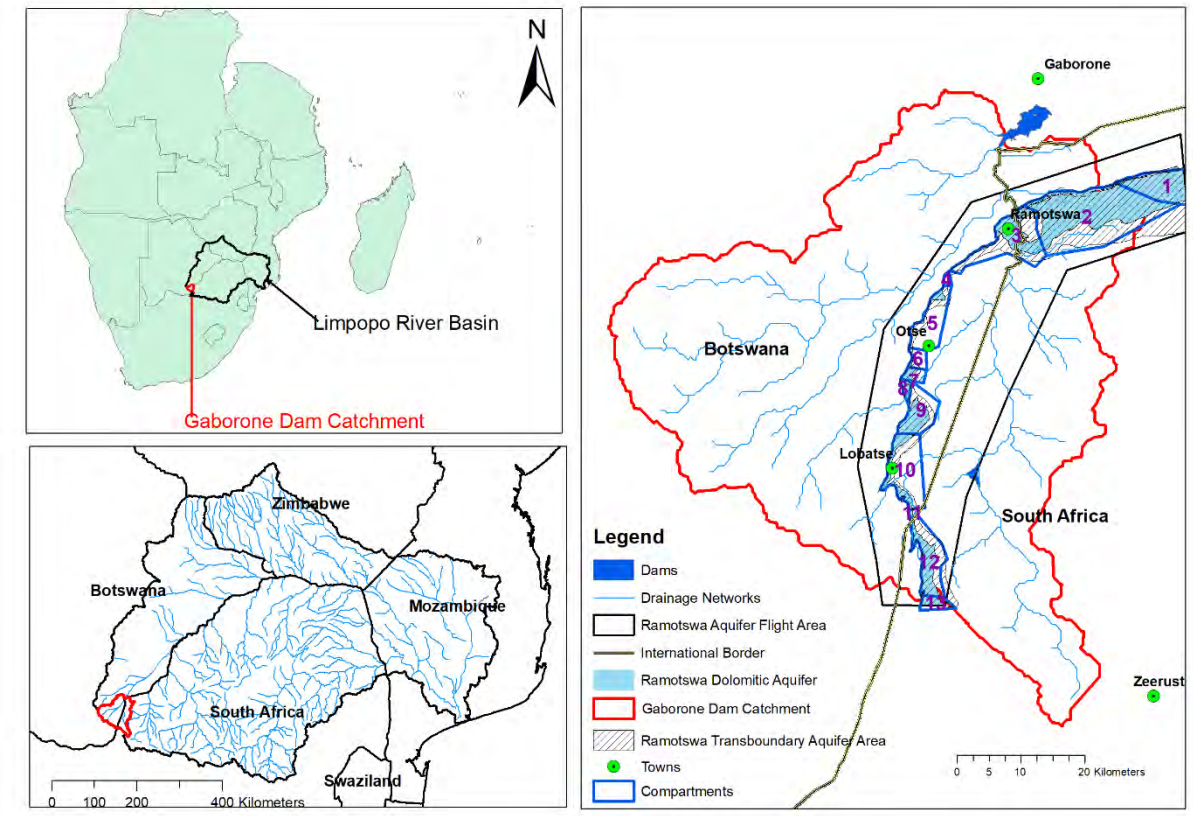

Figure 1: Study area location

2.2 Model area

During the airborne geophysics survey (XRI BLUE, 2016), 13 compartments of the dolomite aquifer were identified in the RTBAA (Figure 1). These compartments were delineated by connecting dikes but also by permeability contrast, by identifying less permeable formations. Out of the 13 compartments, only four compartments (3, 10, 11 & 12] are transboundary. Due to significance in terms of human dependence on the groundwater from the compartment, availability of data for model calibration, its transboundary nature and its size compared to the other three transboundary compartments, compartment 3 was selected for modeling purpose. Compartment 3 comprises the Ramotswa wellfield area that supply water for Ramotswa town. It covers an area of 80 km^2. The Ngotwane River, also known as the Notwane River in Botswana is the largest ephemeral river that crosses the study area. As can be seen in Figure 2, the area is highly urbanized on the Botswana side, while the South African side is less developed. The topographic map of the study area is shown in Figure 3. Catchment elevation in the modelling area ranges from 1019-1210 m above mean sea level. The Sengoma Mountains represent the topographic highs.

Figure 2: Study are of compartment 3 of the Ramotswa aquifer (Google Earth). Black polygon shows the boundary of the model area while the Blue line represents the international border which is also matching with the Ngotwane River. Left of the Ngotwane River is Botswana and on the right side is South Africa. Ramotswa town is indicated.

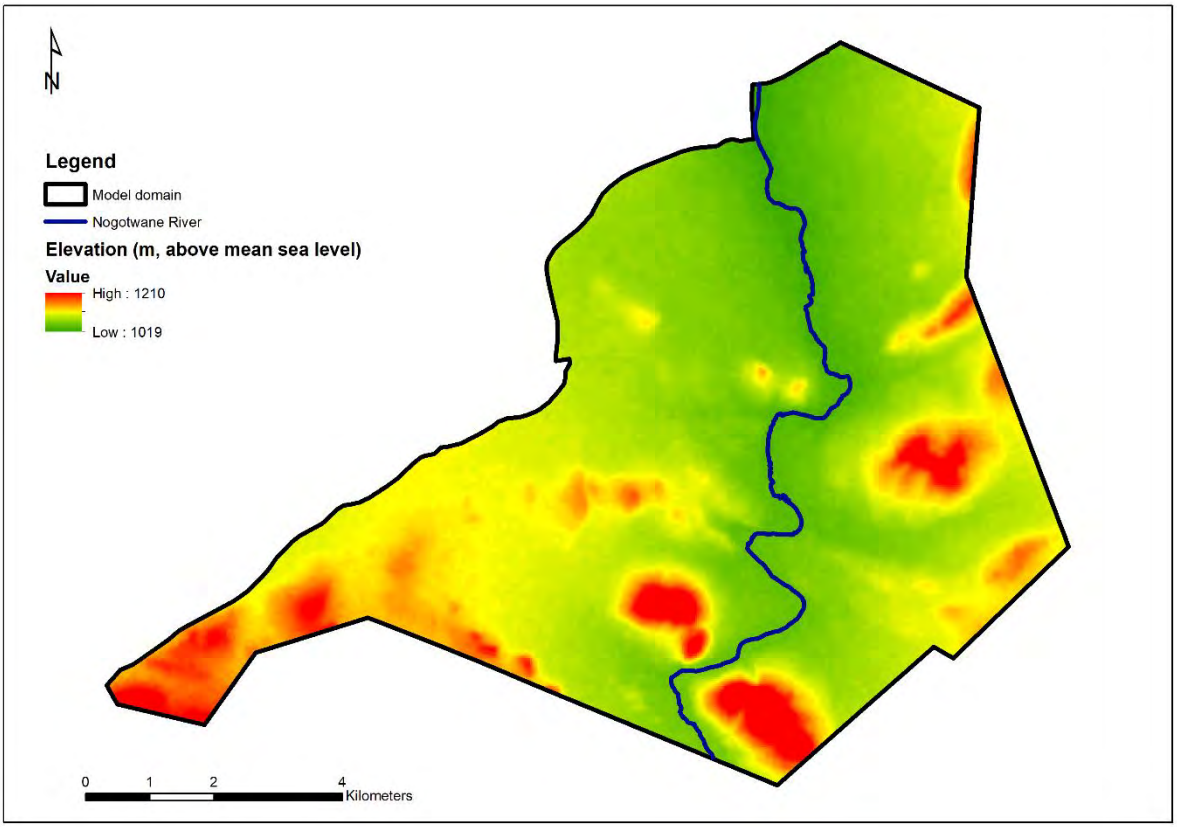

Figure 3: Topographic map of the study area

2.2.1 Climate

The Thiessen polygon method is the most common method used for determining areal average rainfall for a catchment using point rainfall measurements. The method requires the construction of a Thiessen polygon networks. The catchment area is divided into polygons and station weights is calculated based on the relative areas of each measurements station in the Thiessen polygon network (Figure 2). The individual weights are multiplied by the station observation and the values are summed to obtain the average precipitation. In the present study, nine rainfall stations shown in Figure 4 were used to construct the Thiessen polygon networks. However, as can be seen in Figure 4 the study area is fully enclosed in the Thiessen polygon network nearest to the Ramotswa rainfall station. Therefore, Ramotswa station is selected as a representative climate station. It is important to note that whenever a new station is added or removed the Thiessen polygon need to be updated.

Figure 5 shows the annual rainfall for the Ramotswa station. The annual precipitation ranges from 86-915 mm/a. The mean annual precipitation is 493 mm/a, standard deviation of 222 mm/a [1995-2015]. There is high inter-annual variability in annual rainfall (coefficient of variation of 45%). The maximum and minimum annual rainfall occur in year 2013 and 2009, respectively. The long-term mean monthly rainfall data is shown in Figure 6. As can be seen most of the rainfall takes place from October – March. Majority (57%) of the mean annual rainfall occurs [Jan-Mar] and 33% [Oct-Dec].

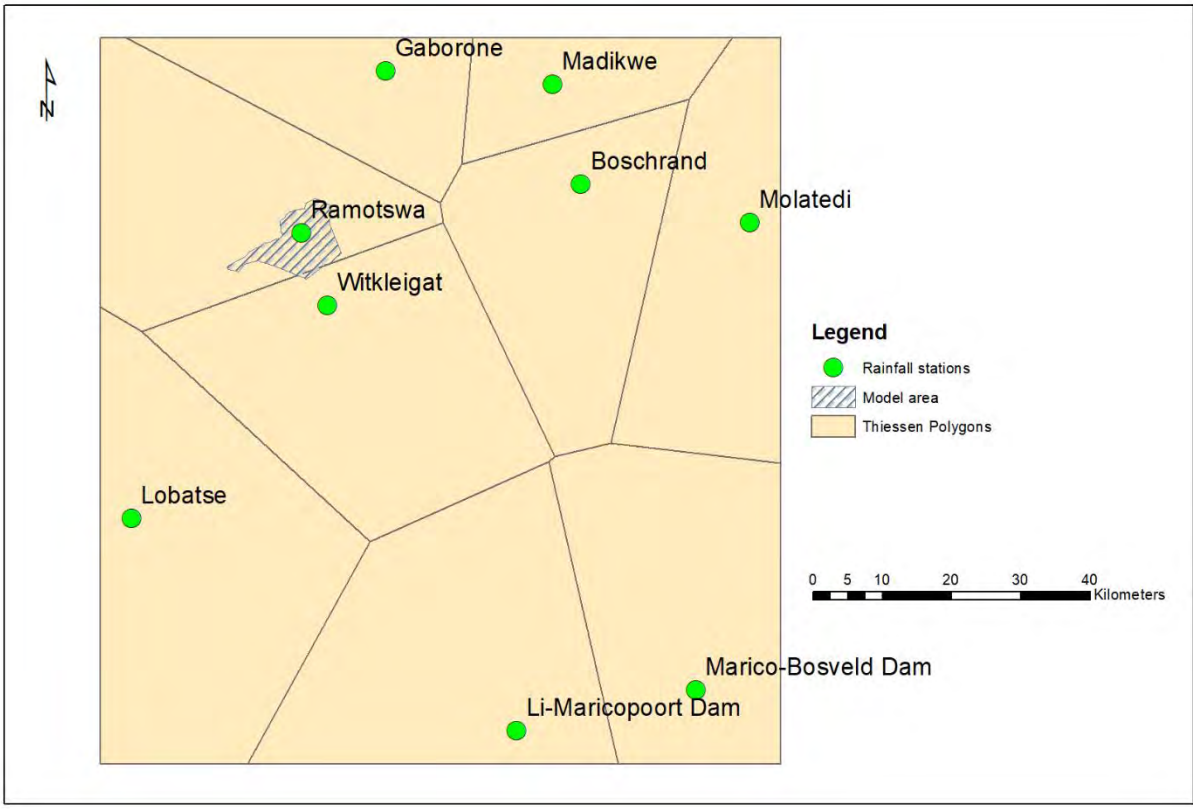

Figure 4: Thiessen polygon method for areal rainfall estimation

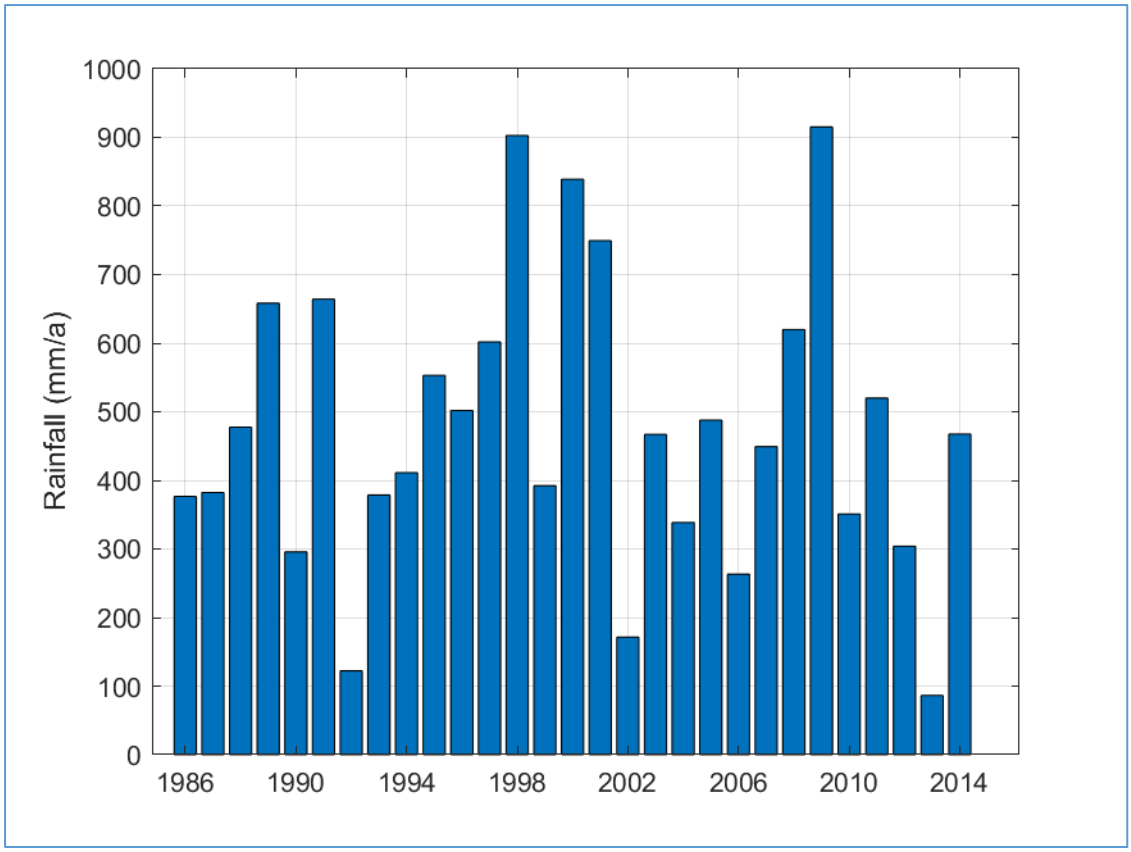

Figure 5: Annual rainfall (data from Ramotswa station)

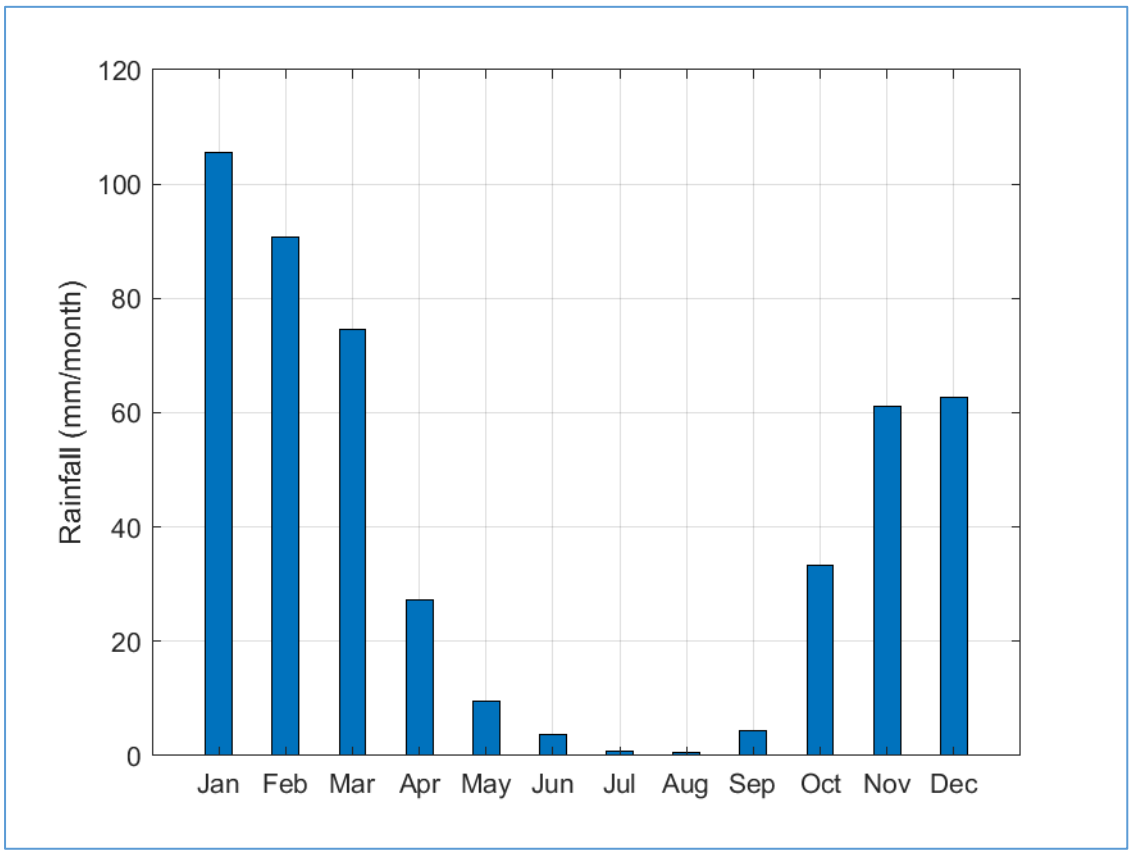

Figure 6: Mean monthly rainfall (data from Ramotswa station [1986-2014])s

2.2.2 Geology

Geologically, the Ramotswa wellfield area is formed from the Transvaal Supergroup. The Transvaal Supergroup is divided into four lithostratigraphic units, i.e. the Protobasinal Rocks, Black Reef Formation, Chuniespoort Group and Pretoria Group (Catuneanu and Eriksson, 1999; Eriksson and Reczko, 1995). Figure 7 presents these lithostratigraphic units and their chronology. The simplified geology of the study area is shown in Figure 8. The lithology of the Black Reef formation is dominated by clastic rocks ranging from conglomerate to sand stones and mudstones (Catuneanu and Eriksson, 1999). The Chuniespoort Group comprises of seven formations, the five dolomite formation in the Malmani Subgroup (i.e, Oakatree, Monte Cristo, Lyttelton, Eccles and Frisco), Penge and Duitschland Formations (Catuneanu and Eriksson, 1999). The five dolomite formations are differentiated based on their chert content and type of stormatolie as well as by interbedded subordinate carbonaceous mudstones and rare quartzite (Catuneanu and Eriksson, 1999; Eriksson and Altermann, 1998). The Malmani dolomite formations starts from the lower most Okatree, succeed Monte Christo, Lyttelton, Eccles and upper most Frisco Formation (Eriksson and Altermann, 1998). The Frisco Formation is overlain by iron-rich facies of the Penge Formation, also known as Ramotswa Formation in the Botswana (Catuneanu and Eriksson, 1999). The Penge Formation consists of micro – to macro-banded iron formations with shard structures and subordinate interbeds of carbonaceous mudstone and intraclastic iron formation breccias (Catuneanu and Eriksson, 1999). The upper most Chuniespoort Group formation is the Duitschland Formation overlying the Penge Formation. The Duitschland Formation comprises predominant dolomitic mudstones with interbedded dolomites and quartzites (Catuneanu and Eriksson, 1999). The Pretoria Group consists of 14 formations dominated by clastic and volcanic lithologies (Catuneanu and Eriksson, 1999).

The lower part of the Timeball Hill and the upper part of the Rooihoogte formation of the Pretoria Group is known as Lephalale formation in Botswana (Altchenko et al., 2017). Lephalale formation also called the Ramotswa shale. The Timeball Hill and Rooihoogte formation covers about 16.26 and 8.66 km^2 of the study area. Together these two formations accounts about 31.15% of the study are and 51.80 % of the area outside of the dolomite and unconsolidated sediment formations.

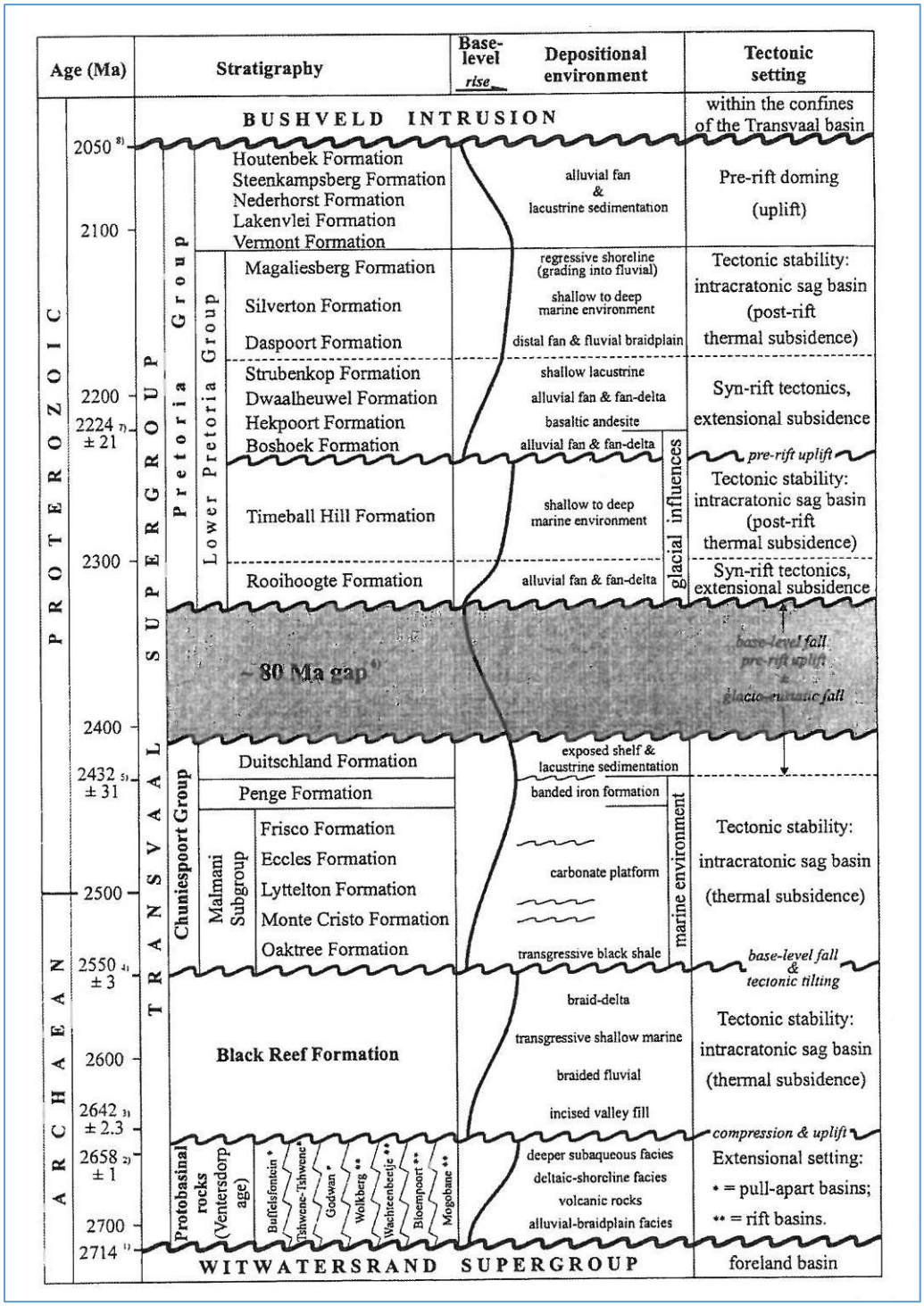

Figure 7: Lithostratigraphy of the Transvaal Supergroup obtained from Catuneanu and Eriksson (1999)

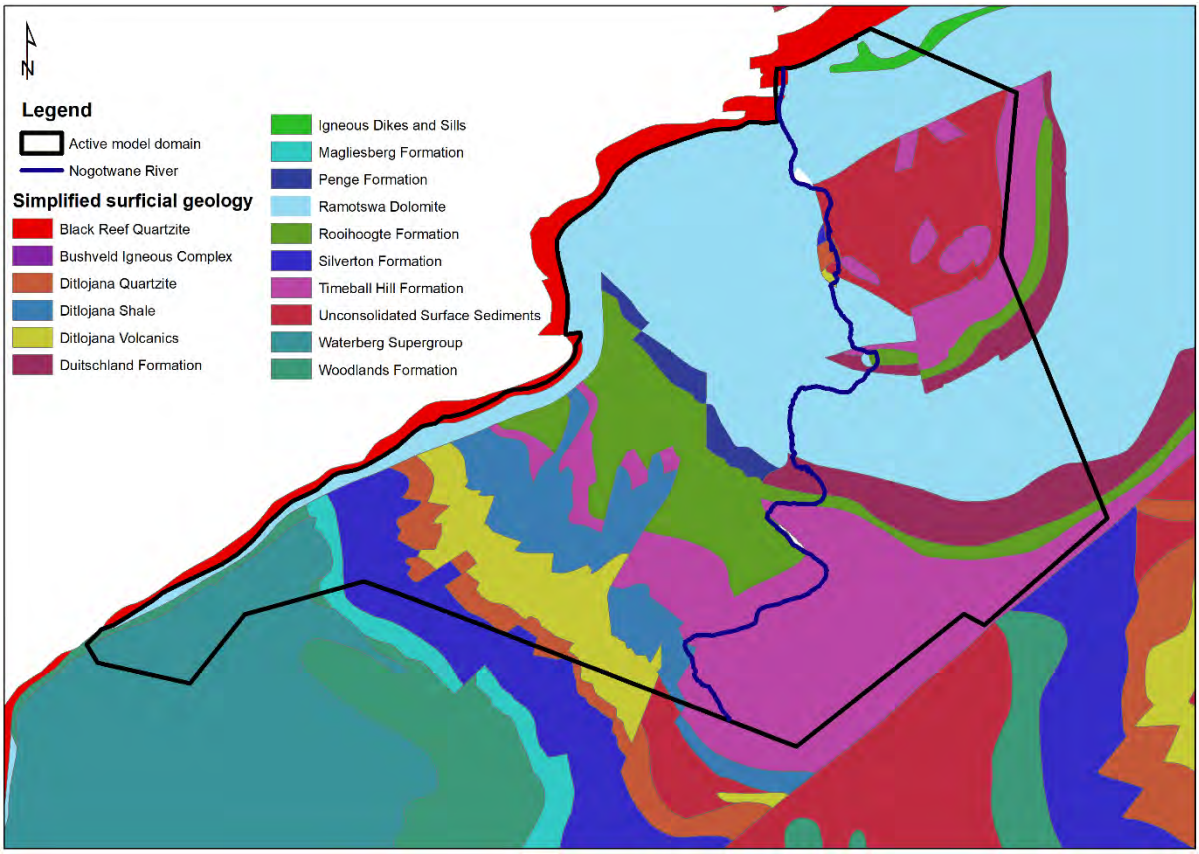

Figure 8: Simplified surficial geology of compartment 3

2.2.3 Hydrogeology

The main aquifer in the RTBAA is the Ramotswa Dolomite formation (Chuniespoor Group, Malmani Subgroup). However, a second aquifer systems exists in the RTBAA, the relatively low-yielding Lephalale formation (lower part of the Timeball Hill and the upper part of the Rooihoogte formation of the Lower Pretoria Group), although some high yielding wells are drilled in this formation (GCS, 2000; Selaolo, 1985). Groundwater in the Ramotswa Dolomite is located in parts of the formation where karstification has occurred. The Ramotswa Dolomite comprises five carbonate formations referred to as either “chert-free” or “chert-rich” dolomite. While the chert-rich formation **Eccles** and **Mont Chisto** are classified as a good aquifer, the other three chert-poor dolomite formations, Oaktree, Lyttelton, and Frisco are regarded as poor aquifers. According to GCS (2000), the Dolomite Aquifer presents two zone of karst development and fissuring. These two zones hydraulically connected.

1) **The upper karstic zone** This zone has a thickness that varies from 20 to 50 m and is thought to be the results of fluctuations in the present water level. Dolomite dissiolution appears preferentially along fractures but the less cherty dolomite also presents karstic features at outcrop. The solution cavities are usually filled with mud or wad.
2) **The deeper karstic zone**. This zone results from older fluctuations in the water level and has a thickness ranging from 25 to 50m. The solution cavities are open and generally do not contian mud or wad filings.

The main groundwater flow direction is from south west to north east and generally follows the natural topography (Altchenko et al., 2017; Selaolo, 1985; Staudt, 2003; WUC, 1989). The aquifer is criss-crossed by impermeable dikes, which affect groundwater flow.

2.2.4 Effect of dikes on groundwater flow

The role of the dikes in relation to the groundwater flow is largely unknown. Based on pumping test in the cave sandstone aquifer, Morpulae, Botswana, Morel and Wikramaratna (1982) found that the transmissivity of dolerite dikes is at least hundred times smaller than the transmissivity of the cave sandstone aquifer. In another study in Botswana, (Bromley et al., 1994) reported that dolerite dikes less than 10 m thickness tend to be permeable due to cooling joints and fractures that generate hydraulic continuity across the intrusion whereas, thicker dolerite dikes serve as groundwater barriers. Based on the water level differences observed across compartment or dike boundaries in Groundwater Region 10, South Africa, Meyer (2014) concluded that the dikes at deeper depth are impermeable while some flow across the boundaries may occur within the upper weathered section of the dike.

Dike intrusions normal to the flow direction would significantly retard the flow of water. If the retardation is sufficient, the principal water flow could change to a direction parallel to the alinement of dikes (Takasaki and Mink, 1985). If the dike intrusions become sufficiently numerous and intersect, the dike-intruded rock section could become a barrier to groundwater flow. The dikes, because they generally retard the flow of water, impound and store water behind them. The limiting height and depth to which water can be stored behind them depend on the geometry of the dyke intrusions, the hydraulic properties of the dike materials that enable them to retain the impounded water, and the water bearing properties of the reservoir rocks (Takasaki and Mink, 1985). Dikes can act as pathways or barrier to the groundwater flow depending upon intensity of fracturing in the dike rock (Gupta et al., 2012). Whether the dikes act as water conduits or as barriers depends on their structure, location and orientation with respect to the groundwater flow (Gupta et al., 2012). Dikes act as potential aquifer when they are jointed/fractured. On the other hand, when they lack primarily porosity and permeability and are not jointed/fracture, they act as groundwater barrier. In such a case the terrain upslope of the dike functions as a good water repository, whereas the downslope remains unproductive (Singh and Jamal, 2002). Thus, even those dikes that are barriers to transverse groundwater flow may be good conduits of dyke-parallel flow. In many areas, for example in Iceland and Tenerife (Canary Islands), dikes are known to collect groundwater and transport it over long distances (Nilsen et al., 2003). Gupta et al. (2012) found that little influence on the groundwater flow for smaller dikes, at least in the hilly part of their study area. The host rock is often fractured close to the dike intrusion (improving flow and storage capacity adjacent to dikes) and this area have been targeted for groundwater development all over South Africa (Du Toit, 2001).

3. Review of Previous Modelling Studies

The Ramotswa aquifer has been the subject of more than three hydrogeological modelling (GCS, 2000; IoH, 1986; WUC, 1989) and other hydrogeological studies (DWA, 2006; Selaolo, 1985; Staudt, 2003; WUC, 2014). All the past hydrogeological modelling studies were: 1) undertaken with perspective of Botswana, not in a transboundary context, 2) focused on groundwater availability assessment and none of the modelling studies were dealing with MAR potential assessment. The present modelling

study is undertaken in the transboundary context, focusing on both understanding of the current aquifer water budget and MAR scenario analysis using more recent information, and data collected in the past two decades. The hydrogeological model boundaries are also defined based on the geophysical study carried out during the first phase of the Ramotswa project (Genco and Pierce, 2016a, b). This report reviews two of the three modelling studies conducted in the past. The WUC (1989) modelling study was not included in the review because of unavailability of modelling report that describes the first phase of the modelling work that the WUC (1989) used as a basis for modelling.

Institute of Hydrology, University of Bloemfontein, South Africa Assessment

The Institute of Hydrology, University of Bloemfontein, South Africa (IoH, 1986) modelled the Ramotswa aquifer using the Garlerkin finite element method. The modelling area is presented in Figure 9. Rectangular elements were used to discretize the area. The rectangular elements have a length of 1 km and refined grid along the river (200 m). Finer grids were used to represent the main linear feature and along the Ngotwane River. Vertically the aquifer is represented using three layers. Spatially, the aquifer area was divided into three zones representing: 1) the massive dolomite rock, 2) the Lephalale formation, and 3) the main E-W linear feature together with its immediate area. All geologic formations except the Ramotswa Dolomite, including the Black Reef Quartzites, were lumped as the Lephalale formation. The E-W linear feature represents areas of dense fractures. This area is located along the principal E-W karst feature in the Southern area where the main production boreholes are located. The study indicated that fractures together with recharge from the Ngotwane and the intersections with other minor valley from east and west have produced favourable conditions for enhanced secondary permeability by chemical dissolution. The width of the E-W linear feature was assumed to be 250 m. According to the study the linear feature extends 2 km on the Botswana side of the international boundary and it may extend NE several kilometre into the South Africa. However, it is unclear if the eastern karst has similar groundwater conditions as the zone in the Botswana.

The study adopted no flow boundary in the North and West, and constant head boundary in the South and Eastern sides. An unconfined aquifer is simulated. The aquifer thickness was assumed to be 85 m. This was divided into three layers with thickness of 15 m for the upper aquifer and 30 m for the middle aquifer and 30 m for the lower aquifer. The hydraulic properties used for the three zones in the three layers are presented in Table 1. To avoid model convergence problems due to abrupt change in hydraulic conductivity, an intermediate zone of 300 m width was introduced into the grid between the main linear feature and unfractured rock massive dolomite. Abstraction from four production boreholes (BH4336m BHZ4400 BH4349 and BH4337) located along the linear feature of the dolomite aquifer were included in the model. The average abstraction rates used in the model for the four boreholes was 2400 m^3/d. Initial conditions representing the pre-abstraction period June 1984 was approximated using constant water level of 1015 m. Recharge was not included in the model. The model simulation was compared with drawdown obtained with the long-term pumping test undertaken from July to September 1984. No calibration was attempted during this period, except adjusting the simulated drawdown by 30% to account for well loss. Although no statistical performance is reported it was argued that without optimizing the aquifer parameters, a good match between observed and model simulated drawdown was observed. Based on the area for each zone and assumed saturated thickness and storage coefficients values, total aquifer storage was computed to be 16.5 Mm^3. This was obtained by multiplying area by saturated thickness and storage coefficient and not by the model.

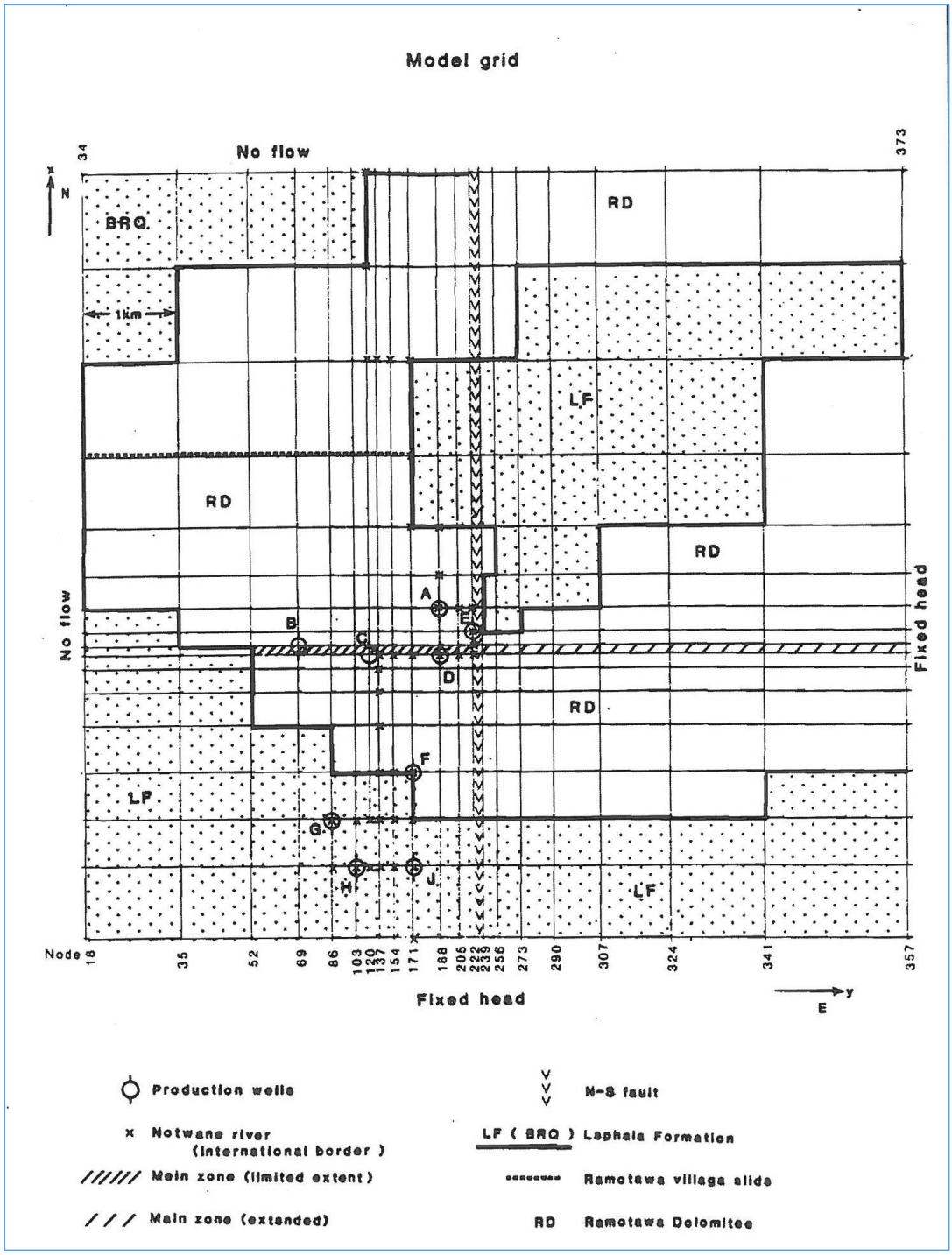

Figure 9: Model area, boundary conditions and model grid used in IoH (1986)

Table 1: Hydraulic parameters used in IoH (1986)

Aquifer zones	Hydraulic properties	Aquifer vertical layers		
		Upper aquifer	Middle aquifer	Lower Aquifer
Massive dolomite	Permeability (m/d)	0.1	0.1	0.1
	Storativity	0.003	0.003	0.003
E-W linear feature	Permeability (m/d)	65	7	7

	Storativity	0.02	0.02	0.02
Intermediate zone of the E-W linear feature	Permeability (m/d)	10	5	5
Massive Lephalale formation	Permeability (m/d)	0.05	0.05	0.05
	Storage coefficient	$3x10^{-4}$	$3x10^{-4}$	$3x10^{-4}$

Geotechnical Consulting Services (Botswana) Report

The Geotechnical Consulting Services team (GCS, 2000) modelled the Ramtoswa Aquifer area in 2000 using the Processing Modflow, PM Version 5. The aim of the modelling work was to reproduce the previous model developed by the Water Utilities Cooperation (WUC), Botswana, in 1989 using GWATER software, to improve the modelling work using the latest dataset and to derive some conclusion regarding the sustainability of groundwater abstraction in the aquifer. The model are, which was modelled by WUC (1989) and later modified by GCS (2000) is presented in Figure 10. GCS (2000) modelled the area using a two–dimensional model, which is a single layer model. The model area was divided into 500 x 500 m grid cells and refined in the proximity of the Ngotwane River using a 200 m grid. The model area extends 10 km in the EW direction and 12 km in the NS direction, however, it lacks geographical reference. The WUC (1989) model was bounded by no flow boundary in the west along the Black Reef Quartzite, no flow boundary in the east approximately 4 km from the Ngotwane River along the flow line, no flow boundary in the southern boundary along the surface water divide, and fixed head boundary of 1000 m amsl along the contact to the Black Reef Quartizite and Ngotwane river. In the GCS (2000) modelling work, the aquifer was modelled as no flow along the perimeter. The fixed head boundary at the north was replaced by no flow boundary. The reason for eliminating the fixed head boundary was that, as it is very close to the wellfield, it may act as an unlimited source of water for the wellfield. The eastern boundary moved 12 km east of the Ngotwane River, so that it coincides with the watershed divide and zone of enhanced faulting in the dolomite.

The aquifer was modelled using two zones: Dolomite and Lephalale formations. Two sources of recharge were included in the model. Recharge from the rainfall was assumed to be 10 mm/a, and recharge from the Ngotwane river was set to be 50 mm/a. Both values were assumed to be constant throughout the simulation period. The Ngotwane River is considered as discharge zone and modelled using a drain package assuming approximate depth of the drain equal to 5 m. The conductance value was calibrated during the steady state calibration.

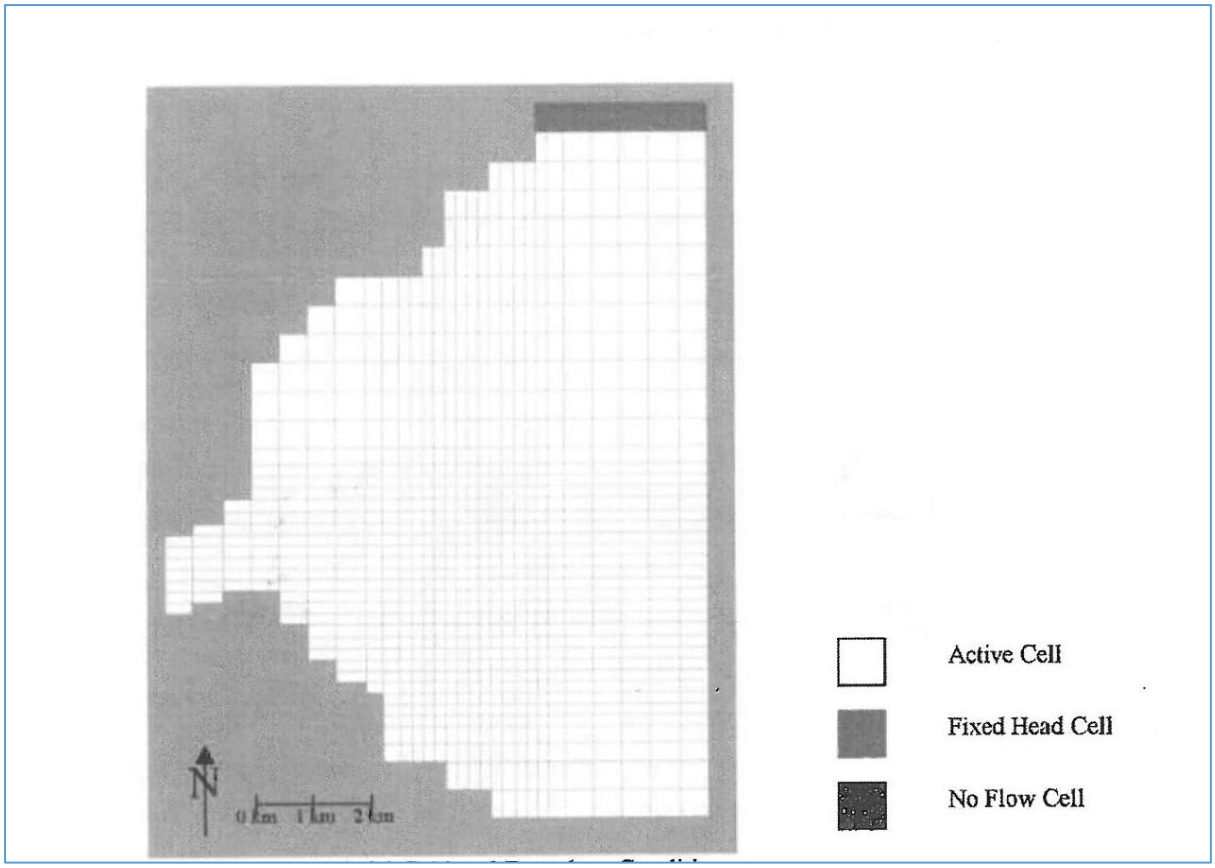

Figure 10: Model area, model grid and boundary conditions used by WLPU Consultants (WUC, 1989) and later modified by Geological Consulting Services (GCS, 2000)

4. Methodology

4.1 Data collection

4.1.1 Borehole elevation survey

Accurate groundwater level data is critical for model calibration. Groundwater level data is commonly obtained by subtracting depth to groundwater from ground elevation of the boreholes. In most cases ground elevation is obtained using hand held GPS. However, hand held GPS provides elevation data with poor accuracy (USGS, 2018b). A rough rule of thumb is that vertical position errors are usually about twice the horizontal ones, so if your handheld GPS is indicating 3-6 m horizontal precision, that is something like 6-12 m vertical precision (Balco, 2017)

Borehole elevation survey/mapping using handheld GPS. GARMIN handheld GPS version 62 was used for mapping borehole elevations during a field campaign May 7-11, 2018. During this campaign, 27 observation boreholes and 8 production boreholes, in total 35 boreholes, were surveyed. The data obtained during this survey was compared with water level data obtained from DWA and water level data calculated based on CGS (2000) borehole ground level. The comparison shows a -6.4 to +6.7m difference in water level between our measurement and CGS (2000) report. To minimize the error in borehole elevation using multiple handheld GPS measurement, we re-surveyed the borehole elevations using Differential GPS (DGPS).

Borehole elevation survey/mapping using DGPS. DGPS is an enhancement to GPS that calculates an error correction vector based on the difference between the known location of the base station and the perceived location of the base station from the current received satellite information. This correction vector can then be sent to the rover receiver to correct its estimated location (Koenig and Wong, 2010). DGPS called MicroSurveyFieldGenius9 was used for the surveying work. Real-Time Kinematic (RTK) Surveying using Global Navigation Satellite Systems (GNSS) was used. RTK Surveying is a relative positioning technique, which measures the position of two GNSS antennas relative to each other in real-time. One antenna is setup on a static point with fixed coordinates and is known as the base station**.** The RTK base station transmits its raw observation to the rover in real-time and the rover uses both the rover and base observations to compute its position relative to the base. A rover is a survey tool used to receive signals from satellites and a base station to calculate slope. The precision of RTK decrease as distance to the base station increase. Real-Time Network (RTN) surveying tool has been developed to extend this base-to-rover range limitation. The RTN concept is that a group of reference or base stations collect GNSS observations and send them in real time to a central processing system. The central processor then combines the observations from all (or a subset) of the reference stations and computes a network solution. From this network solution, the observation errors and their corrections are computed and broadcast to rovers working within the bounds of the RTN. Table 2 summarizes the major difference between RTK and RTN surveying methods.

South Africa has 67 base TrigNet network across the county, which have a maximum inter-station spacing distance of 300 km (Vorster and Koch, 2014) . The data from these base stations is streamed, via dedicated leased lines, to the National Geo-Spatial Information office in Cape Town where it is processed and made available, free of charge, to national and international users.

Table 2: Major differences between RTK and RTN surveying methods (Donahue et al., 2017)

Description	RTK	RTN
Base station	Requires base stations, which makes it costly	Do not require base station. RTN users required only to purchase a network subscription for access to the base station (network operator)
Communication	RTK survey normally uses UHF, VHF or broad spectrum radios. Communicate with the base station using radio links (Bluetooth) and avoids reliance on cellular coverage	Uses cellular phone networks, which means corrections only be received where cellular coverage exists.
Solution quality	The precision of RTK decrease as the distance from the base station increase	Gives comparable results anywhere within network range up to 50 km from a base station.

RTK method. Borehole elevation survey was conducted only in the Botswana side. This is because, all observation and production boreholes are located in Botswana. DGPS survey with the RTK method require setting up the base station and on site calibration or localization. The base station should be located where there is clear and unobstructed view of sky. Where ever possible it is important to set up the base station for maximum view or in the place where it maximize the satellite signal reception.

Wire fences, high voltage power sources significantly affect the work. Trees and high rise building also obstruct satellite signals. To detect the effect of a signal limiting source it is always advisable to check the number of currently tracked satellite at the rover and base station using the controller instrument, and the measurement errors. Localization also known as Site calibration is the process of relating local grid coordinate to the GPS earth centred earth fixed ellipsoidal datum. The process involves collecting control points with known coordinate and allowing the software to calculate transformation parameters. A minimum of three control point are required for horizontal control and one for vertical control. Localization is performed at the beginning of the survey, unless the base station is moved. The control point should encompass the survey area.

Survey procedure Location and elevation of the control points (bench marks, trig beacons and reference points) were obtained from Department of Survey and Mapping (DSM), Botswana. Bench marks are known point with correct x, y and z, whereas trig stations are correct in x, y but they have error in elevation in the range of plus minus 2m. Reference points are points that are transferred from trig stations and have x, y coordinate only. Three bench mark location and five trig station locations are obtained from DSM. Figure 11 shows the location of the trig stations. Figure 12 shows the DGPS instrument setup at BPQ42 (selected base station for maximum view and to maximize the satellite signal reception). Figure 13 shows the different nature of Bench marks in Ramotswa.

Figure 11: Trig stations location in Ramotswa (Left) and Trig beacon PBQ42 (Right)

Figure 12: Instrument setup at Trig station BPQ42

Figure 13: bench marks in Ramotswa (1/71 right and 1/78 left)

4.1.2 Groundwater level data

Depth to groundwater was monitored at 18 observation boreholes using a dip meter on the Botswana side. This is a once-off simultaneous monitoring of groundwater levels across the study area to determine the spatial distribution of groundwater levels (piezometric surface). The objective was gain understating of groundwater flow direction. Water level monitoring was not possible where observation boreholes were equipped with data logger as the boreholes are locked. Water level

measurement was not possible in the South African side as all boreholes were equipped. However, the Department of Water and Sanitation managed to measure the water level in five boreholes July–September 2018. Figure 15 shows the spatial distribution of water level in the study area interpolated using kriging. The groundwater level contour map was developed using water level data monitored during July 23, 2018 field campaign in the Botswana side and additional water level data monitored by DWS, South Africa on August 18 & September 10, 2018.

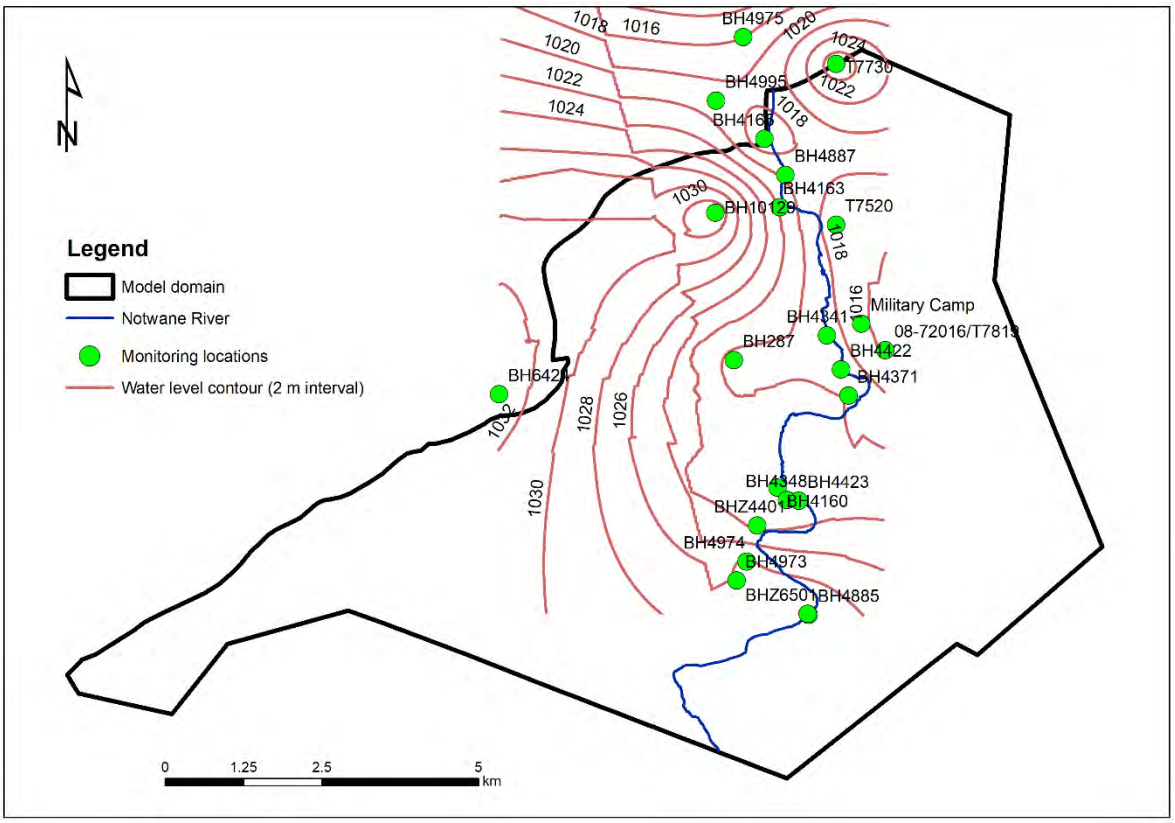

Figure 14: Groundwater level contours interpolated using kriging of water levels in 22 observation wells, July-2018

4.2 Modelling approach for karstic aquifers

Groundwater flow in karst aquifers occurs due to a combination of diffuse, fracture, and conduit flow (Quinn et al., 2006). Three approaches can be used to simulate flow in a karst aquifer. These approaches are: Equivalent porous medium approach (EPM) (Long et al., 1982), dual porosity model, and discrete fracture network models (Cook, 2003; Singhal and Gupta, 2010). Two conceptualization can be followed to represent flow in conduit network, 1) flow through conduit can be modelled using pipe flow concept and coupled with matrix flow, 2) conduits can be considered as narrow zone of high hydraulic conductivity zone. In the first approach the pipe geometry such as diameter, length, roughness and hydraulic radius need to be known. As there are no known network conduit in the study area, none of the approaches are used in the present study.

Some of the challenges in karst aquifer modelling pertain to:

1) Aquifer heterogeneity, aquifer parameters are difficult to estimate
2) Duality in flow ranging from matrix flow to conduit flow

3) Traditional models were designed for laminar flow and poor in representing flow through conduits

The EPM concept assumes that by averaging highly fractured and interconnected rocks over a large volume, the average flow resemble flow through a porous medium (Hassan et al., 2014).This approach is based on the assumption that the groundwater flow is not controlled by a small number of fractures, instead, the fractures are assumed to form a network of interconnected conduits, similar to pore space within a granular medium (Kaehler and Hsieh, 1994). In Equivalent Porous Media approach individual fractures or conduits cannot be adequately represented, rather the spatially averaged system properties are simulated (Teutsch and Sauter, 1991). This simplification is necessary because accounting individual fractures is a complex process. The EPM approach can be used for poorly karstified aquifer. However, for mature karst aquifers with well-developed conduit network, this approach results in poor approximation. The dual porosity model approach assumes that the porous medium consists of a fracture network and matrix blocks, which is less permeable. The discrete fracture network approach assumes that the fracture network forms only pathways for groundwater flow, and the matrix is impervious (Lee et al., 1999).

The EPM approach has been successfully applied in Karst aquifer (Ghasemizadeh et al., 2015; Larocque et al., 1999; Panagopoulos, 2012; Scanlon et al., 2003). Kuniansky (2016) tested the application of EPM approach based on MODFLOW 2005 and MODFLOW-CFP (MODFLOW-Conduit flow process model) in Florida Karstic aquifer and reported that, for monthly and seasonal time scales both models reproduced well the observed data. Based on this comparison, Kuniansky (2016) concluded that for monthly and seasonal time scale flow modelling in karst aquifer the increased effort required such as the collection of data on conduit location, and increased computational burden is not necessary. In the present study we adopted the EPM approach because it has proved adequate in previous studies.

4.3 Hydrogeological model description

The groundwater flow system was modelled using MODFLOW 2005 (Harbaugh, 2005) using the ModelMuse modelling environment/user interface (Winston, 2009). MODFLOW was selected for the present study for the following reasons: 1) It is available in the public domain and freeware that facilitate the use and further refinement of the model by the project partners, 2) It is one of the industrial standard groundwater models developed by the USGS (United State Geological Survey), 3) It is well documented and adequately tested, and previously applied to model groundwater flow in karst aquifer. ModelMuse is a freely avialble graphich user interface that has the functionaliy of importing, veriew and exporting GIS data.

MODFLOW is a three-dimensional finite-difference hydrogeological model for simulating and predicting groundwater conditions and groundwater/surface-water interactions. The transient 3D groundwater flow equation in MODFLOW is described using Equation 1. Equation 1, when combined with boundary and initial conditions, describes transient three-dimensional groundwater flow in a heterogeneous and anisotropic medium, provided that the principal axes of hydraulic conductivity are aligned with the coordinate directions (Harbaugh, 2005). Equation 1 is solved using the finite-difference method. The finite difference method uses a series of algebraic equations, which are based on conservation of mass and Darcy's law. These algebraic equation are solved for unknown heads at discrete nodes located in an orthogonal network. Since equation 1 is solved using a backward finite difference form, a head distribution at the beginning of a time step is required to calculate the head

distribution at the end of the time step. For each time step, the head distribution at the start of one time step is set equal to the head distribution at the end of the previous time step. External drivers, like climate and pumping influences how the heads change from one time step to the next. The chain of calculations is started with "initial heads" specified by the user. After the first time step, initial heads are no longer used to calculate heads. However, they are critical as they have a strong initial and lingering effect on the model results as the simulation progresses.

$$\frac{\partial}{\partial x}\left(K_x \frac{\partial h}{\partial x}\right) + \frac{\partial}{\partial y}\left(K_y \frac{\partial h}{\partial y}\right) + \frac{\partial}{\partial z}\left(K_z \frac{\partial h}{\partial z}\right) - W = Ss \frac{\partial h}{\partial t} \quad (1)$$

Where Kx, Ky, and Kz are hydraulic conductivities in x, y, and z directions (L/T), h is hydraulic head (L), t is time (T), W is a source-sink term (1/T) representing recharge, pumping, evaporation, etc., and Ss is specific storage (1/L), which when multiplied by the saturated thickness gives the confined aquifer storage coefficient, S (-), or the unconfined aquifer specific yield Sy (-).[-]. In general kx, ky, kz and Ss are a function of space and W may be a function of space and time.

MODFLOW was designed in a modular way, so that additional capabilities can be added over time. MODFLOW supports several primary packages. In the following sections, the MODFLOW packages used in this study are described.

4.3.1 Recharge package

Recharge from rainfall (diffuse recharge) occurs evenly over a large area and recharge from the river channel is calculated using the recharge package. Recharge flux is directly applied to the saturated zone and the volumetric rate of flow into a cell is calculated as by multiplying the recharge flux rate with the horizontal area of the cell. It is important to note that recharge rate is independent of the head in the cell.

4.3.2 Drain package

The Drain Package is applied to describe the discharge of groundwater from the aquifer to the river. The rate at which water seeps into a drain (river in our case) in the saturated zone of an aquifer is approximated in the model using the equation 2.

$$Qd = cd\ (h - d) \quad (2)$$

Where Qd is the rate of water flow into the drain (L^3/t), h is the head in the aquifer near the drain (L), d is the head in the drain (L) and cd is the conductance of the interface between the aquifer and the drain (L^2/t)

The head in the drain is assumed to be the bottom elevation of the drain. Thus, the flow into the drain is assumed to be proportional to the head above the drain. This equation only holds when the head in the aquifer is greater than the head in the drain. When the elevation of the drain is greater than the head in the aquifer, the flow into the drain is set to zero. Focused recharge from the river cannot be simulated with this approach. The input data which are specified by the user at the beginning of each stress period consists of the location of the drain (row, column and layer), elevation and conductance of the drain. Water discharged to the river is lost to the system. I.e., it is not routed through the river or made available for further downstream recharge to the aquifer.

4.3.3 General Head Boundary Package

A General Head Boundary (GHB) in MODFLOW is a boundary condition specifying a given head at the boundary of the model area. This can be specified as a time series of varying head. It is used to represent a boundary condition where water enters or leaves the model area at a rate proportional to the head difference between the specified head and the head in the model cell. The rate at which water is supplied to the model area or removed is expressed by Equation 3.

$$Q = Cm\,(H - h) \tag{3}$$

Where Q is the rate at which water is supplied from the boundary or water leaving through the boundary (L^3/t), Cm is hydraulic conductance of the material between the boundary and adjacent aquifer cell in the model area (L^2/t, H is the head at the source boundary (L), and h is the head in the adjacent aquifer cell (L). The input data requirements are the location of the boundary cell (layer, row and column), the boundary head and conductance of the material between the model area and boundary.

4.3.4 Evapotranspiration package

The Evapotranspiration (ET) Package in MODLFOW simulates the effects of plant transpiration and direct evaporation removing water from the saturated groundwater regime. The ET rate determined by the ET Package depends on the position of the aquifer head relative to two given ET reference elevations--ET surface and ET extinction elevation. When the groundwater table is at or above the evapotranspiration surface, water is extracted at maximum evapotranspiration rate. When the groundwater table is below the extinction depth - no extraction takes place. When the groundwater table is between the evapotranspiration surface and the extinction depth the extraction varies linearly with the groundwater table elevation. The ET rate is assumed to be proportional to the saturated thickness above the given ET extinction elevation. The ET rate is expressed in terms of flow out of the aquifer as

$$ET = 0 \;\; when\; h < Extinction\; elevation \tag{4}$$

$$ET = Maximum\; ET \left(\frac{h - Extinction\; elevation}{Extinction\; depth}\right) when\; the\; ET\; surface\; elevation \geq head\; in\; the\; aquifer \geq Extinction\; elevation \tag{5}$$

$$ET = Maximum\; ET\; when\; head\; in\; the\; aquifer > the\; ET\; surface\; elevation \tag{6}$$

Where

Extinction elevation, h, ET surface and Extinction depth in unit of (L) and ET and Maximum ET rate in unit of (L^3/t). Extinction depth is ET surface elevation minus extinction elevation.

4.3.5 Well Package

A well package in MODFLOW is used to simulate a specified flux to individual cells (L^3/t). A recharge well is viewed as a source of water and its flux is assigned as positive value. A discharging well is a recharge well with a negative recharge rate. The input data requirement include the location of the well (row, column and layer) and rate at which the well is recharging the aquifer or pumping water out of the aquifer. The screen level in each well determine the location of the sink in Equation 1.

4.4 Hydrogeological model setup

4.4.1 Conceptual Model

A conceptual model is the foundation of the model analysis (Bredehoeft, 2005). Generally, it includes information about the water budget that defines flow into and out of the aquifer system and boundary conditions. Conceptual model development involves an iterative process (Bredehoeft, 2005). The conceptual model may be redesigned as more data and information become available. During the conceptual model development, simplification is necessary to meet data limitations. However, such assumptions should be reasonable and consistent with the hydrogeology of the aquifer system. According to Bredehoeft (2005), the appropriateness of the conceptual model cannot be tested until a numerical model, based on the conceptual model, is built and comparisons made between observations and model simulation results. As such, the best approach is presumed to be concurrent and iterative development of conceptual and numerical models rather than waiting until a 'perfect' conceptual model is formulated before starting to assemble the numerical model. Conceptual models of carbonate aquifers can be found (White, 1969, 2012). The conceptual model for the present study is developed based on a previous study referred to above (GCS, 2000).

Developing a conceptual model consists of the following five steps (ASTM Standard D5447, 2010):

1. Specify the physical extent of the aquifer systems that impact or control the groundwater flow system, and analysis of groundwater flow directions
2. Determine appropriate physical and hydrological model boundaries
3. Define distribution and configuration of aquifer and confining units. Of primary interest are the thickness, continuity, lithology and geological structures
4. Determine relative hydraulic properties for each aquifer unit. This include specifying hydraulic conductivity, storage characterises of the aquifer system such as specific yield and storage coefficients
5. Identifying the source and sinks of water to the aquifer system. Source and sinks include pumping wells, infiltration, evapotranspiration, drains, and leakage across confining layers, and flow to or from surface water bodies.

The GCS (2000) modeling study adopted two–dimensional (2D) Areal flow model. The 2D areal flow model assumes that the aquifer is a 2D planar feature where groundwater flow is predominantly in the horizontal plane. However, as pointed out by Merz (2012), this assumption is usually valid for aquifers that have a horizontal extent that is much larger than the aquifer thickness and for aquifers that have high horizontal hydraulic conductivity so that vertical head gradients within the aquifer are negligible. These two assumptions are difficult to achieve in the Ramotswa aquifer. Hence, in the present study, we used a 3D flow model. Figure 15 presents a schematic diagram of the conceptual model used in the present study. The schematic conceptual model was derived from the geological-x section provided in the airborne geophysical survey. However, it is important to note that dipping in the dolomite formation and others is not shown. The main inflow occurs due to recharge (diffuse recharge from rainfall and concentrated or focused recharge from the Ngotwane ephemeral stream). The outflow from the model domain is mainly through domestic pumping, groundwater evapotranspiration and outflow though boundaries. Leakage from sewer pipes and wastewater discharge also contribute to aquifer recharge, but they are not accounted for in the model, assuming they are less important.

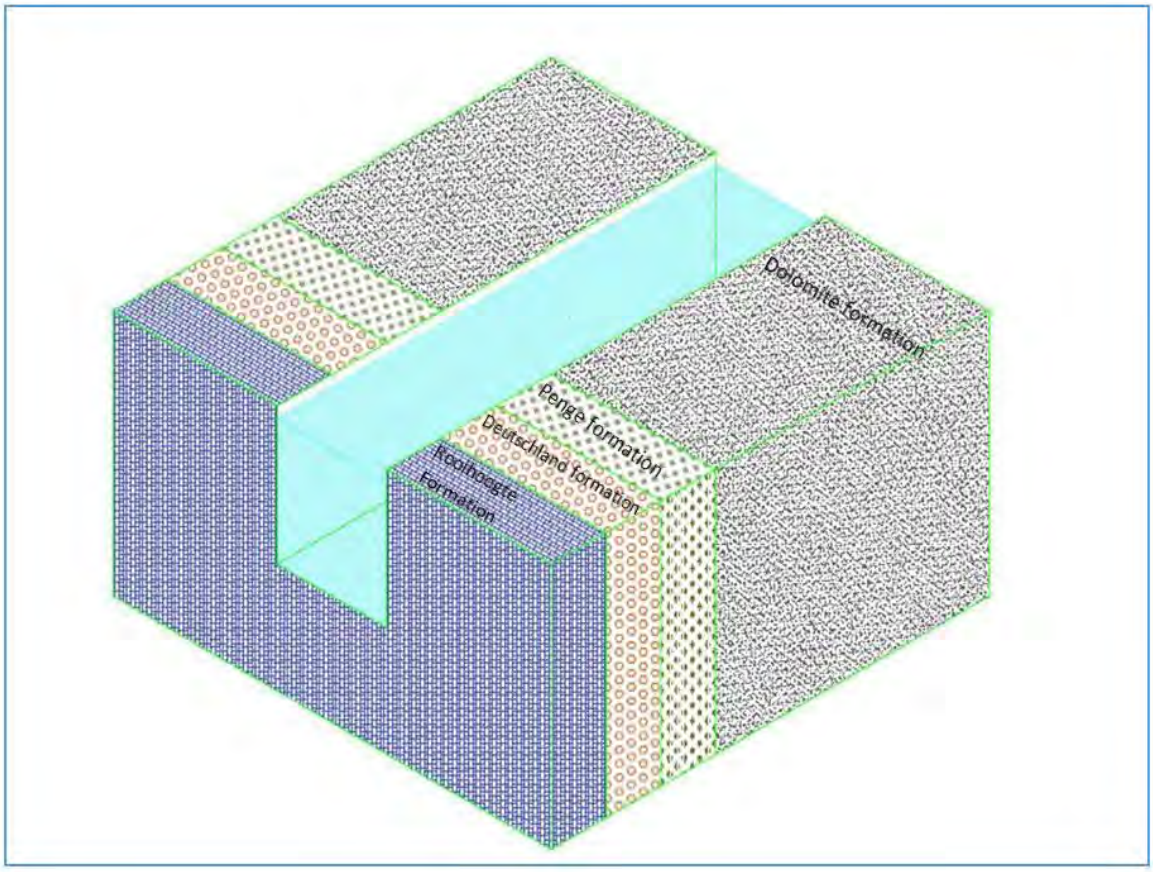

Figure 15: Schematic conceptual model (the dolomite dipping to the south is not shown)

4.4.2 Spatial model discretization

Spatially, the model area was divided into a grid cell size of 90 x 90 m (Figure 16). Vertically the model is discretized into two layers representing the upper karstic zone and the deeper layer. The thickness of the aquifer is specified based on the deepest borehole depth drilled in the area and specified as 150 m. This represents the level at which groundwater flow presumably becomes negligible underlying the lower water-bearing unit. The thickness of each layer is largely unknown. Williams (2008) reported that in arid and semi-arid region, the highly weathered and karstified layer below the soil layer may have a maximum thickness of 30 m while in other climatic regions it is typically limited to 3-10 m. Hence, in this study, we assumed 30 m thickness for the top layer and 120 m for the deeper (second layer). The elevation of the top layer was defined based on Shuttle Radar Topography Mission (SRTM) 30 x 30 m Digital Elevation Model (USGS, 2018a). The water-bearing formations are assumed to be in hydraulic connection with each other. The upper layer was assumed to be unconfined while the second layer was treated as convertible based on groundwater level in the deeper aquifer. If a layer is convertible, the code checks whether the head in the lower level is above or below the top of the layer as the simulation progresses and treats the layer as confined or unconfined, accordingly. Values of both confined and unconfined storage parameters are input for convertible layers (Anderson et al., 2015).

4.4.3 Temporal model discretization

Temporally, the 18 year's simulation period (2000-2017) was divided into 216 monthly stress periods. A stress period is an interval of time over which specified inputs are constant. Monthly stress period was selected in order to allow simulation of seasonal change in groundwater use, recharge, evapotranspiration and seasonal aquifer storage and recovery options through MAR. Each monthly stress period was further divided into weekly computational time steps.

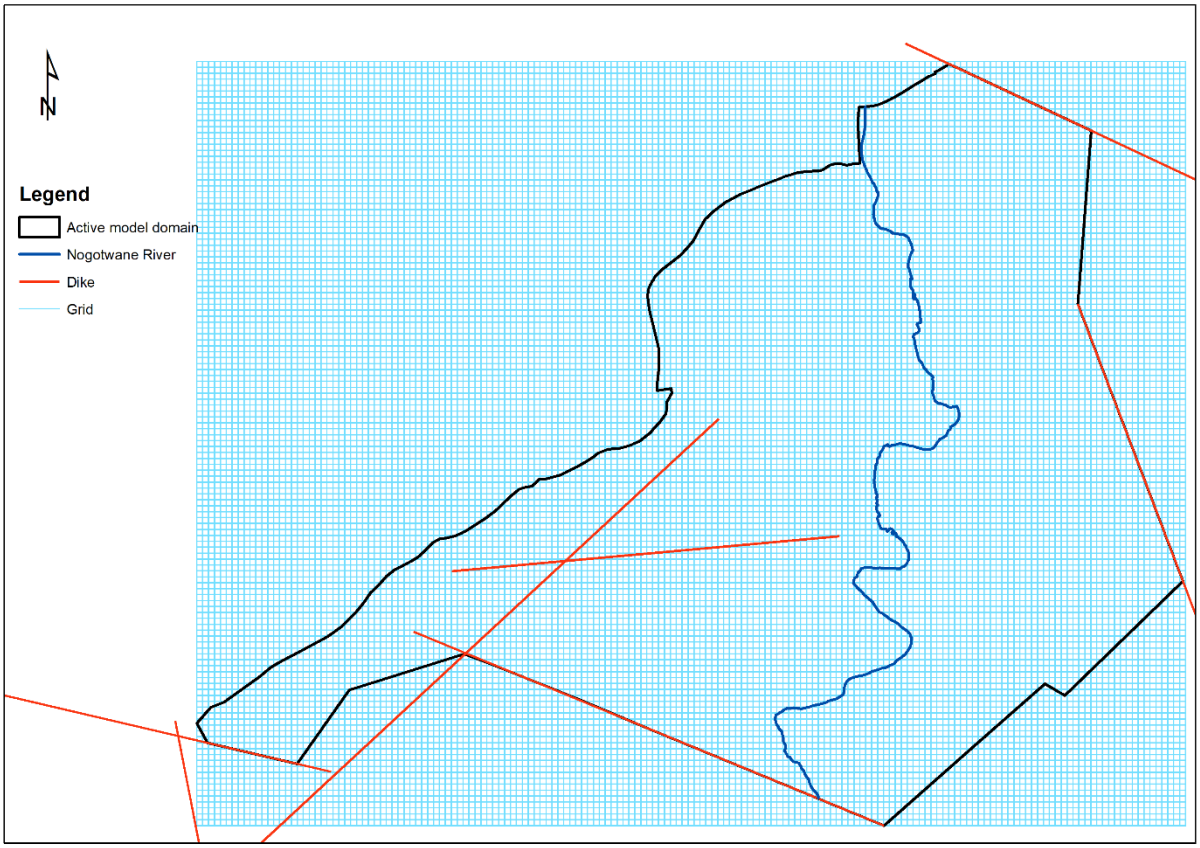

Figure 16: Model domain and grid (grid size of 90 m by 90 m)

4.4.4 Boundary Conditions

The identification and assignment of appropriate boundary conditions is critical for developing a proper conceptual model. The model boundaries need to be specified in a manner consistent with natural hydrologic features. The boundary conditions in this study were defined based on the previous studies (GCS (2000), IoH (1989)) and presumably nearly impermeable dikes, identified during the airborne geophysical survey. In general, the model domain is assumed to be bounded by no flow boundaries in all directions, except towards the north where the Ngotwane River crosses the Black Reef Quartzite where a General Head Boundary (GHB) was used to define outflow (Figure 17). Water level for the GHB was assigned based on observed water level at observation well BH4165. The conductance term of the GHB was estimated using model calibration. The following boundary conditions were assigned along the perimeter of the model domain (Figure 17).

- **North:** This boundary was represented by a no flow boundary along the contact between the dolomite aquifer and the Black Reef Quartzite and GHB where the Ngotwane River

crosses the Black Reef Quartzite.

- **Northeast:** no flow boundary along the dike.
- **East**: Represented by a no flow boundary along the contact between the unconsolidated surface sediment formation with the Tsokwnae Quartizite of the Timball Hill formation
- **South** The southern boundaries were represented by a no flow boundary along the contact between the Lephalale Formation and the Tsokwnae Quartizite
- **Southeast**: The southeast boundary was specified as no flow along the dikes
- **Southwest**: A no flow boundary along the dikes

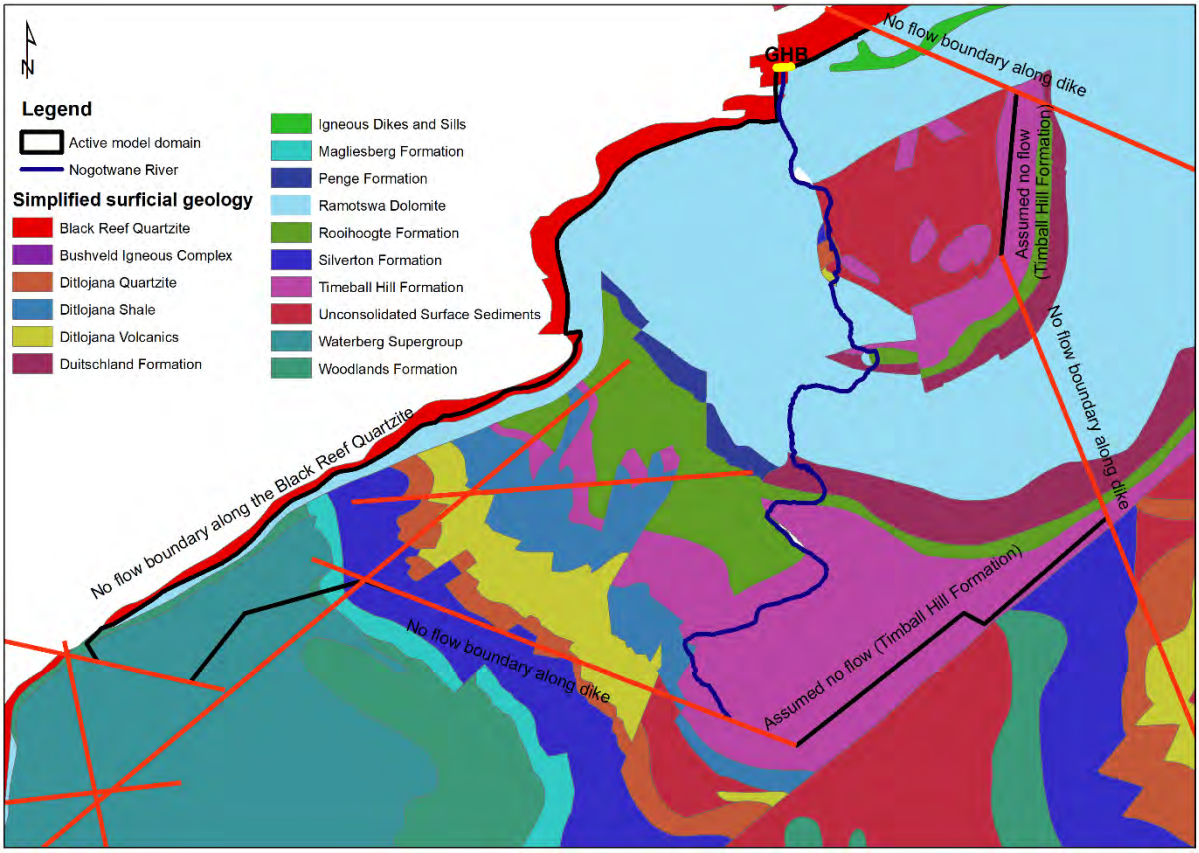

Figure 17: Boundary conditions

4.4.5 Modelling the effect of dikes on groundwater flow

The effect of dikes on groundwater flow can be simulated using two approaches: 1) assuming zone of low hydraulic permeability e.g. Comte et al (2017), 2) using Horizontal Flow Barrier Package (HFB) of MODFLOW (Hsieh and Freckleton, 1993). For the present study, dikes inside the model domain (Figure 17) were simulated using HFB as demonstrated by Gebreyohannes et al. (2017) and Faunt et al. (2004). In the HFB Package, dikes are conceptualized as being located in the boundary between two adjacent finite difference cells in the same layer. The HFB package then adjusts the horizontal hydraulic conductance computed by Layer property Flow package or Block centred Flow package to account for the barriers. The key assumption underlying HFB is that the width of the barrier is negligible as compared to the horizontal dimensions of the cells in grid so that the original conductance calculation is not affected (Harbaugh, 2005). The HFB package requires two parameters to be specified; the

hydraulic conductivity and the thickness of the barrier. Barrier thickness is not explicitly considered in the package, but included implicitly in a hydraulic characteristics which is the ratio of the hydraulic conductivity to the thickness of the barrier. Hence, HFB allows the capability to use hydraulic characteristics as calibration parameters. The geometry of the dikes are assumed to be vertical, and extend from the surface of the ground to the bottom of the model layer.

4.4.6 Initial Conditions

In a transient solution, the initial heads provide the reference elevations for the heads solution. The classical approach for defining initial heads for the transient model simulation follows a two-step procedure, calibrating steady state model for pre-development time period and using the output of the steady state model as initial head for the transient simulation. Using model-generated initial head ensures consistency between the initial head data and the model hydrologic inputs and parameters (Anderson et al., 2015). Incorrect initial head may result in an extreme (large or small) volume of water being stored in the aquifer, and when simulations are performed with this initial head, the flow condition will be dominated by the wrong positioned water and mask the influences of recharge and abstractions (Lloyd, 1981). The initial condition affects transient model simulation with reduced effect as time progresses. Initial condition for the transient model was specified based on calibrated steady state model for the average water level conditions 2000-2012.

4.4.7 Groundwater Pumping

According to WUC (2014), the Ramotswa wellfield was commissioned in the 1980s for emergency water supply to Gaborone city. The wellfield started its operation with four production boreholes. After the completion of the Gaborone dam in 1984, water supply from Ramotswa wellfield to Gaborone city was discontinued and the Ramotswa wellfield was used to supply Ramotswa town at a rate of approximately 1000 m^3/d (WUC, 2014). Later, in 1989, the number of production boreholes were increased to ten and in that year the average daily abstraction rate also increased to 1696 m^3/d. In 1996, abstraction from the Ramotswa wellfield was totally stopped due to high nitrate level in the groundwater and re-operated in 2014. However, the exact re-opening date of the wellfield is not known. At the moment, nine production wells shown in Figure 18 are operational. The depth of these wells ranges from 102-120 m below the ground surface. Figure 19 presents total monthly abstraction for the period March 2015-Augst 2017. Figure 20 shows the average daily abstraction rate per production borehole. As can be seen in Figure 19, the abstraction in the Ramotswa wellfield reached a maximum of 8923 m^3/d in October 2015.

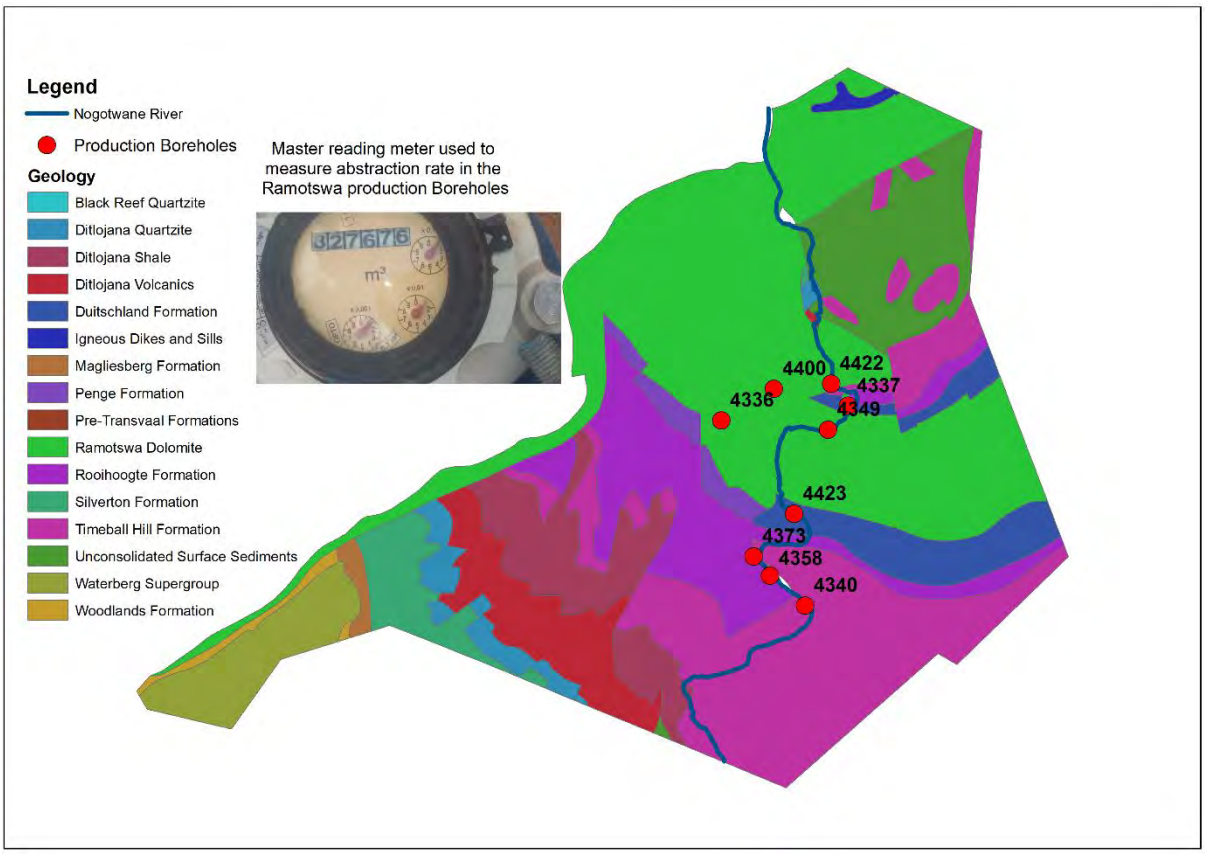

Figure 18: Location of production boreholes (Total N= 9) 5 in Ramotswa dolomite and 4 in other formations

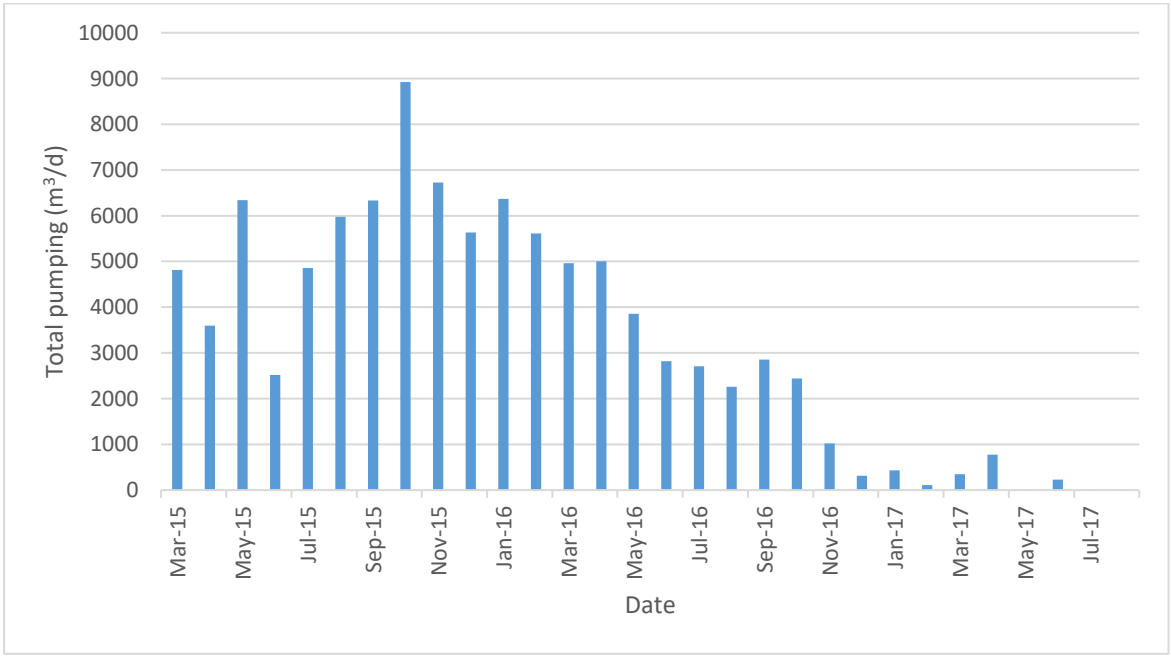

Figure 19: Total monthly abstraction (N=9 production boreholes) for the period March 2015-Augst 2017 from WUC

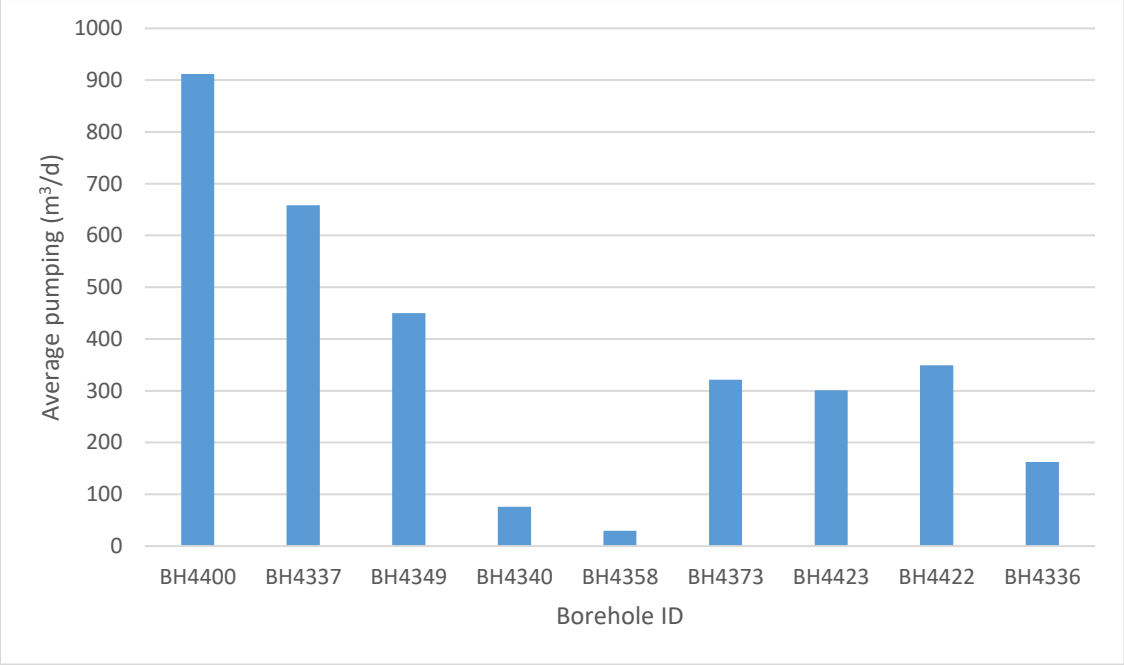

Figure 20: Average daily pumping per production boreholes for the period March 2015-Augst 2017 from WUC

4.4.8 Groundwater Evapotranspiration

Groundwater Evapotranspiration (GWET) occurs in areas where the depth to groundwater is shallow and plant roots penetrate to the zone of saturation. GWET in Ramotswa occurs along the Ngotwane River where groundwater is relatively close to the surface. The minimum depth to groundwater from ground surface for observation wells within distance of 200 m from the River channel ranges from 0.88 – 2.61 m (Figure 21). To simulate GWET using the ET package, maximum evaporation rate, evapotranspiration surface and extinction depth need to be specified in the model. A maximum evapotranspiration rate is assumed to occur when the water table is at land surface. The ET extinction depth was determined based on Shah et al. (2007) study for a given soil type and land cover. The soil type in the study area is sandy clay loam. This was determined using soil global dataset (Soilgrid 250 m ISRC World Soil information). For sandy clay loam soil type and land cover type bushes and grass, the ET extinction depth was determined to be 3 m. The potential or reference evapotranspiration was estimated using the Hargreaves Method (Hargreaves and Samani, 1985; Samani, 2000), Equation 6. RA can be estimated using Equation 7 or tables (Allen et al., 1998; Samani, 2000). Figure 22 shows the calculated monthly ET rate using the Hargreaves Method based on temperature data from Gaborone city (Figure 1).

$$ETo = 0.00023 \times RA \times Ta^{0.50} \times (Ta + 17.8) \quad (6)$$

$$Ra = \frac{1440}{\pi}(G_{sc} \times d_r) \times (\sigma \times \sin\varphi \times \sin\delta + \cos\varphi \times \cos\delta \times \sin\sigma \quad (7)$$

Where

ETo is potential evapotranspiration (mm/d)

G_{sc} is the solar constant (0.0820 Mj/m^2/min)

d_r is inverse relative distance from the earth to sun and expressed by

$d_r = 1 + 0.033 \times \cos(\frac{2\times\pi\times JD}{365})$, JD- is day of the year

$$\delta = solar\ declination\ (rad) = 0.409 \times \sin(2 \times \pi \times \frac{JD}{365} - 1.39)$$

$\varphi = lattitude\ of\ location(rad)$

σ = sunset hour angle (rad)

$\sigma = arcos[-\tan(\varphi) \times \tan(\delta)]$

Ra = extra-terrestrial radiation (MJ/m2/d) but to use it in the Hargraves equation, it has to be converted to mm/d. MJ/m2/d can be converted to mm/d as; mm/d = (MJ/m2/d)/2.43

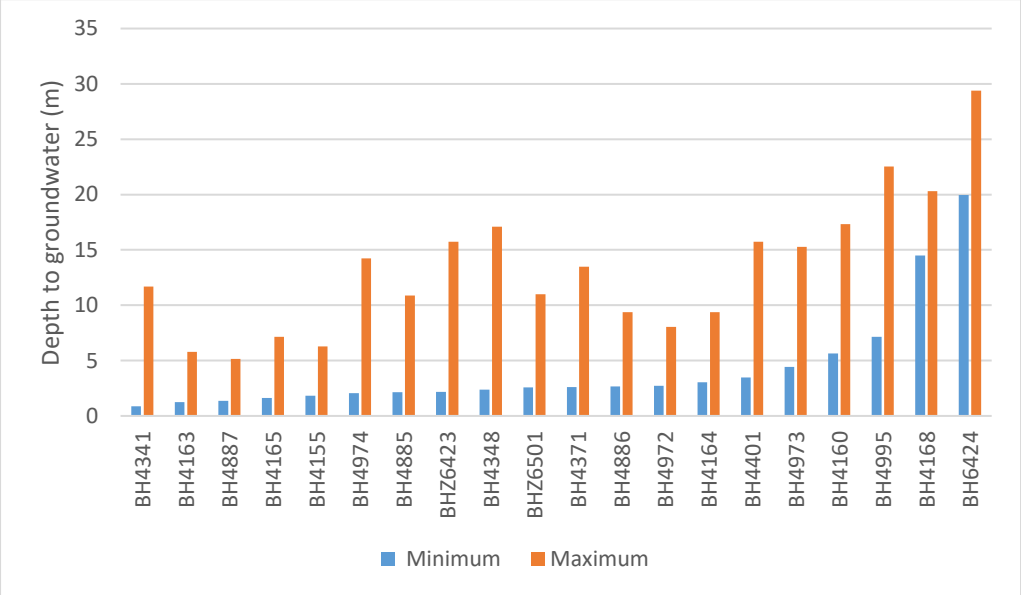

Figure 21: Minimum and maximum depth to groundwater from ground surface for all observation wells

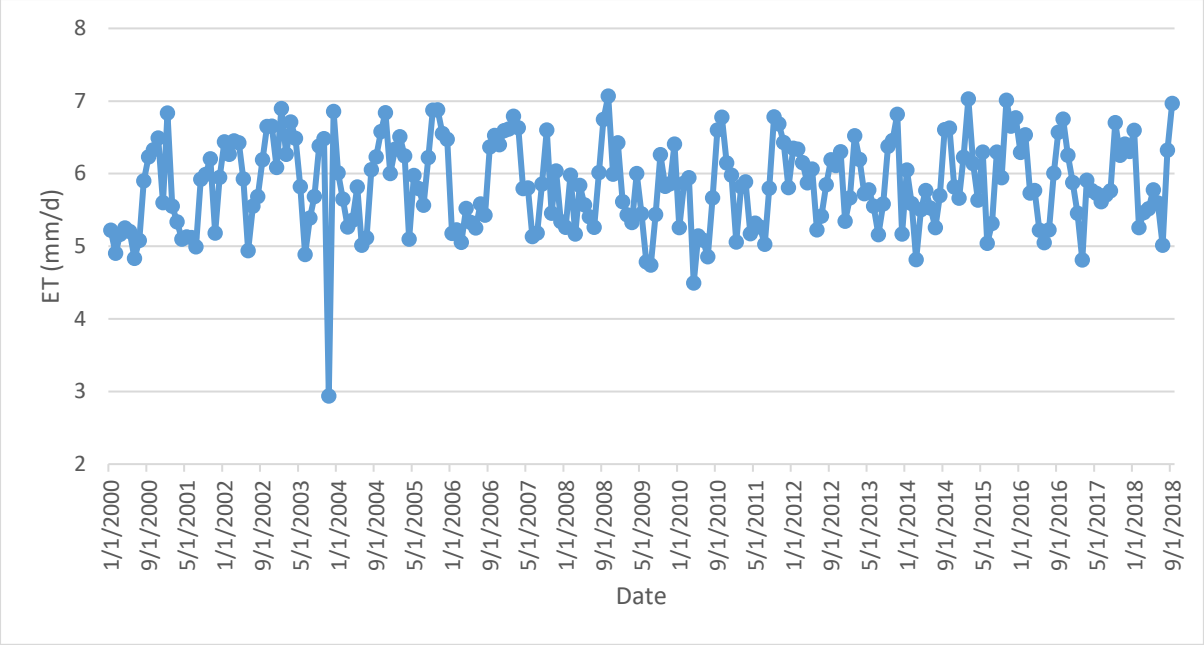

Figure 22: Monthly evapotranspiration using Hargraves method

4.4.9 Groundwater Recharge

The primary sources of recharge to the Ramotswa aquifer is via leakage from Ngotwane ephemeral stream, and more diffusely from rainfall. In drylands, recharge from ephemeral streams is predominant (Goodrich et al., 2004). Recharge from precipitation occurs when rainfall infiltrates the land surface and percolates past the root zone to the water table. It is generally a small fraction of the total precipitation in dry climates. The diffuse recharge processes are arguably more widely understood but major uncertainty exists in areas where recharge from ephemeral water bodies dominates (Doll and Fiedler, 2007). Recent review of recharge estimation methods from ephemeral streams is presented by Shanafield and Cook (2014). The seven methods reviewed include: 1. controlled infiltration experiments, 2. monitoring changes in water content, 3. heat as a tracer of infiltration, 4. reach length water balances, 5. flood wave front tracking, 6. groundwater mounding, and 7. groundwater dating. All of these methods require data focused on the river itself. However, river gauging station data is not available in Ngotwane River in the study area. Furthermore, the field studies conducted as part of this study are limited to river bed infiltration tests. Hence, rigours application of any of the methods listed above was not possible.

In the present report, recharge from precipitation (diffuse recharge) and recharge from the Ngotwane River (focused recharge) was simulated using the recharge package. Recharge rates were estimated as a fraction of precipitation, assuming that focused recharge occurs in conjunction with rainfall. The monthly rainfall values were specified in the model as potential/upper recharge flux and this was multiplied by two multiplying factors, one representing recharge zone 1 (recharge form rainfall) and one representing recharge zone 2 (from the river), Figure 23. The multiplying factors were estimated during model calibration. Ebrahim et al. (2015) have used a similar approach for estimating recharge from a Wadi Samil in Oman.

Recharge is also estimated using the Water Table Fluctuation (WTF) method using water level observed in observation wells close to the river. The WTF method is presented in Annex 1. It is important to note that the river channel is highly variable as shown in Figure 24 and may not be

recharging the aquifer in all sections. Soil infiltration tests was conducted at six points inside the channel and nine locations outside of the river channel (Figure 25). Results of the infiltration test shows that the infiltration rate is low inside the river channel compared to outside/in the field (Figure 26). The average infiltration rate inside the river channel and outside/in the field was0. 51 and 3.41 m/d, respectively. Detail information about the infiltration test and field procedure can be found in the deliverable on Managed Aquifer Recharge (December 2018). It is important to note that infiltration rate in the bedrock areas of the river may be high. However, this was not confirmed as the soil infiltration test cannot be applied in these areas. However, fractured/ karstifed rock bed areas (picture left centre) may be a source of recharge for the aquifer and aquifer discharge may occur in the other areas such as close to BH4163 picture top left corner). Based on pumping test analysis, DWA (2006) found that the river is a recharge zone as opposed to previous assumptions as discharge zone (e.g. GCS, 2000, IoH, 1989). Depending on season, the river may function as a recharge zone (e.g. early in the wet season), and as discharge zone (latter parts of the wet season when groundwater levels in the area have gone up).

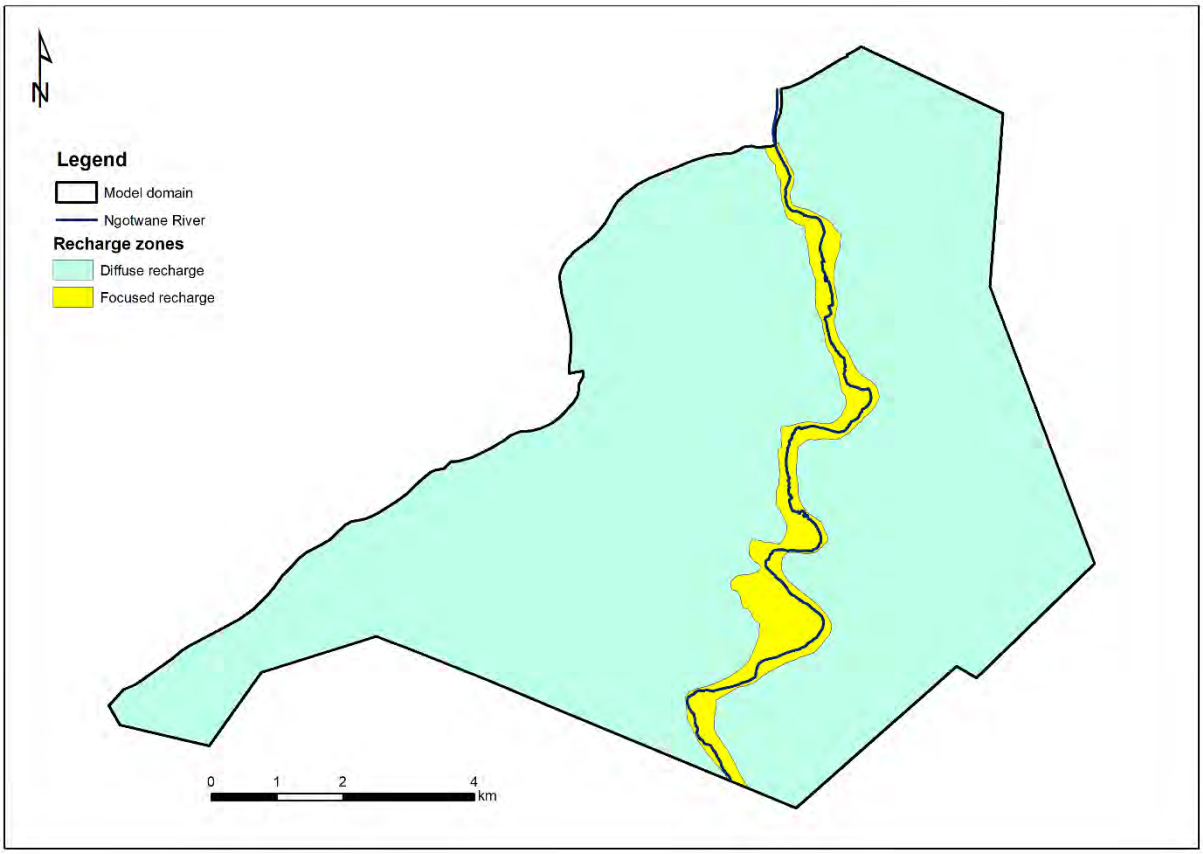

Figure 23: Recharge zones

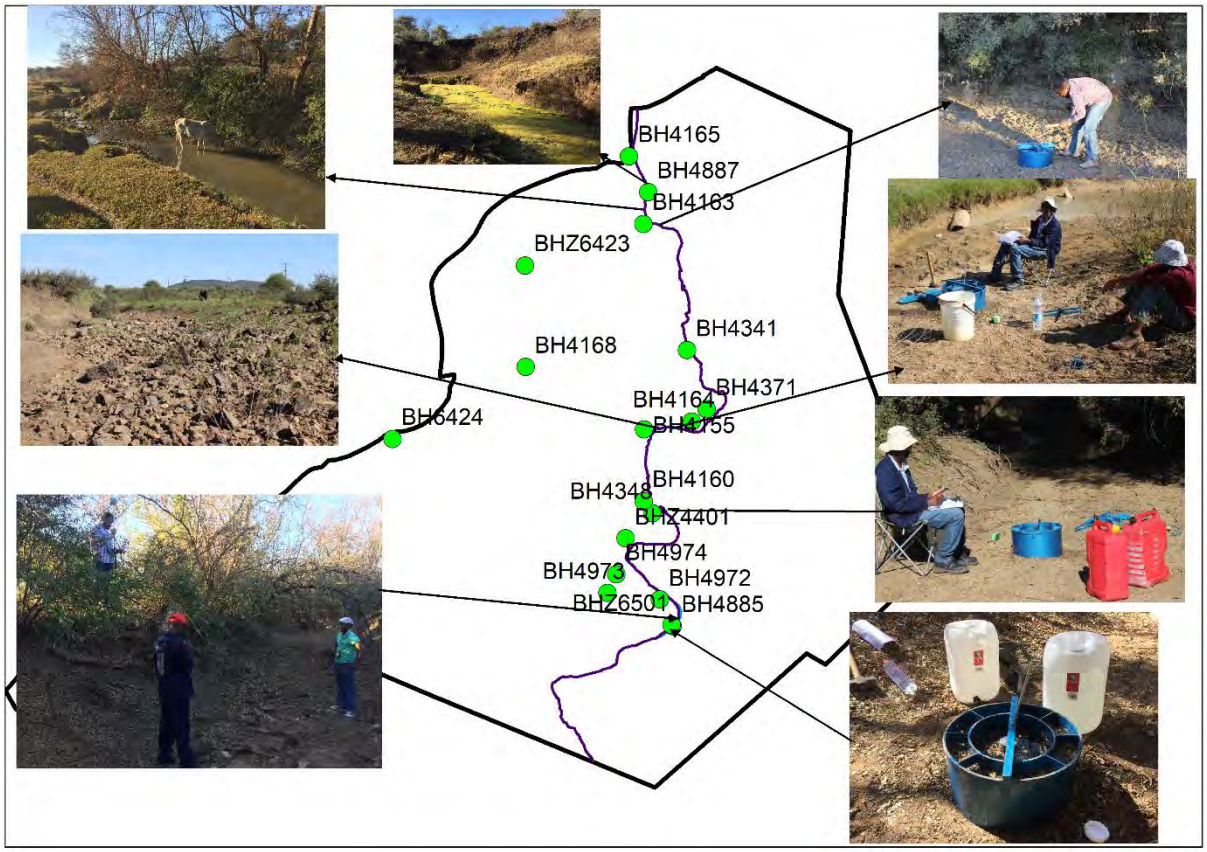

Figure 24: Riverbed sections at different river segments

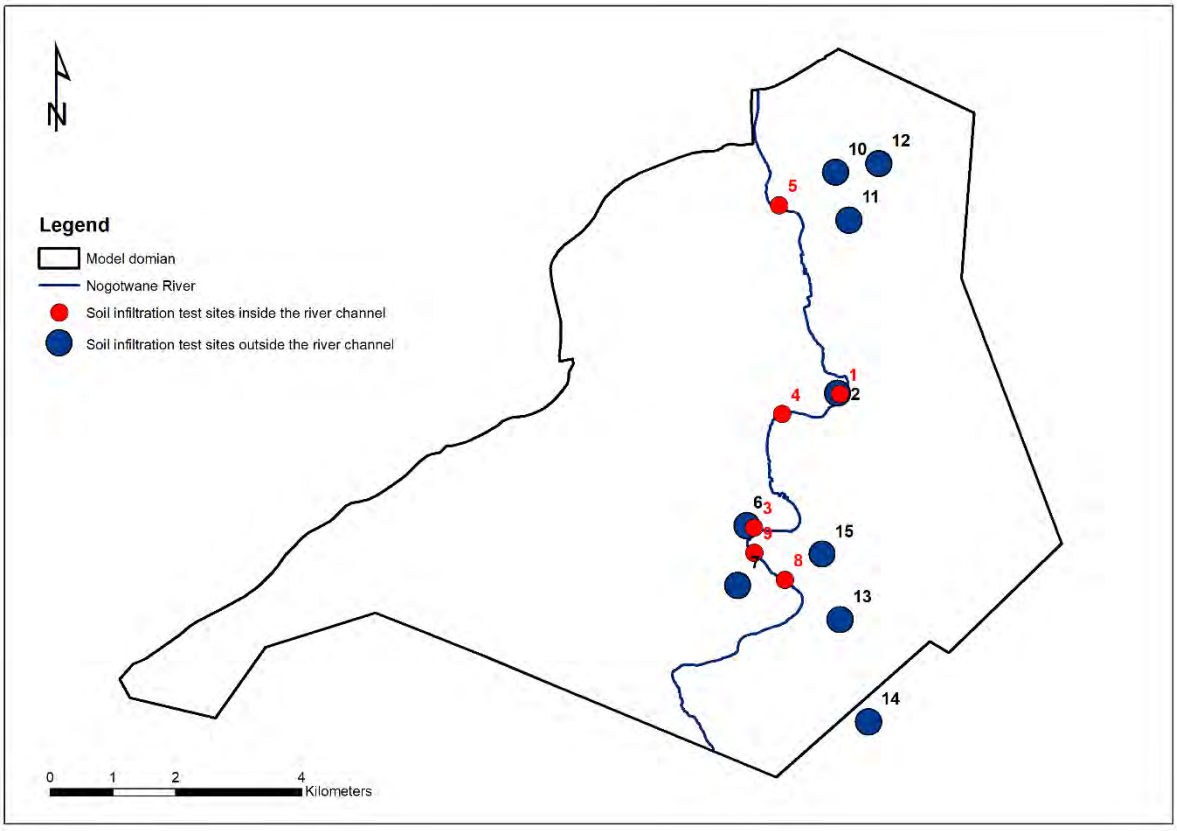

Figure 25: Soil infitration test sites in the Ramotswa aquifer (Labels in the dot corssponds to site ID in Table 5)

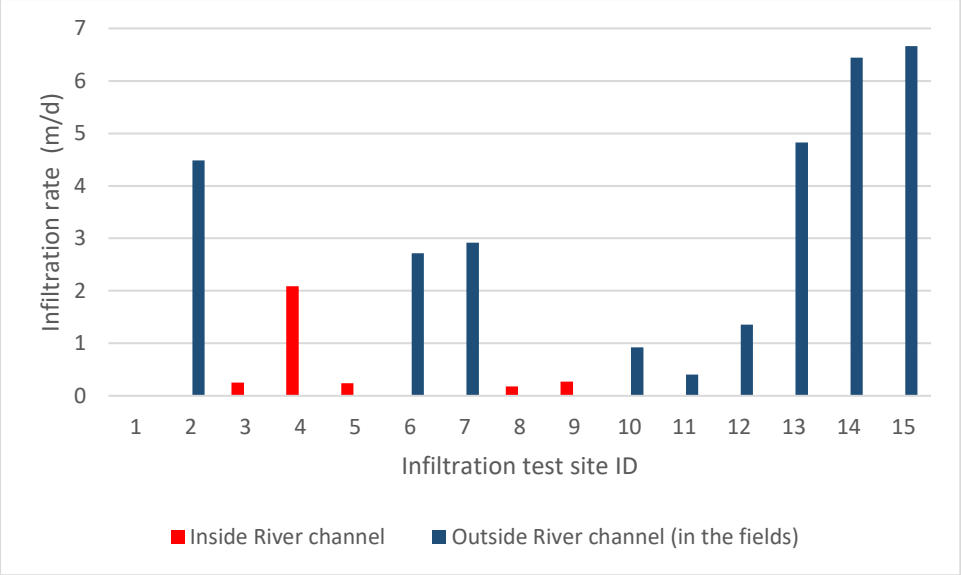

Figure 26: Double ring infiltrometer soil infiltration test results in Ramotswa

4.4.10 Groundwater discharge to the River

Quantifying river-aquifer interaction in ephemeral streams is the most difficult and uncertain. Different studies have used different approaches to model the stream-aquifer interaction in ephemeral streams. Varalakshmi et al. (2012) used the River Package of MODFLOW, to simulate stream-aquifer interaction. Burns et al. (2012) and Ruhl and Cowdery (2004) used the Drain Package of MODFLOW to simulate groundwater discharge to ephemeral streams. The Drain Package was initially developed to simulate agricultural drains that removes water from an aquifer at a rate proportional to the difference in water level between the aquifer and drain elevation. When the groundwater level exceeds the ephemeral stream bed elevation, an outflow is simulated; otherwise no recharge is simulated from the ephemeral stream to the aquifer. Stream flow packages (Niswonger and Prudic, 2005; Prudic, 1989; Prudic et al., 2004) were developed and incorporated into MODFLOW to simulate river –aquifer interactions. Although these packages simulate river-aquifer interaction better than the Drain Package, they require more data including inflow data from upstream reaches, riverbed hydraulic conductivity, Manning roughness coefficient, river channel geometry and surface runoff to each river segment, which is not available in our case. Therefore, for the present study we used the Drain Package and simulated groundwater discharge to the ephemeral Ngotwane River and used separately specified recharge along the stream to account for focused recharge.

For the Drain Package, river bed elevation was determined from nine river cross-sections surveyed using DGPS. River bed elevation obtained using the DGPS was correlated to elevation from SRTM 30 x 30 m and applied to cells defining the river channel. This is because, the drain elevation need to be specified at river cell and the DGPS points are not enough to make interpolation. The conductance term in the Drain Package was determined using model calibration. Previous studies (e.g. GCS, 2000) used Drain Package to simulate groundwater discharge to the river.

5. Model Calibration

Model calibration is the process of reproducing the field measured groundwater levels. The calibration process entails: 1) defining calibration target, calibration parameters and initial values, 2) sensitivity

analysis to determine the most sensitive parameters for model calibration, 3) steady state model calibration, and 4) transient model calibration and validation.

5.1 Calibration target

Groundwater level data available for the period 2000-2012 and 2015-2017were used as calibration targets. During the period 2012-2014, water level monitoring stopped for a while due to reform in the water sector (email communication, Alfred Petros, 2017, DWA, Botswana). Water level data are available starting from March 2015 however the data till late November 2016 are not reliable because the technician who were responsible for monitoring water level, was not following the correct procedure; in some instance the instrument malfunctioned (personal communication, Phemelo Makoba, 2018, DWA, Botswana). During the period 2000-2012, there is no pumping in the Ramotswa wellfield. The wellfield was closed due to elevated nitrate in 1996. Wellfield operation re-started sometime in 2014 and abstraction data is available from March 2015-2017 from WUC, Botswana. Figure 27 shows the spatial location of observation wells used for model calibration and Table 3 presents the coordinate and ground elevation, casing height and distance of each observation well from the Ngotwane River. In total, 17 observation wells were used for model calibration and validation. As can be seen in Figure 27 and Table 3, nine out of the 17 observation wells are located within 100 m distance of the river. No production boreholes (Figure 18) were used as observation wells, due to the influence of the pumping on the groundwater level. Due to better spatial density of observation wells in the vicinity of the river we believe that the river-aquifer interaction parameters could be adequately represented during the model calibration.

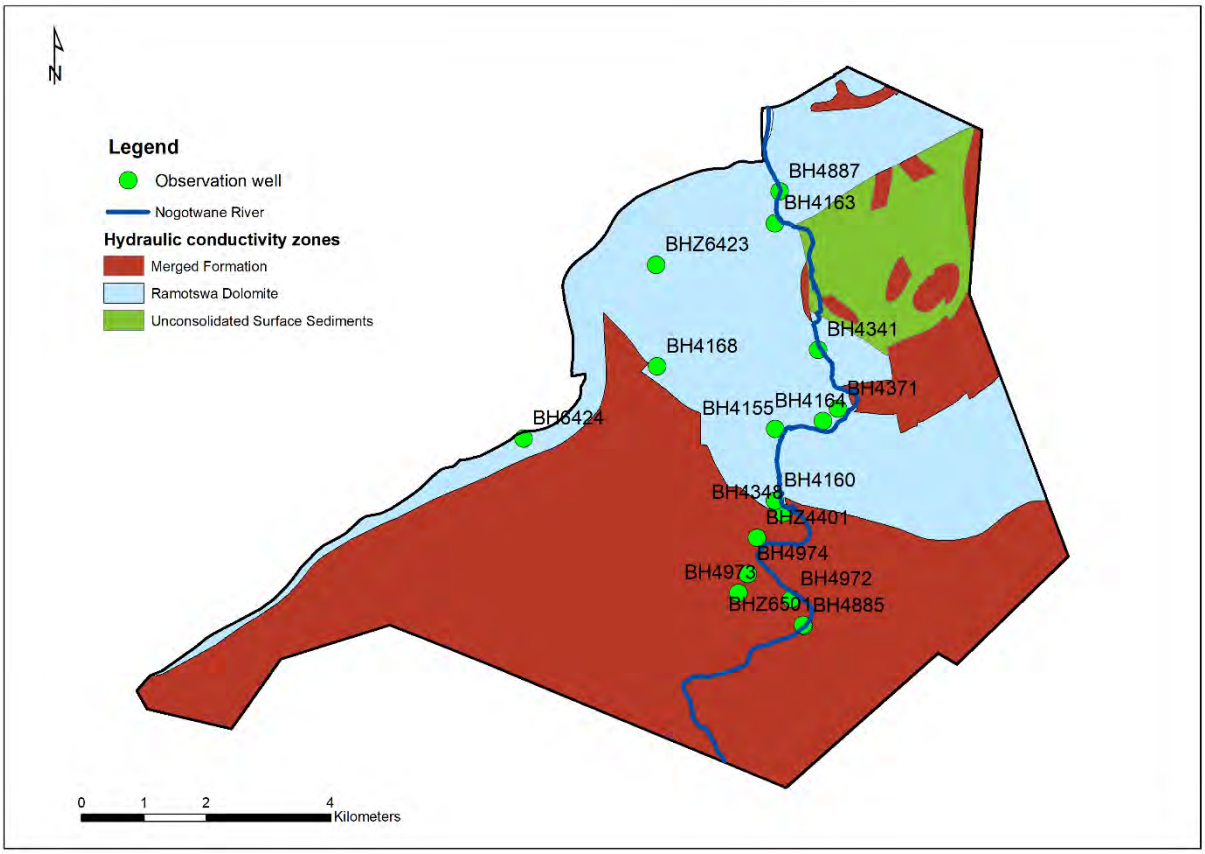

Figure 27: Hydraulic conductivity zones and location of 17 observation wells used for model calibration and validation

Table 3: Observation wells used for model calibration and validation, giving location and elevation obtained using the differential GPS survey (projection system WGS UTM 35S), casing height measured during the survey and distance of each observation well from Ngotwane River calculated using the Near tool in ArcGIS. Depth to groundwater is usually measured from the top of the casing hence the acsing height need to be deducted to obtain actual groundwater below the ground surface

Observation well name	X coordinate (m)	Y coordinate (m)	Elevation (m)	Casing height above ground (m)	Distance to the Ngotwane River (m)
BH4887	386522.601	7250870.869	1015.540	0.435	13.7
BH4885	386913.669	7243893.643	1027.930	0.290	21.6
BHZ6501	386898.503	7243911.384	1027.940	0.410	44.5
BH4341	387143.766	7248328.829	1019.810	0.299	44.9
BH4160	386447.044	7245903.542	1027.680	0.461	92.9
BH4348	386587.348	7245709.627	1025.200	0.251	96.0
BH4163	386446.784	7250359.809	1019.140	0.512	97.7
BH4972	386711.351	7244321.073	1027.090	0.140	100.9
BH4155	386452.467	7247057.822	1024.240	0.403	153.2
BH4164	387222.628	7247183.051	1024.310	0.222	161.4
BHZ4401	386158.085	7245305.574	1025.720	0.745	163.6
BH4371	387461.964	7247381.082	1023.340	0.559	168.9
BH4974	386009.640	7244727.478	1028.370	0.500	281.4
BH4973	385864.221	7244424.470	1032.230	0.580	598.0
BHZ6423	384536.293	7249692.121	1038.170	0.693	2105.5
BH4168	384552.502	7248059.391	1043.600	0.160	2298.8
BH6424	382405.417	7246903.687	1056.830	0.550	4089.6

5.2 Aquifer hydraulic properties

The magnitude and spatial distribution of aquifer properties such as hydraulic conductivity and storage coefficient (specific storage and specific yield) are required for the model. Hydraulic conductivity is one of the highly variable parameters in space. In most of the cases, our knowledge regarding the values of the hydraulic conductivity is limited to randomly located point measurements or no measurement at all. Initial estimates of the aquifer hydraulic properties were made based on past studies in the study area (WUC, 2014, DWA, 2006; Staudt, 2003, GCS, 2000, IoH, 1986; Selaolo, 1985) and other literature for karstic aquifer (Cobbing, 2018; Meyer, 2014). Initial horizontal hydraulic conductivity values were determined from pumping test data (DWA, 2006) (Table 3). Staudt (2003) reported transmissivity value of 1170 and 492m^2/d for the Ramotswa dolomite and Lephalale formation, respectively. The initial value of the hydraulic conductivity of the first layer was assumed to be half of the mean horizontal hydraulic conductivity determined from pumping test, while for second layer initial value was set equal to the mean value. This is because even if the upper layer is highly karstified compared to the lower layer the solution cavities are reported to be filled by mud or wad while the second layer cavities are open and generally do not contain mud or wad fillings (GCS, 2000).

The vertical and horizontal anisotropies were determined from literature values. Anisotropy is defined as having different properties in different direction. Anisotropy is commonly attributed to the presence of preferred flow directions along sub-parallel set of fractures in the rock (Kaehler and Hsieh, 1994). Vertical anisotropy is defined as hydraulic conductivity in the x-direction divided by z-direction

(kx/kz). Vertical anisotropy ratios commonly are on the order of 10:1 (horizontal to vertical direction) or greater (Tucci, 1997). As the vertical anisotropy ratio increase, the groundwater flow path increasingly deviate from the vertical direction. Horizontal anisotropy is the ratio of hydraulic conductivity along the x-direction to the y-direction (kx/ky). According to Tucci (1997), as horizontal anisotropy increases, flow pattern becomes increasingly skewed in the direction of maximum hydraulic conductivity. However, model calculated flow patterns may be insensitive to changes in anisotropy ratios beyond some threshold value that may be site dependent. In the present study, the initial value of vertical and horizontal anisotropy were assumed to be 10 and 1, respectively. The same values for anisotropy for the first and second layer were used. Staudt (2003) reported a storage coefficient of 5.7 $x10^{-2}$ for the Ramotswa dolomite and $8.7x10^{-4}$ for the Lephalal formation. Shevenell (1996) reported specific yield of 1 to $8X10^{-4}$ for conduit dominated karstic aquifer and 1 $x10^{-3}$ for the fractured dominated karst aquifer. A sensitivity analysis of these parameters is presented in the next section (Section 5.3).

Table 4: Hydraulic conductivity calculated from DWA 2006 pumping test results

BH No	Depth (m)	Water Strike (m)	Water Level (at time of drilling) (m)	Estimated yield (at time of drilling) (m^3/hr	Transmissivity (T) (m^2/d)	Saturated thickness (b) (m)	K (T/b) (m/d)
4336	102	24 – 32, 45	14.32	24, 30	800	87.68	9.124
4337	118	36, 81 - 82	5.51	12, 90	500	112.5	4.444
4340	120	14, 30, 42	7.12	15	5	112.9	0.0442
4349	120	11, 37, 112	4	24	550	116	4.741
4358	102	45	8.05	15	8	94	0.085
4373	120	40, 56, 75, 96	7.09	90	14	113	0.0124
4422	120	70 - 72	4	50 – 60	12	116	0.013
4423	120	24 - 44	6	2	210	114	1.842
4400	102	47	6.1	150	500	96	5.208

Transmissivity values are from DWA 2006 (Evaluated hydraulic parameters from test pumping and step-drawdown testing (C-factor)

5.3 Sensitivity analysis

In this study, sensitivity analysis was carried out using PEST (described in Section 5.4). Sensitivity analysis is a procedure that evaluates the model sensitivity to variations in the input parameters. The procedure involves keeping all input parameters constant except for the one being analysed. Sensitivities are calculated as the derivatives of change in simulated head to change in parameter. According to Hill and Tiedeman (2006), since sensitivities are measured in units of the simulated value divided by the units of the parameters, both of which may vary considerably, it is important to compare the relative importance of different observations using a common scale. Composite scale sensitive parameter is one of the dimensionless sensitivity parameters that is used to determine the aggregate information provided by the observations for the estimation of one parameter (Hill and Tiedeman, 2006).

Twenty-three parameters were selected for the sensitivity analysis. It is important to note that during the sensitivity analysis, the parameter zonation defined based on geologic formation shown in Figure

28 was used. The parameters used in the sensitivity analysis were Recharge multiplier(multi1), horizontal hydraulic conductivity of merged/Lephalale formation in layer 1 (kh11) and layer 2 (kh12), horizontal hydraulic conductivity of dolomite formation in layer 1 (kh21) and layer 2 (kh22), horizontal hydraulic conductivity of unconsolidated sediment formation in layer 1 (kh31) and layer 2 (kh32), horizontal anisotropy of all formations for layer 1 (hani11) and layer 2 (hani12), vertical anisotropy of all formations for layer 1 (vani11) and layer 2 (vani12), specific storage of merged/Lephalle formation in layer 1 (ss11) and layer 2 (ss12), specific storage of dolomite formation in layer 1 (ss21) and layer 2 (ss22), specific storage of unconsolidated sediment formation in layer 1 (ss31) and layer 2 (ss32),), specific yield of merged/Lephalale formation in layer 1 (sy11) and layer 2 (sy12), specific yield of dolomite formation in layer 1 (sy21) and layer 2 (sy22), specific yield of unconsolidated sediment formation in layer 1 (sy31) and layer 2 (sy32),conductance term of the GHB (ghb_cond) and drain (drn_cond) and hydraulic characteristic of dikes (dyke_hydr).

During the sensitivity analysis, each parameter value was increased by 50% one at a time while keeping the other parameter values unchanged. The output from the sensitivity analysis was used to calculate the composite relative sensitivity (Figure 28). Recharge multiplier (multi1), hydraulic conductivity of the dolomite formation of the second layer (kh22) and hydraulic conductivity of the merged Lephalale formation of the second layer (kh12) were found to be very sensitive.

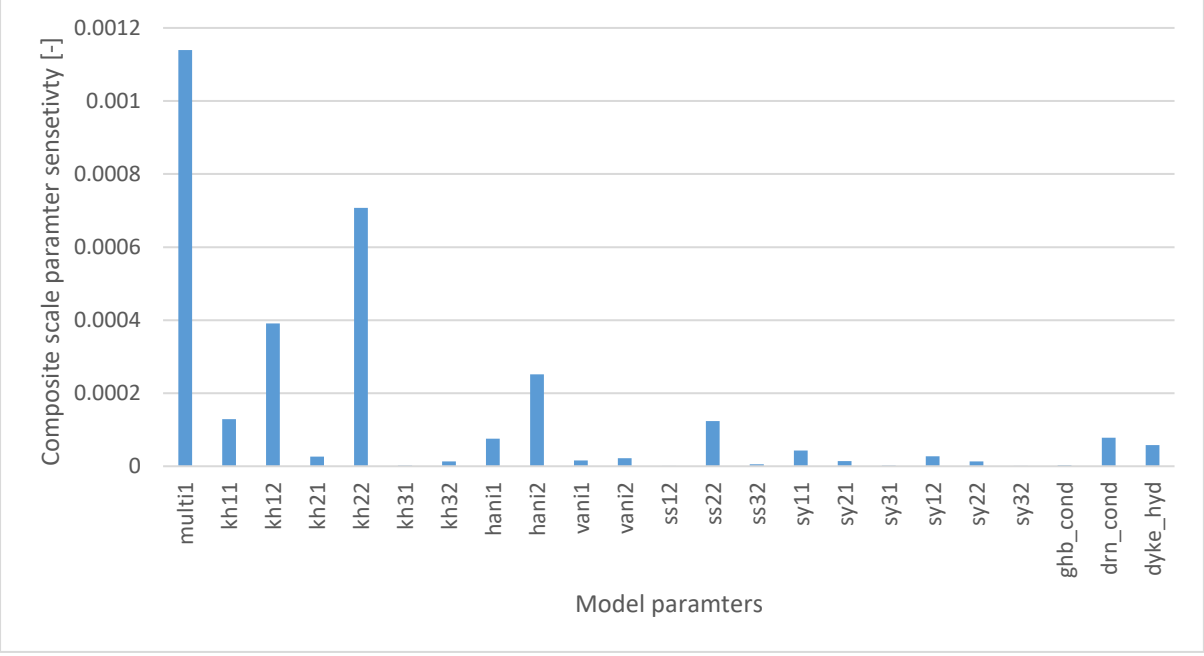

Figure 28: Composite-scaled parameter sensitivities calculated by PEST using water level data from 17 observation wells in the study area

5.4 Calibration approach

Steady sate and transient model automatic calibrations were performed using the automated parameter estimation code PEST (Doherty 2000). PEST is a model-independent non-linear parameter estimator. PEST automatically minimizes the sum of square errors using the Gauss-Marquardt-Levenberg optimization algorithm in a weighted least-square sense using the measured and simulated values (Equation 8). Since its inception in the mid-1900s, PEST has become the industrial standard in

the calibration of all kinds of environmental modelling problems (Doherty and Johnston, 2003). In the course of parameter estimation, PEST is required to run the model many times as part of the process of calculating the Jacobian matrix (i.e. the matrix of derivatives of observation with respect to parameter increment). During the optimization, observations were assumed to be of equal weight (equal importance in determining the optimization outcome).

$$\phi_k = \sum_{k=1}^{N_{pbs}} (w_k h_m{}^k - w_k h_s{}^k)^2 \quad (8)$$

Where ϕ is the objective function value, w_k is the weight applied to the difference between the measured (h^k_m) and simulated (h^k_s) parameter of the same type k, and N_{pbs} is the total number of measured parameter values of the same type.

The pilot point calibration approach (Doherty, 2003) was used to spatially vary and calibrate the most sensitive parameters. (Recharge multiplier (multi1) and horizontal hydraulic conductivity of dolomite formation in layer 1 (kh21) and layer 2 (kh22),) However, due to computational limitations, only hydraulic conductivities in both layers were calibrated using the pilot point approach. One of the advantages of the pilot point approach is that it does not require prior definition of zonation. The zonal method approach, which often used for hydrogeological model calibration, requires the model area to be divided into zones of uniform hydraulic parameters, and the parameters assigned to each zone is adjusted either manually or using automatic parameter estimation software until the error between observed and simulated heads are minimized. According to Doherty (2003), this approach has some shortcomings. First, this approach requires the delineation of zones of uniform hydraulic properties prior to parameter estimation. In most cases geological boundaries are only approximately know. Hence, modellers have to use trial and error to define as many zones as possible to obtain a good fit between the observed and simulated values. This approach is very laborious and time consuming. Furthermore, the final results may not be a true representation of the geological heterogeneity.

In a pilot point approach, the necessity to define a zonation scheme in advance of the parameter estimation process is removed. The approach allows the calibration process itself to decide where heterogeneity must exist within the model domain for model outcomes to match field measurements. This approach is more likely to approximate geological reality than a distribution based on pre-determined zones of piecewise hydraulic property uniformity (Doherty, 2003). In the pilot point approach, hydraulic property values are assigned to a set of points distributed throughout the model domain rather than directly to the grid of a numerical model. Property values are then assigned to model grids through spatial interpolation from the pilot point to the grid. This results a smooth variation of the hydraulic property over the model domain. Parameters estimated through the model calibration process are the hydraulic property values assigned to the pilot points. As normal calibration practice, the assignment of parameters to these pilot points is done in a way that minimizes the discrepancies between model outputs and field measurements. Kriging is used for spatial interpolation from pilot point location to the model grid or mesh.

5.5 Steady state model calibration

The steady state flow model was calibrated using long-term average water level data [2000-2012] measured in 17 observation wells. This period was selected because there was no pumping during this

period and hence groundwater levels are assumed to represent quasi-equilibrium conditions. During model calibration, parameter values were adjusted until the simulated water level matched the observed values.

Table 5 presents the selected calibration parameters and their calibrated values for the steady state model. Both manual and automatic calibrations were used for calibration. Pilot point calibration points (n=81) were used to calibrate the hydraulic conductivity of layer 1 and layer 2 (Figure 29-30). Recharge in two zones (diffuse recharge from rainfall away from river) and focused recharge in the river and along the flood plain, drain conductance, dyke hydraulic characterises and GHB conductance were included in the calibration, but assuming that they are spatially uniform. Steady state calibration results provided a very good fit for the long-term average water level in 17 observation wells (Root Mean Square Error (RMSE)=1.2192]. However, the calibrated rainfall multiplier for the two zones were 0.044 for the diffuse recharge and 1E-3 for the river channel and flood plain. This result seems unrealistic. The results along the river and flood plain should be at least equal or greater than the recharge from the rainfall that occur diffusively. Also, the water level along the river (as indicated in the observation wells) specifically show underestimation during the transient model run, which leads us to the manual calibration of recharge multiplier for the section along the river. By manual calibration, we found a recharge multiplier of 0.18 with a comparable value of RMSE (1.441).

Table 5: Parameters selected for steady state model calibration and their calibrated values. Hydraulic conductivity of layer 1 and layer 2 were calibrated using the pilot point and other parameters were calibrated assuming spatially uniform.

Parameter	Units	Initial	Lower bound	Upper bound	Calibrated value	Parameter zone
kh11*	m/d		0.01	5.00	Pilot point	Layer 1 Lephalale and merged formation
kh21	m/d		0.01	10.00	Pilot point	Layer 1 dolomite formation
kh31	m/d		0.01	10.00	Pilot point	Layer 1: unconsolidated sediment
kh12	m/d		0.01	5.00	Pilot point	Layer 2 Lephalale and merged formation
kh22	m/d		0.01	10.00	Pilot point	Layer 2 dolomite formation
kh32	m/d		0.01	10.00	Pilot point	Layer 2: unconsolidated sediment
hani1	(-)	1	0.01	10.00	1.80513	Layer1
hani2	(-)	1	0.01	10.00	5.27761	Layer 2
vani1	(-)	10	1.00	20.00	9.96671	Layer 1
vani2	(-)	10	1.00	20.00	9.83645	Layer 2
rch multi1	(-)	0.0345	0.01	0.3	0.0441	Recharge multiplier from rainfall

rch multi2	(-)	0.0345	0.01	0.3	0.001	Recharge multiplier along the river and flood plain
drain cond1	m^2/d	535	10.00	1.00×10^3	535	Drain conductance dolomite formation
drain cond1	m^2/d	535	10.00	1.00×10^3	535	Drain conductance Lephalale formation
GHB cond	m^2/d	2666	10.00	1.00×10^3	2666	GHB conductance
Dike hydr	1/d	1.00×10^{-5}	1.00×10^{-10}	1.00×10^{-3}	4.253×10^{-10}	Dike hydraulic characteristics

**Hydraulic conductivity for both layer 1 and layer 2 were calibrated in steady state model using pilot point. However, in the pilot point calibration initial parameter values can be defined using zones. Hence we use the three zones classified based on geology to constrain the lower and upper bound of parameter variation.*

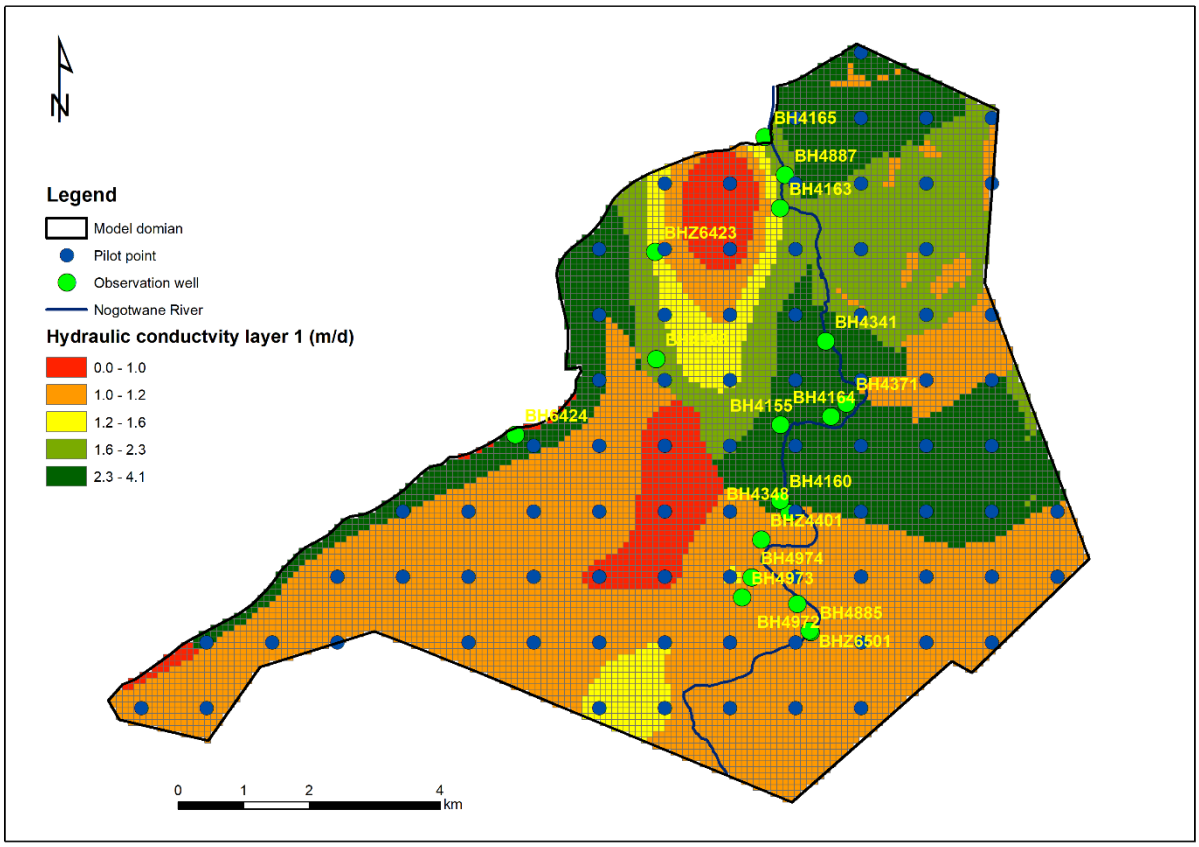

Figure 29: Hydraulic conductivity for layer 1, calibrated using plot point calibration method

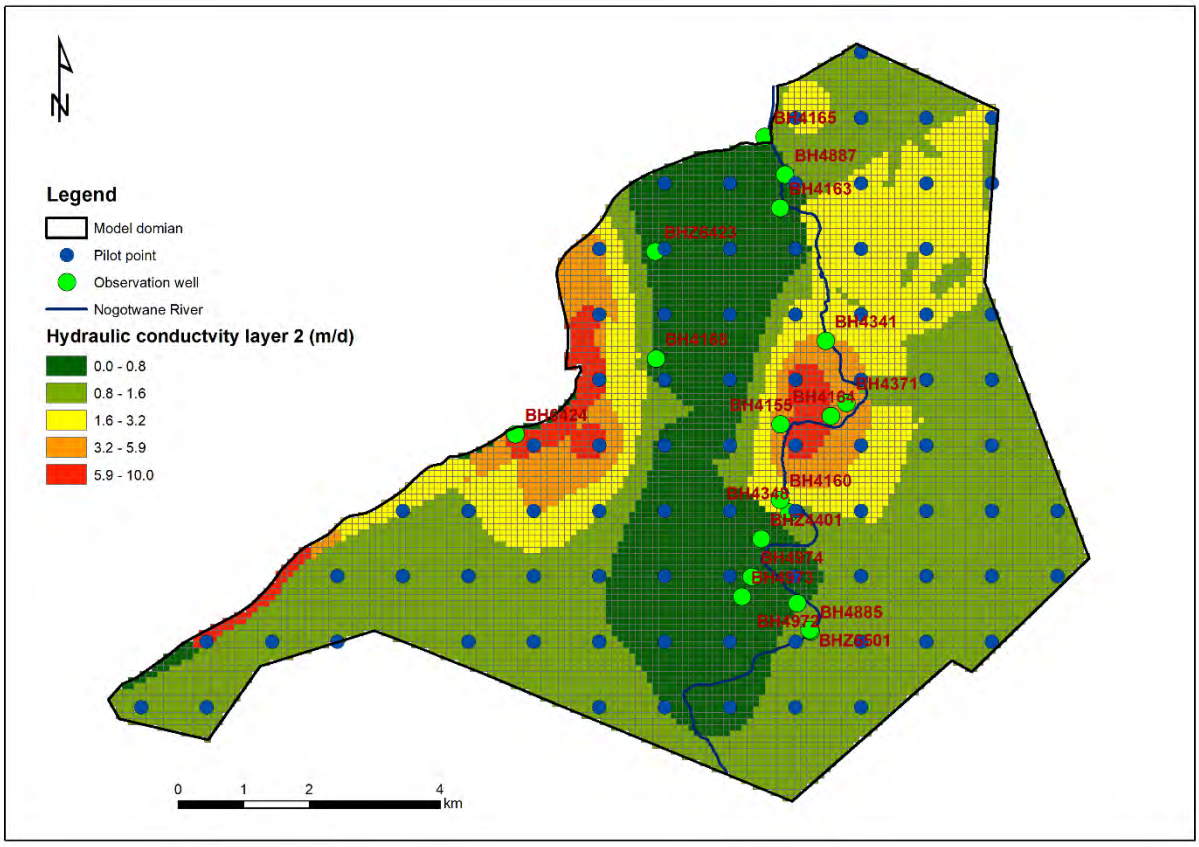

Figure 30: Hydraulic conductivity for layer 2, calibrated using plot point calibration method

5.6 Transient model calibration and validation

The 18 year simulation period [2000-2017] need to be divided into the calibration and validation period. Based on data availability, the period 2000-2008 were selected as a calibration period and 2009-2012 as validation period. However, the recent water level data for the year 2017 were used as post-validation, as this period includes pumping from the wellfield unlike the previous periods. During transient model calibration, only parameters related to storage and recharge were calibrated. As shown in Figure 31, five zones were defined to account for the spatial variation in storage related parameters representing: 1) Zone representing Lephalale and all other geological formations lumped along with it, 2) Zone represented by Ramotswa dolomite. No distinction in the dolomite lithological classes were made. 3) Zone representing areas covered by unconsolidated sediments, 4) Areas along the Ngotwane river cutting through the dolomite formation, which is highly karstified due to shallow water level. 5) Areas along the Ngotwane River cutting through the Lephalale formation, representing fissured zone. The zone along the river was digitized from Google Earth assumed flooding area. Flood marks observed during the field visit were used as supplemental information. Fifteen selected parameters for transient model calibration and final calibrated values are presented in Table6.

Selaolo (1985) estimated sotrativity value of 0.03 for dolomite formation while the Institute of hydrology (IoH, 1986) reported sorativity value of one order of magnitude less for the same formation which is 0.003. Based on these two studies GCS (2000) adopted an average value, which is 0.01 for the dolomite formation. The Storativity values of dolomite formations reported for Grootfontein area, South Africa were 0.025 for Oakatree dolomite formation, 0.008 for Monte Christo and Lyttleton dolomite formation and 0.12 for Eccles dolomite formation (DWAF, 2006). According to Cobbing

(2018) and reference cited therein, the most common value of specific yield in dolomitic aquifer is 2-4%, but it can have a value as high as 18%. We found specific yield of 2.88% for the first layer and 2.99 for the second layer of the dolomite formation. Which shows that our calibrated value are within the range of what is found in similar aquifer.

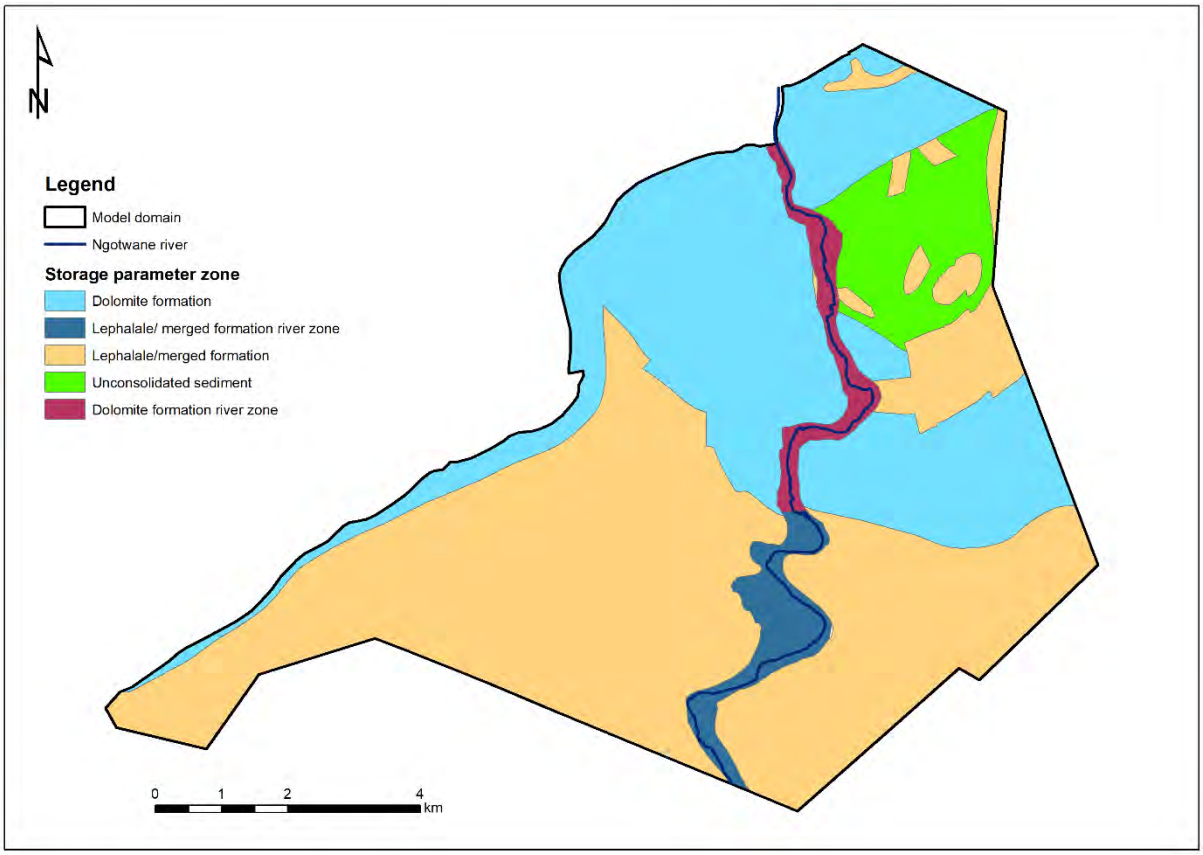

Figure 31: Storage parameter zones

Table 6: Parameters selected for transient model calibration and their calibrated values

Parameter	Units	Initial	Lower bound	Upper bound	Calibrated value	Parameter zone
sy11	(-)	0.05	0.01	0.20	1.00 x10^{-4}	Layer 1 Lephalale and merged formation
sy21	(-)	0.10	0.01	0.20	2.88 x10^{-2}	Layer 1 dolomite formation
sy31	(-)	0.20	0.01	0.30	0.15	Layer 1: unconsolidated sediment
sy12	(-)	0.06	0.01	0.20	1.47 x10^{-2}	Layer 1 Lephalale and merged formation
sy22	(-)	0.08	0.01	0.20	2.99 x10^{-2}	Layer 1 dolomite formation
sy32	(-)	0.12	0.01	0.20	0.100	Layer 1: unconsolidated sediment

sy41	(-)	0.0635	0.001	0.20	6.35×10^{-2}	Along river channel layer 1 dolomite formation
sy51	(-)	0.00657	0.0001	0.20	1.08×10^{-2}	Along river channel layer 1 Lephalale formation
ss12	(1/m)	1.00×10^{-4}	1.00×10^{-7}	5.00×10^{-3}	6.34×10^{-5}	Layer 2 Lephalale and merged formation
ss22	(1/m)	7.00×10^{-4}	1.00×10^{-7}	5.00×10^{-3}	3.60×10^{-6}	Layer 2 dolomite formation
ss32	(1/m)	1.00×10^{-3}	1.00×10^{-7}	5.00×10^{-3}	5.00×10^{-3}	Layer 2: unconsolidated sediment
ss42	(1/m)	3.04×10^{-5}	1.00×10^{-7}	5.00×10^{-3}	8.23×10^{-5}	Along river channel layer 1 dolomite formation
ss52	(1/m)	2.36×10^{-5}	1.00×10^{-7}	5.00×10^{-3}	4.17×10^{-3}	Along river channel layer 1 Lephalale formation
rch multi1	(-)	0.044	0.01	0.3	0.055	Recharge multiplier from rainfall
rch multi2	(-)	0.18	0.01	0.5	0.180	Recharge multiplier along the river and flood plain

6. Results

6.1 Steady State Model Calibration Results

Figure 32 shows residual between observed and simulated water levels for the steady state model. Figure 33 shows scatter plot of observed and simulated water levels. The obtained pattern of simulated water level contours is presented in Figure 34. In general, good correlations between the observed and simulated groundwater levels were obtained (R^2=0.94). The RMSE between the observed and simulated groundwater level values was 1.441. The simulated water level contours are also consistence with the observed overall regional groundwater flow direction (Figure 14). As indicated in Figure 33, the model simulation very much underestimate water level at observation well BH6423 (large blue dot in Figure 34). Local scale heterogeneity in aquifer property and spatial variability in recharge could be the reason for the underestimation. The residuals are randomly distributed, which is a good indication for good calibration (Figure 34).

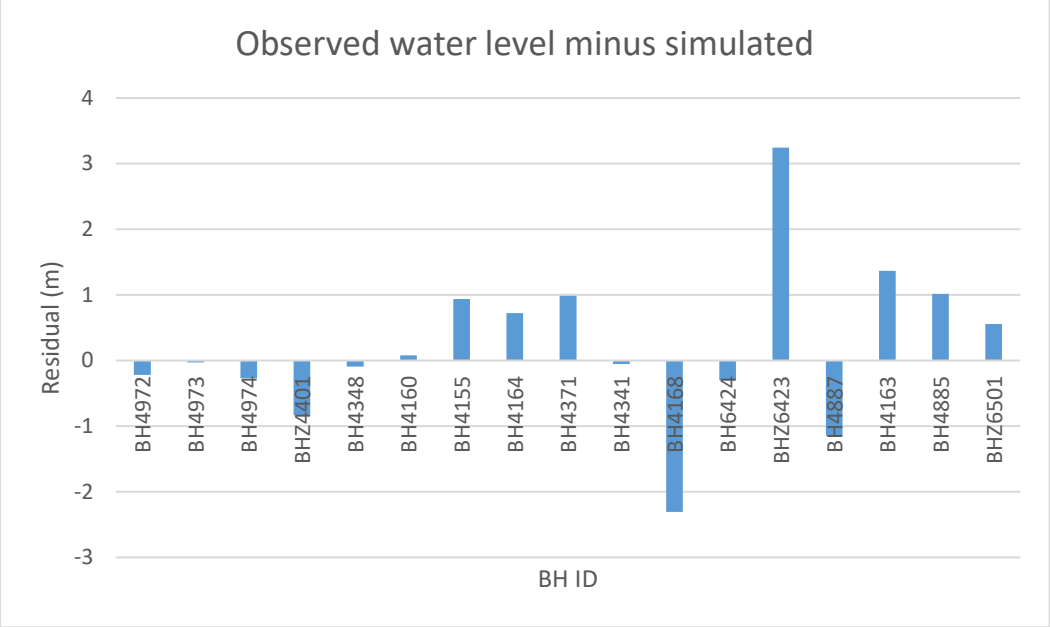

Figure 32: Steady state model calibration, residual in water level (observed minus simulated), RMSE=1.441

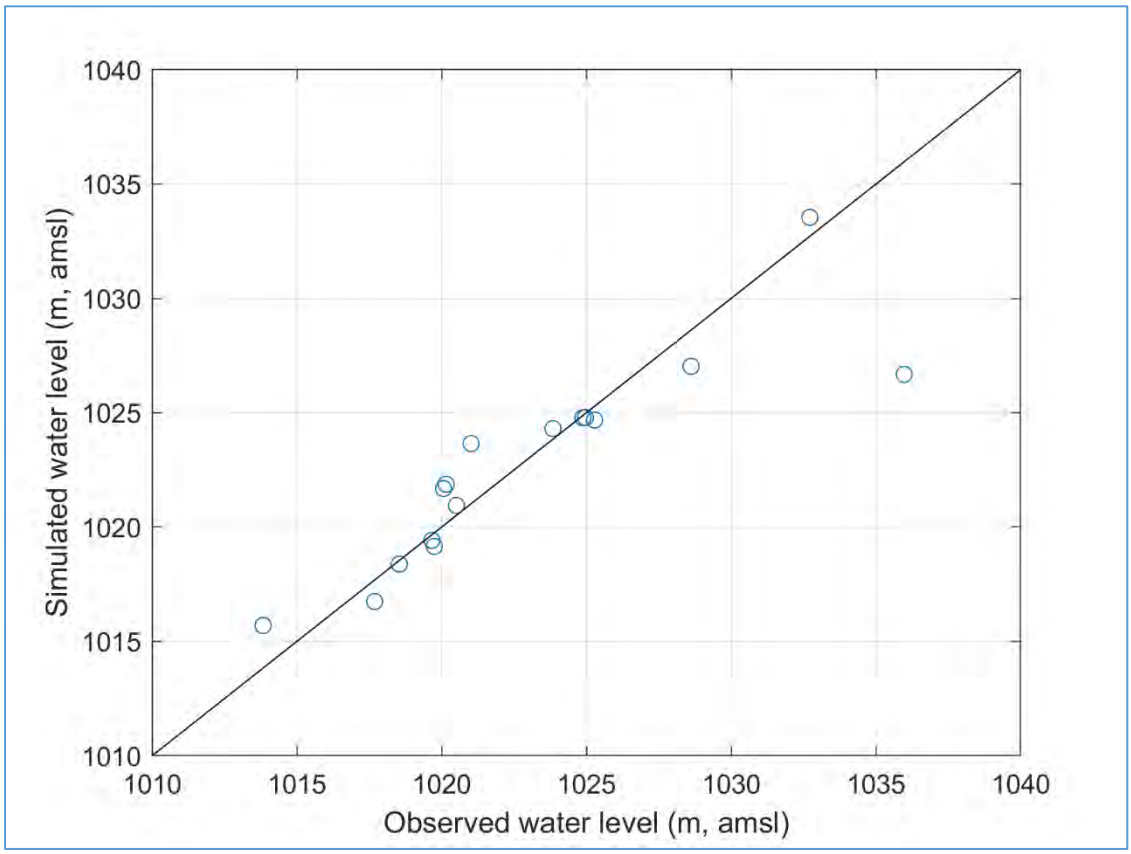

Figure 33: Observed vs simulated water level scatter plot, steady state model calibration.

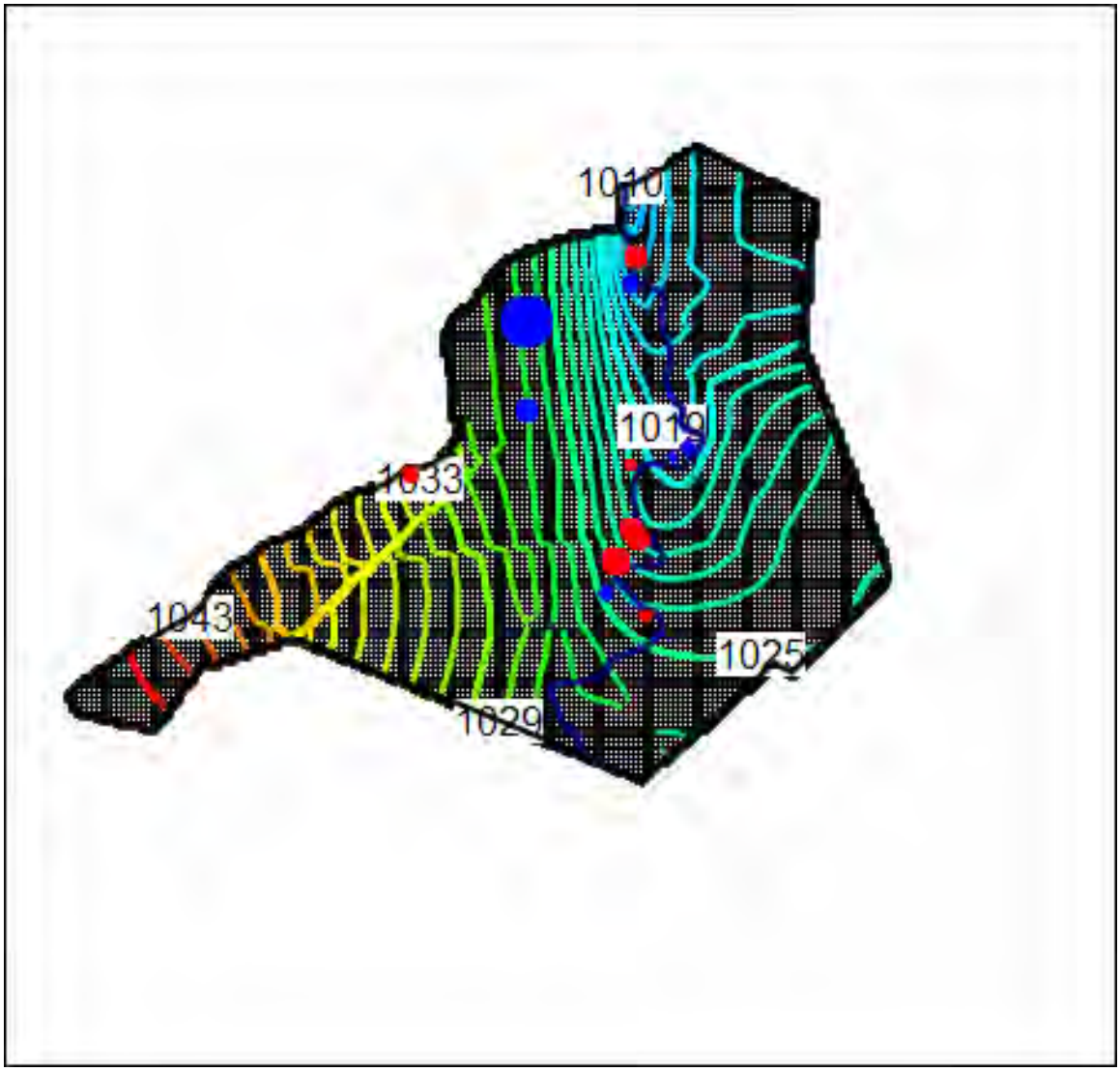

Figure 34: Steady state head distribution from the second model layer (simulated head lower than observed is shown in blue dot, while the red dots show areas where simulated head is higher than the observed value. The size of the dot represent the residual difference)

6.2 Transient Model calibration Results

The time series of groundwater levels from the transient model calibration are presented in Figures 35-42. Figure 43 shows water level scatter plot for year 2017 simulation which is used as post verification period. The MAE and RMSE between the observed and simulated water level for calibration period were 1.35 and 1.74 m respectively. The MAE and RMSE during the validation period were 1.54 and 2.28 m respectively. Figure 44 shows the MAE and RMSE for calibration and validation period each observation wells. The MAE and RMSE are reasonably good. The transient model is able to produce the trend in groundwater level, however the simulated groundwater dynamics in relatively small compared to the observation. Possible reason for the lack of dynamics in the simulated water levels is provided in the discussion section.

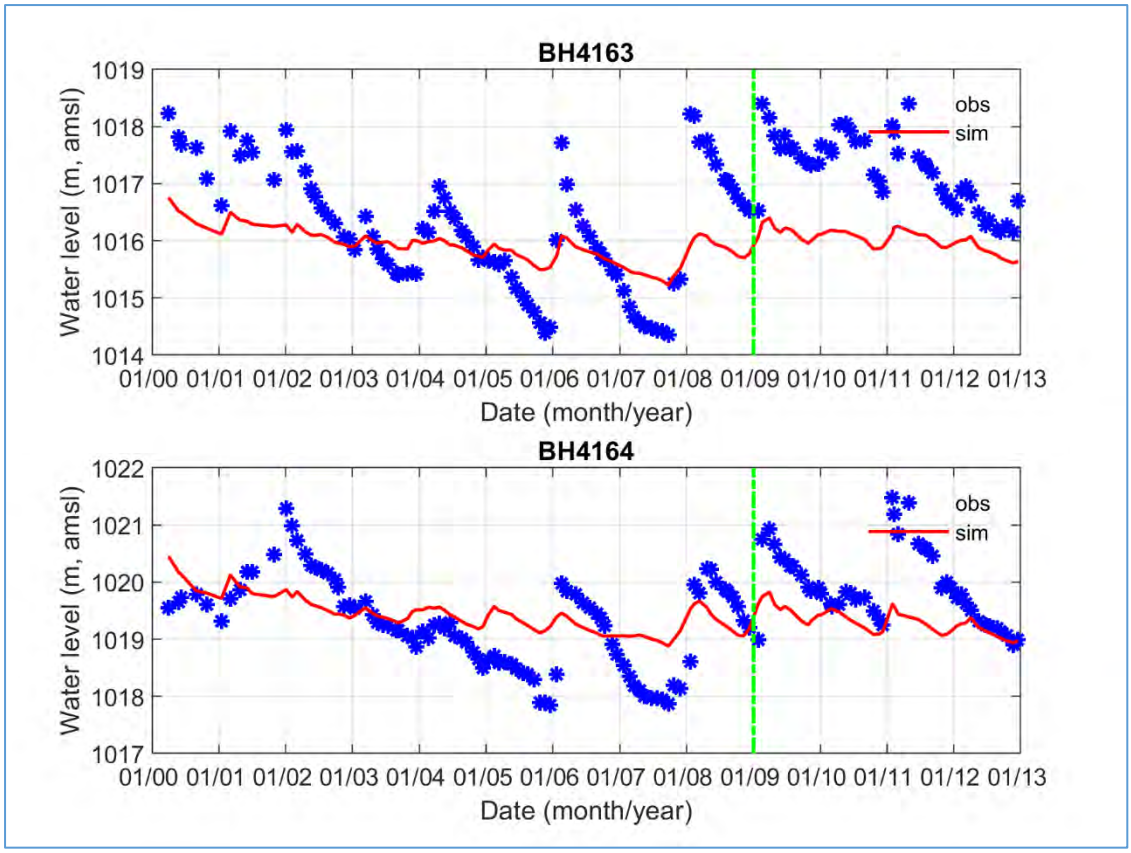

Figure 35: Observed and simulated water levels for BH4163 and BH4164, the latter from the calibrated transient model (vertical broken green line separates the calibration and validation period)

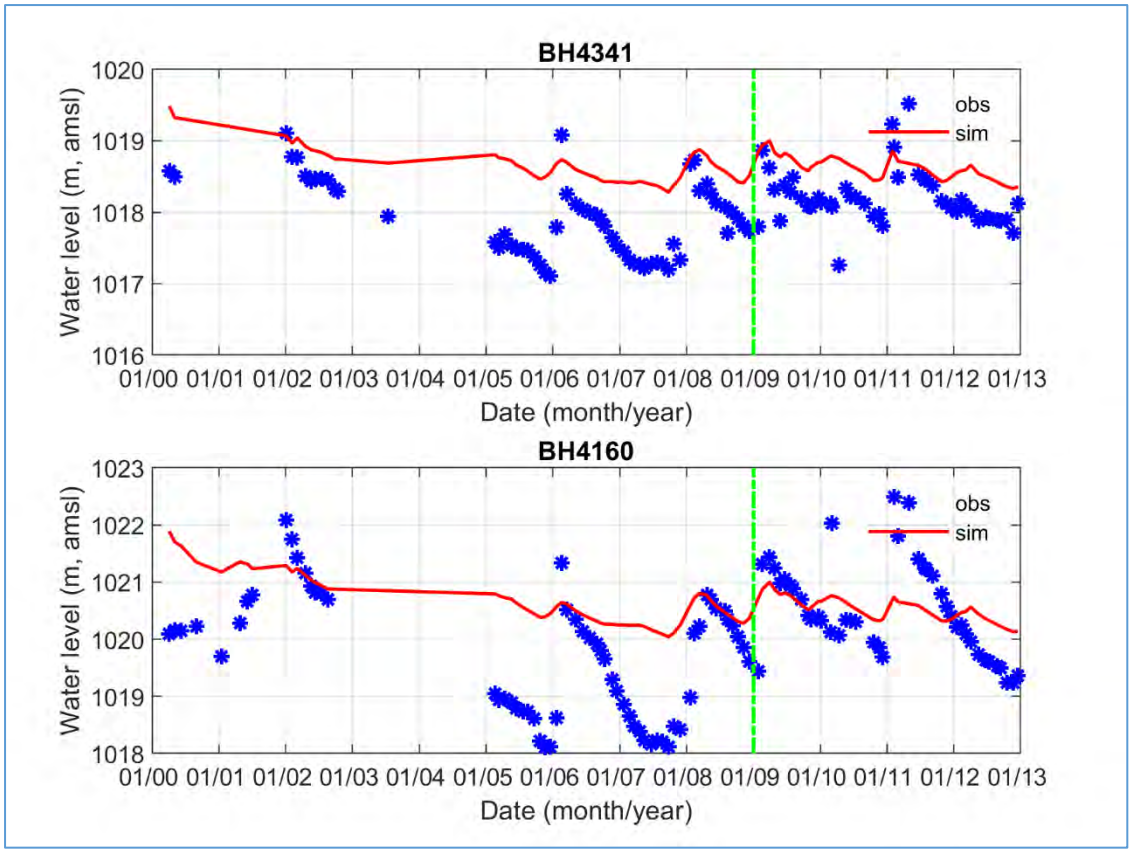

Figure 36: Observed and simulated water levels for BH4341 and BH4160, the latter from the calibrated transient model (vertical broken green line separates the calibration and validation period)

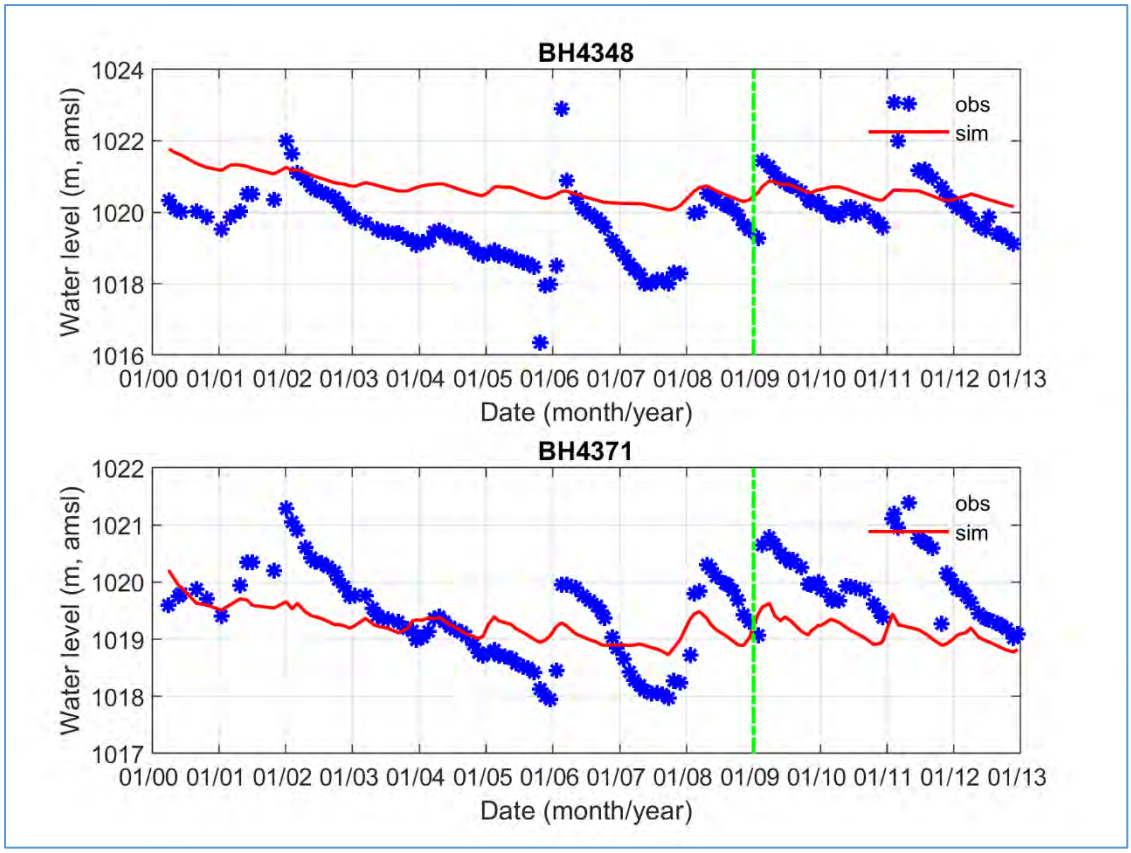

Figure 37: Observed and simulated water levels for BH44348 and BH4371, the latter from the calibrated transient model (vertical broken green line separates the calibration and validation period)

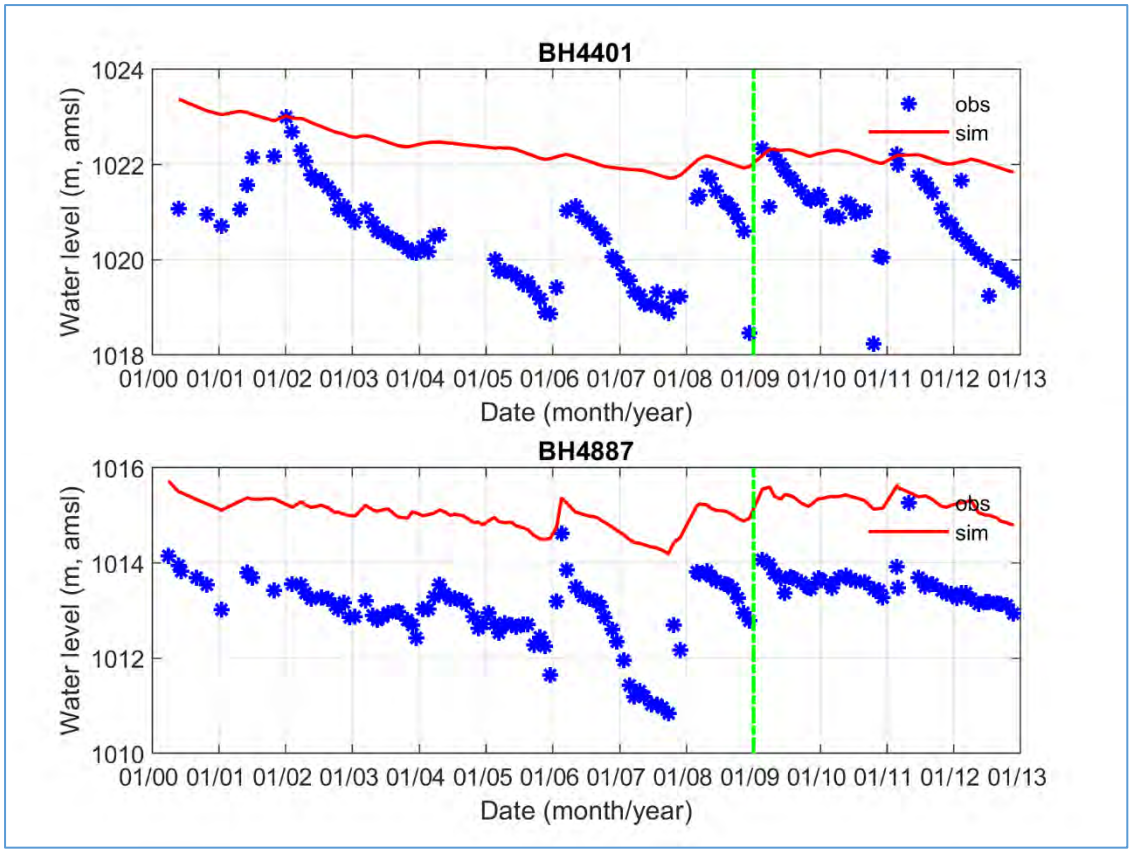

Figure 38: Observed and simulated water levels for BH4401 and BH4887, the latter from the calibrated transient model (vertical broken green line separates the calibration and validation period)

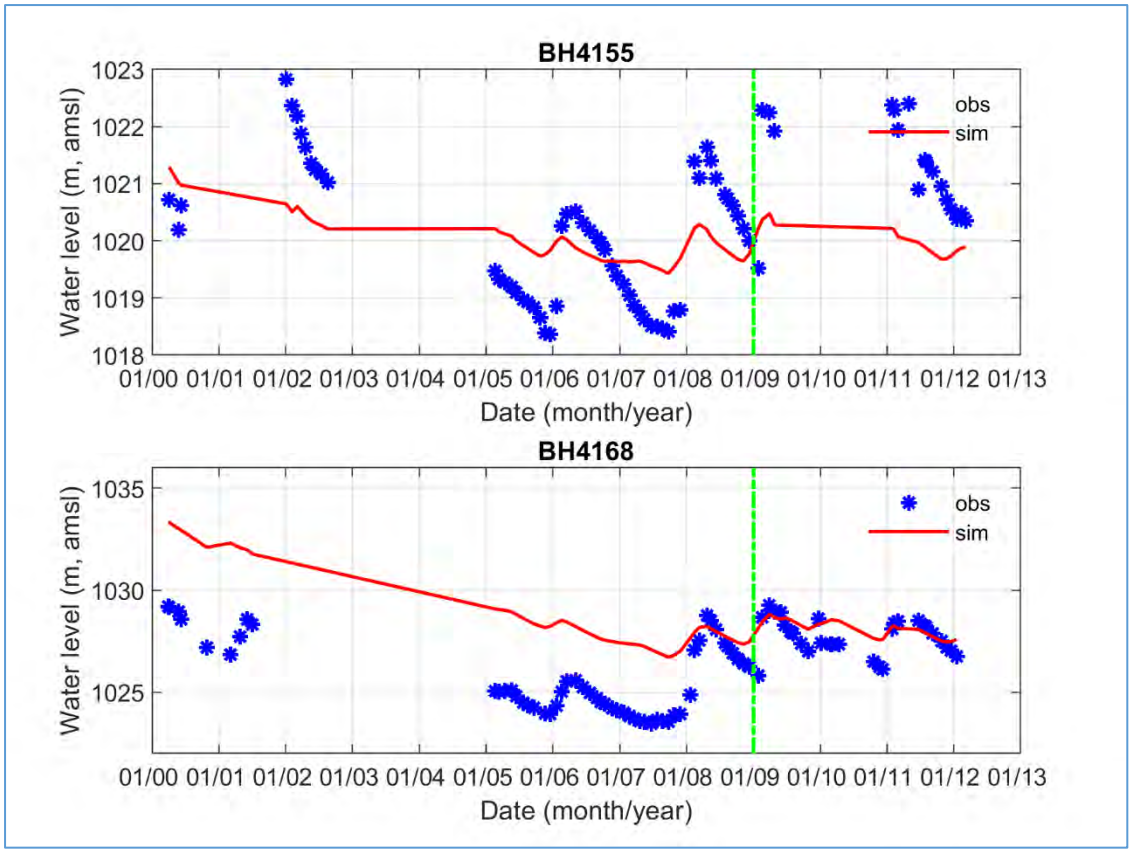

Figure 39: Observed and simulated water levels for BH4155 and BH4168, the latter from the calibrated transient model (vertical broken green line separates the calibration and validation period)

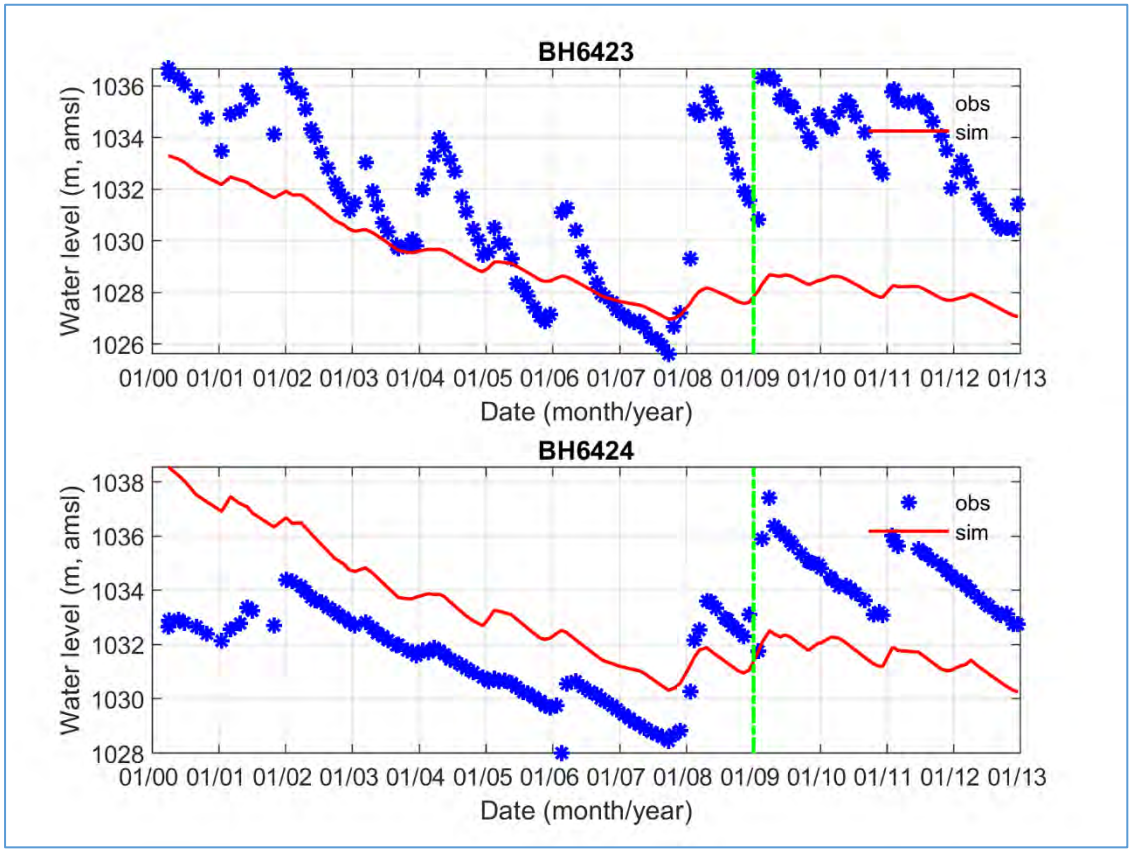

Figure 40: Observed and simulated water levels for BH6423 and BH6424, the latter from the calibrated transient model (vertical broken green line separates the calibration and validation period)

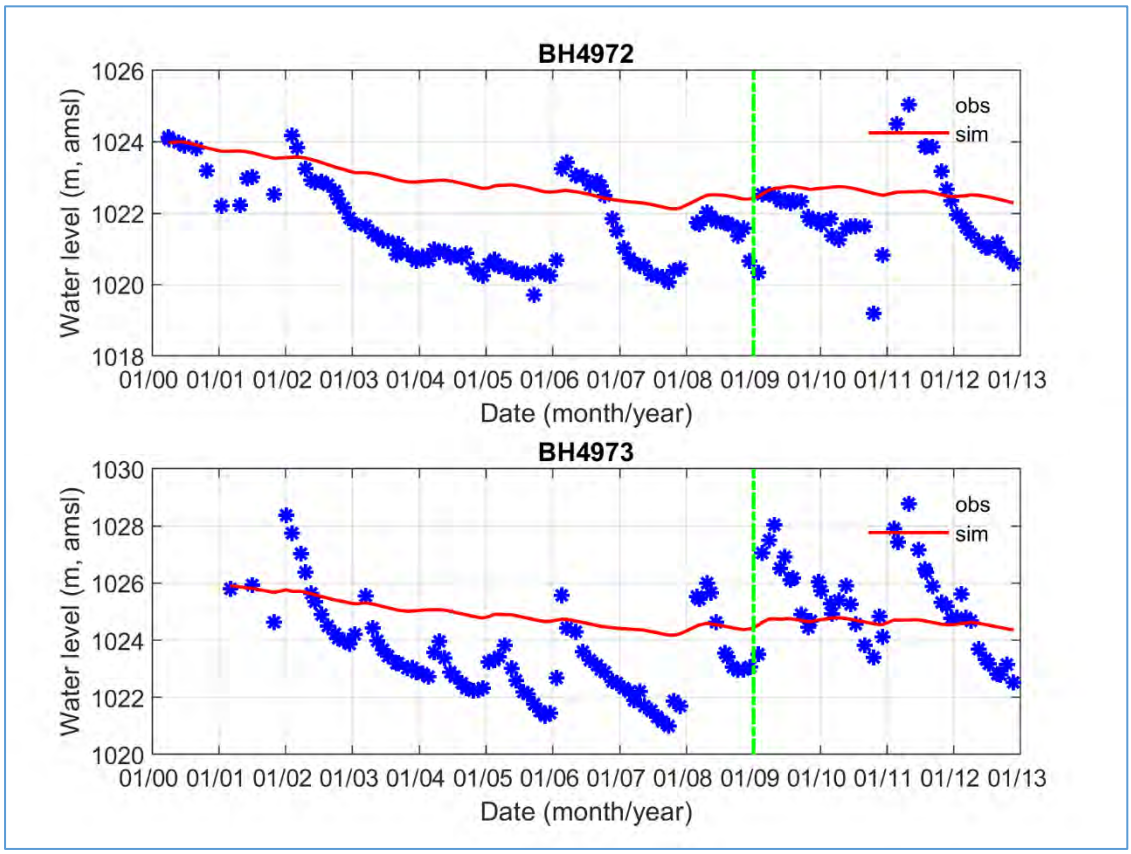

Figure 41: Observed and simulated water levels for BH4972 and BH4973, the latter from the calibrated transient model (vertical broken green line separates the calibration and validation period)

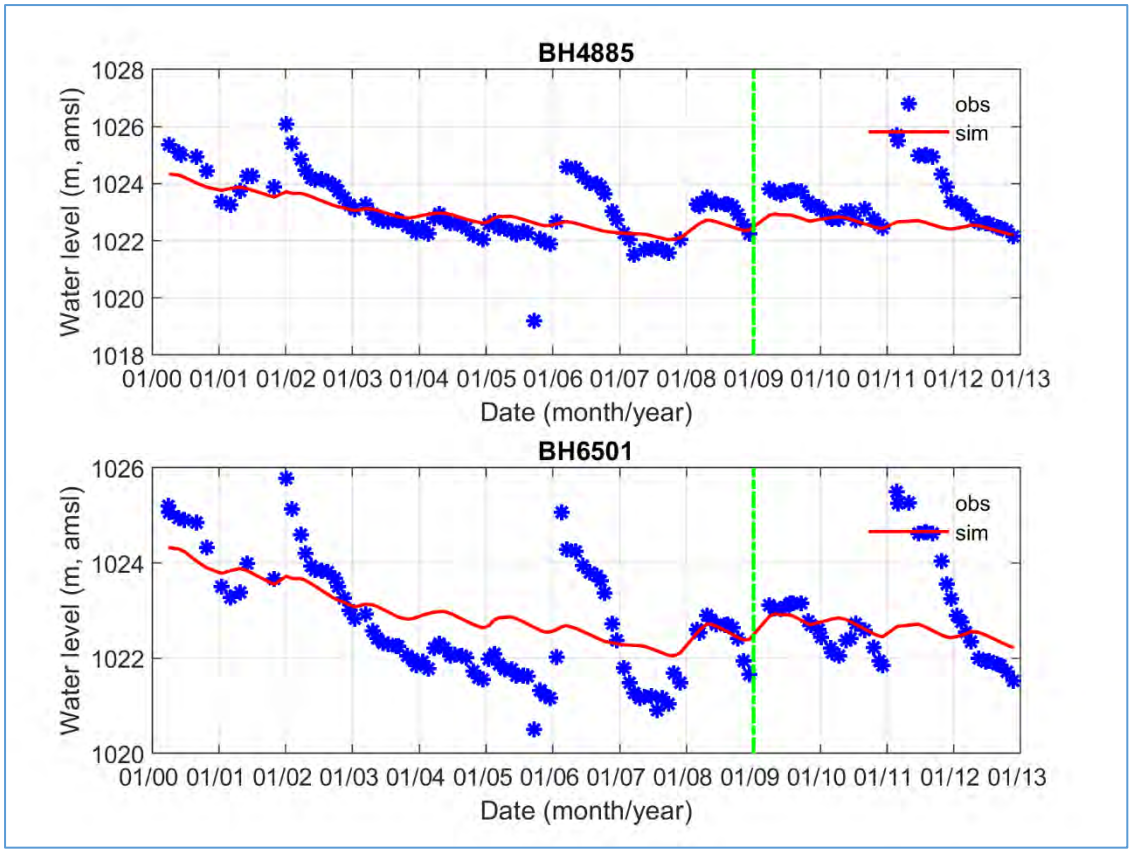

Figure 42: Observed and simulated water levels for BH4885 and BH6501, the latter from the calibrated transient model (vertical broken green line separates the calibration and validation period)

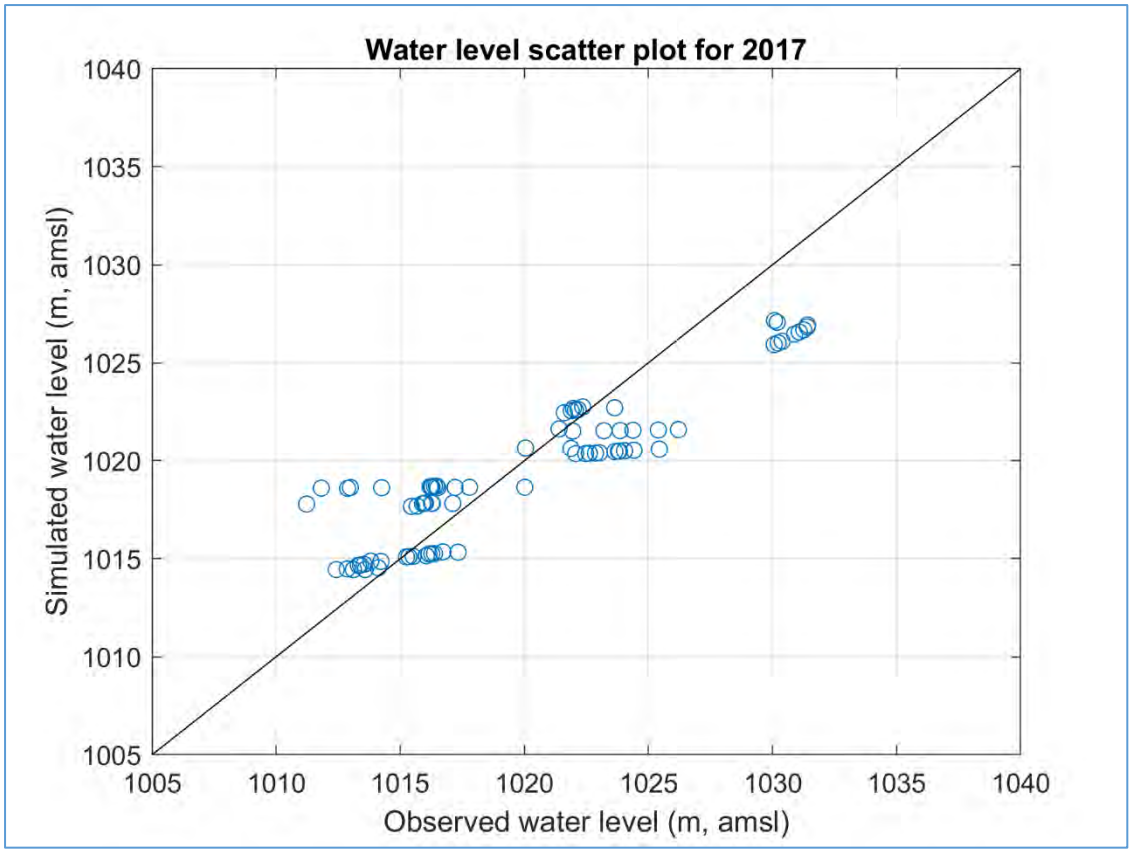

Figure 43: Observed and simulated (calibrated transient model) water level scatter plot for the year 2017 [post validation], for 11 observation wells

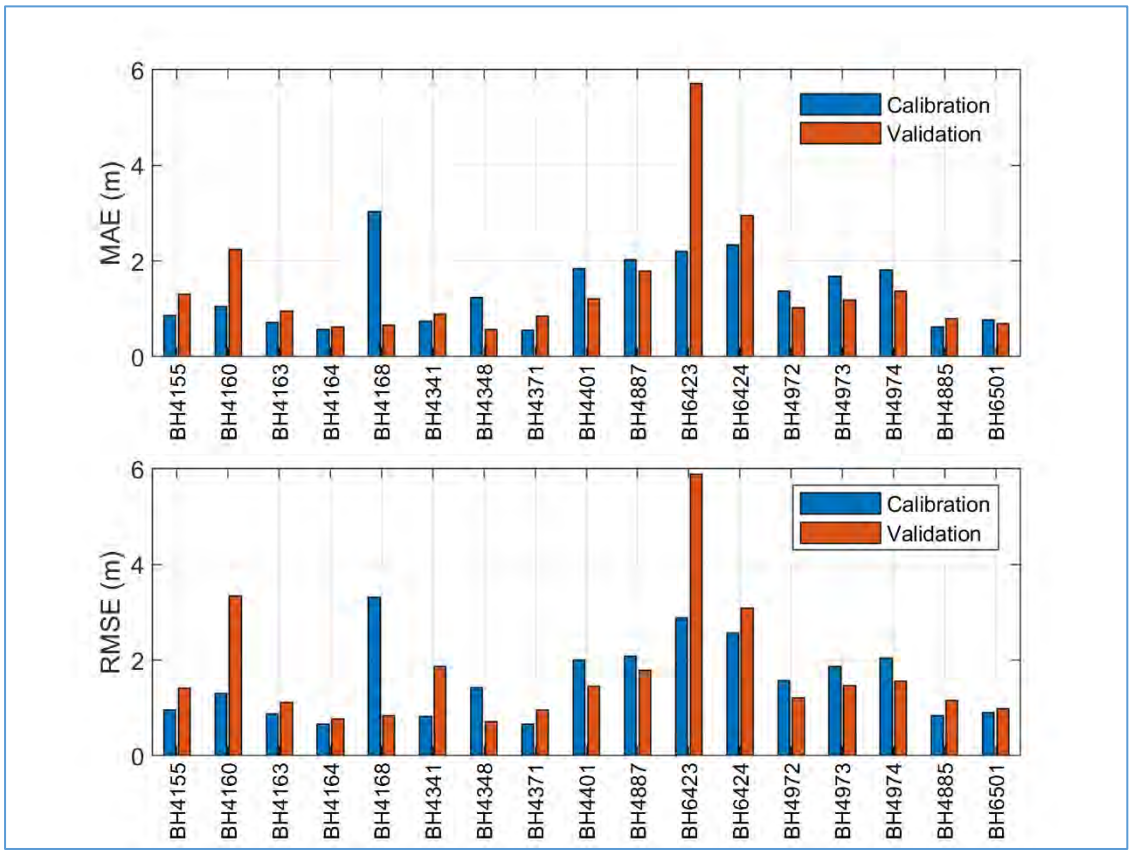

Figure 44: MAE and RMSE between the observed and simulated groundwater levels during the calibration and validation periods for each observation wells.

6.3 Water Budget Analysis

Groundwater budget analysis for the entire model domain was carried out using ZONEBUDGET (Harbaugh, 2009) and analysed with the USGS GW_Chart program. Anderson et al. (2015) described aquifer water budget using Equation 9.

$$\text{Inflow} = \text{Outflow} +/- \Delta \text{ in Storage} \quad (9)$$

When outflow is not balanced by inflow change in storage occurs, resulting in either increase or decrease in groundwater level. For the steady state model, the change in storage is assumed to be zero. The difference in inflow and outflow during the model simulation is recommended not to be larger than 1%. Difference of more than 1% in the mass balance indicates possible numerical problem and may invalidate simulation results (ASTM Standard D5447, 2010).

6.3.1 Steady state model

The water budget of the entire model domain from the calibrated steady state model is presented in Figure 45. Recharge is presented as the sum of diffuse recharge from rainfall and recharge along the river and flood plain. During the calibration period, there is no groundwater abstraction from the aquifer. Hence, at dynamic equilibrium, the total recharge should be balanced by GWET, out flow through the GHB, and groundwater discharge to the river. As shown in Figure 44, GWET accounts for about 90.7% of the total outflow while groundwater outflow across the model boundary accounts for the remaining 9.3%. The recharge (diffuse and focused) calculated by the steady state model was about 37.3 mm/a. This is in the range of recent study by Baqa (2017), who reported recharge rate in the area ranging from 2.1 to 73 mm/a using the chloride mass balance method. A previous study by GCS (2000) used constant value of 50 mm/a for recharge along the river and 10 mm/a for diffuse recharge from rainfall. As noted in Lerner (2002), it is important to note that due to strong inverse correlation between recharge and hydraulic conductivity when calibrating hydrogeological model against groundwater, the calibration generally provides an estimate of R/K instead of R alone. Additional calibration data such as tracer, spring discharge etc. provide additional information that helps to independently calibrate the two parameters. This to say that due to high correlation between recharge and hydraulic conductivity, simultaneous calibration of these two parameters may not result unique parameter value.

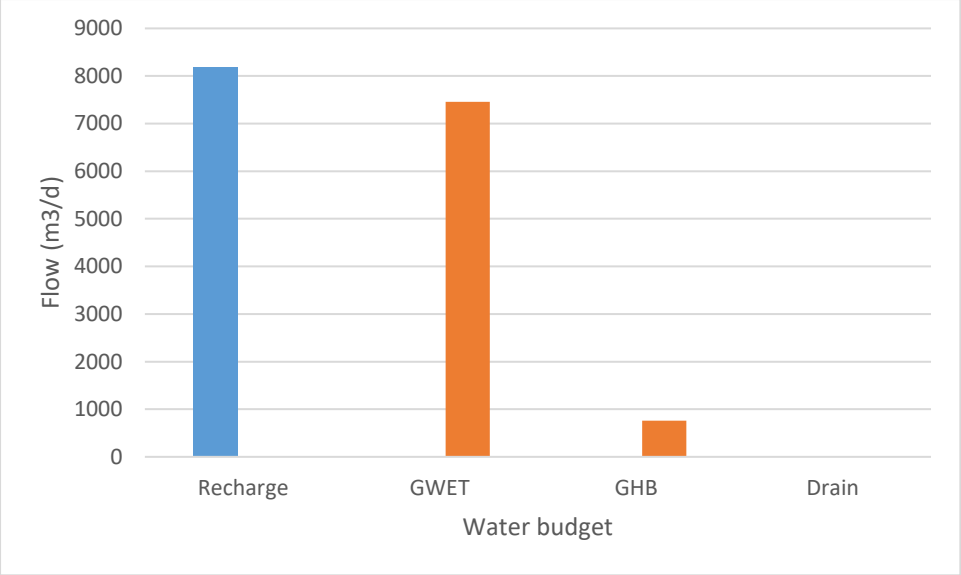

Figure 45: Water budget of the entire model domain obtained from steady state model

6.3.2 Transient model

Annual water budget together with annual rainfall during the simulation period is shown in Figure 46. Simulated total recharge rate (diffuse and focused) during the simulation period ranges from 0.43 – 53.2 mm/a (a mean of 24.5 ± 14.4 mm/a, or, of 5.6 ± 1.3 % mean annual rainfall. As can be seen in Figure 46, recharge is highly variable between the wet and dry years. The minimum and maximum recharge occurs in 2017 and 2009, respectively. Evapotranspiration directly from the groundwater (GWET) is a significant component of the groundwater budget. It ranges from 14.7 – 40.0 mm/a (with a mean of 27.0 ± 6.8 mm/a), which is exceeding the recharge rate. Evapotranspiration from the groundwater mainly occurs along the river where the depth to groundwater is relatively shallow. Groundwater discharge to the river is the smallest component of the water budget with a mean of 2.4 ± 1.64 mm/a. Groundwater outflow from the model domain through the specified GHB is 1.9 ± 1.41 mm/a. Groundwater abstraction only occurs during the recent period [2015-2017] and it ranges from 0-25.37 mm/a (with a mean of 2.76 ± 6.80 mm/a). Annual change in groundwater storage is highly variable ranging from -31.4 – 15.7 mm/a (with a mean of -11.4 ± 11.3 mm/a). Annual groundwater storage change is strongly correlated with annual rainfall (R^2=0.88). The annual storage change is a measure of the volume of water lost or gained in the basin during the year.

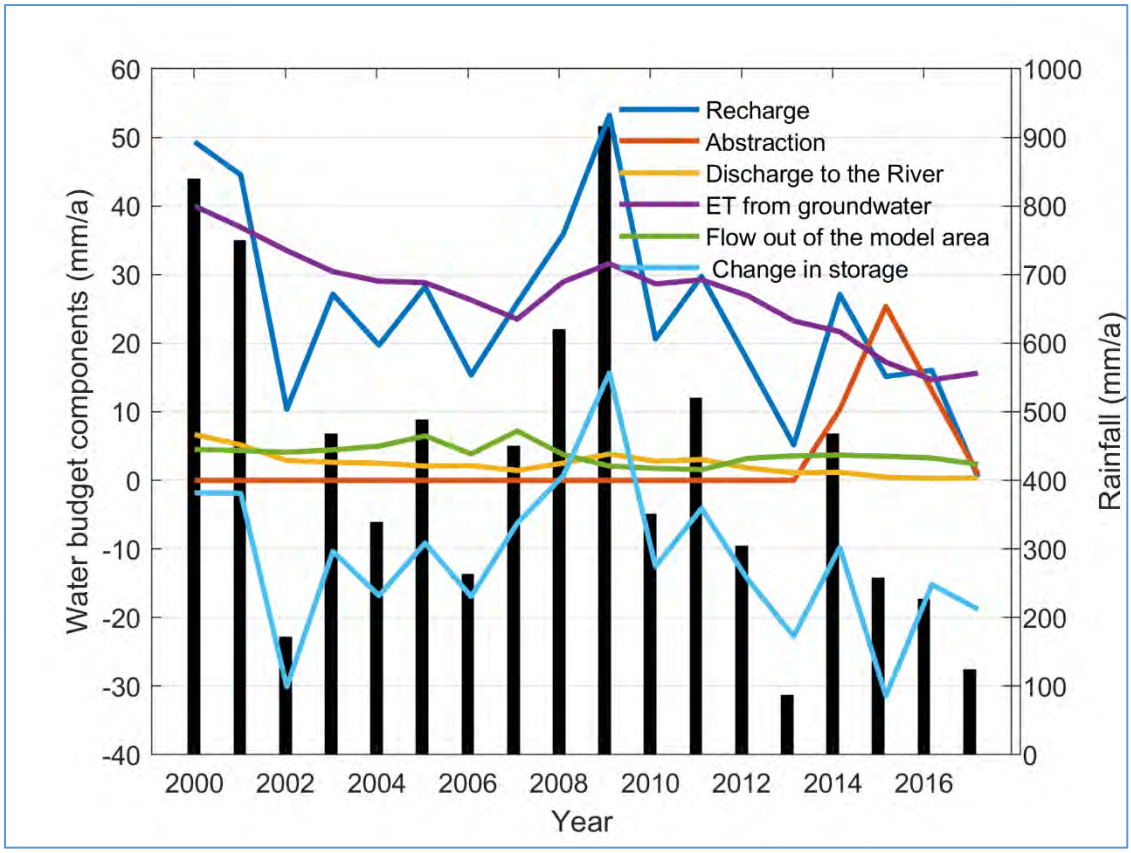

Figure 46: Annual water budget for the transient model during the simulation period 2000-2017 and annual rainfall

7. Discussion

Hydrogeological model developed in the context of transboundary aquifer management. In view of the need for groundwater development in Ramotswa town in the past, more than three hydrogeological models were developed to assess groundwater potential of the aquifer. However, none of these models were developed in a transboundary aquifer management context. The present model builds on these studies and developed the first hydrogeological model in a transboundary aquifer management context. It is also important to note that it has been almost two decades since the last model was developed (GCS, 2000). There has been significant data collection efforts since then. Hence, the main achievement of the present report is to improve the hydrogeological model with recent data, improved conceptual model, improved model calibration approach and to assess the groundwater budget (to investigate the use and movement of groundwater, recharge, discharge and storage process), and to use this model to assess the feasibility of MAR through model scenario analysis. Toward this end, a 3D transient hydrogeological model was developed for the period of 2000-2017 for compartment 3, encompassing Ramotswa town with catchment area of approximately 80 km^2.

Reasonable match between observed and simulated water level was obtained. The transient hydrogeological model was calibrated using observed groundwater level data in 17 observation wells for the period 2000-2012 and validated for the period 2009-2012. The validated model was further verified using recent water level data in 2017. In general, there is good correlation between observed and simulated water level data. The model obtained good agreement between observed and

simulated water levels. The model is also able to reproduce the observed groundwater dynamics in the observation wells but the variability is low.

The first reason for lack of water level dynamics in simulated water level could be non-linearity in recharge dynamics. In the present model recharge (diffuse and focused) were estimated using as linear fraction of monthly rainfall. Where by two recharge zones representing the diffuse recharge (outside of the river channel) and combined diffuse and focused recharge (along the river channel) were used to represent spatial variability in recharge. It is important to note that recharge process is nonlinear by nature linear assumption of linear fraction of rainfall may result poor approximations (Petheram et al., 2002). Allison et al. (1994) presented empirical equation for estimating recharge from rainfall $R = k_1(P - k_2)$, where P is rainfall and k_1 and k_2 are constants. However, Allison et al. (1994) suggested to use this method where annual recharge is fairly high > 50 mm/a. According to the author, this method is rarely used in semi-arid or arid region where recharge is low. The focused recharge from the River section and flood plain areas are more related to the magnitude of the flood, flooded area, frequency of flooding etc. and do not correlate with rainfall. or Daily or sub-daily recharge events that are not captured by the model due to its monthly temporal resolution could be the likely reason for the model not simulating very well the groundwater dynamics at the observation wells.

The second reason is GWET. GWET is highly depend on specified extinction depths. Shah et al. (2007) reported extinction depth for different soil type and land use. For Sandy clay loam soil, Shah et al. (2007) estimated extinction depth of 2, 3 and 4 m respectively for land cover type bare soil, grass and forest. In this, we followed a conservative approach and determined extinction depth to be 3 m, which is corresponding to land, cover type grass. However, the major land use/land cover type in the study area is Shrubs (45%), grassland (28%), urban built (13%), cropped land (8%) and Trees (6%). In MODFLOW ET package, GWET is assumed to decrease linearly with increasing depth to groundwater, reaching a value of zero at extinction depth. However, Soylu et al. (2011) found difference of a factor two as a result of using different soil parameters and concluded that the impact of soil hydraulic parameters are much greater than soil texture. We also observed that the ET estimated using the Hargreaves method has low temporal variability range as compared to ET estimated from pan evaporation from Molatedi dam (Figure 47). There is significant difference in the two ET estimate mainly during low ET periods. These need to be investigated further.

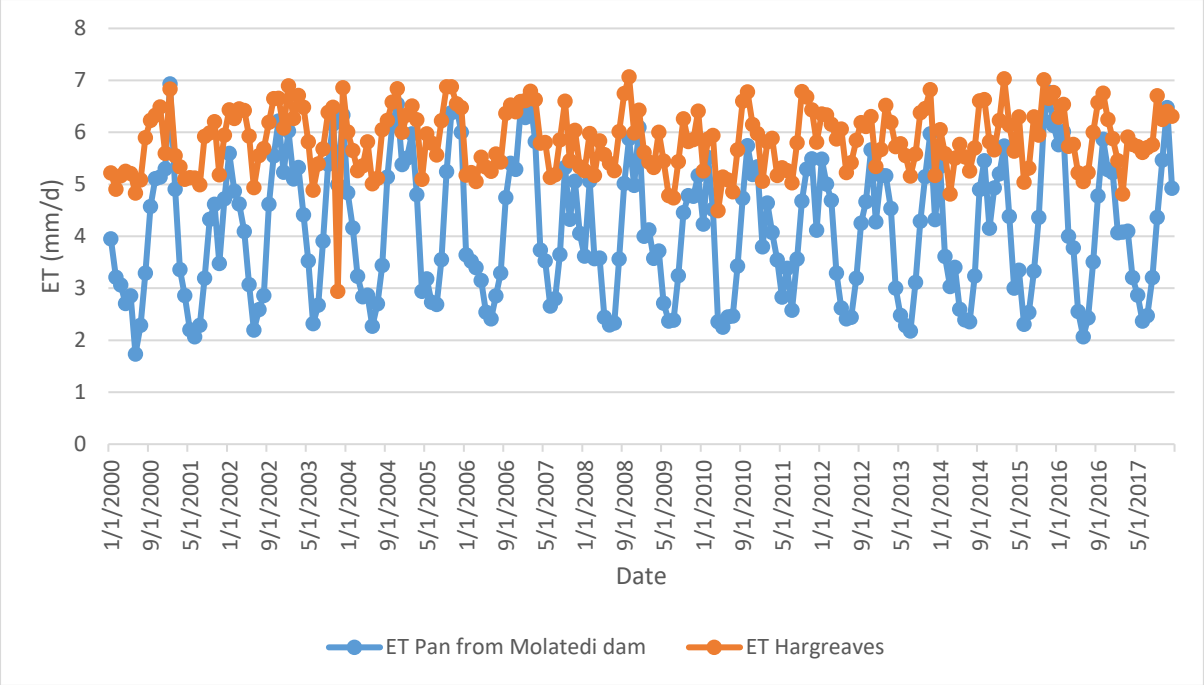

Figure 47: Monthly ET determined using Hargreaves method and ET determined from Pan Evaporation data from the Molatedi dam and Pan Coefficient of 0.85

Water budget in the study area is highly variable. The calibrated model was used to compute annual water budget for the study area. Results show that the water budget in the study area is highly variable between dry and wet years. Little recharge occurs during the dry period which leads to negative storage. There is strong correlation between annual storage change and annual rainfall. Positive storage change occurs when the aquifer is recharged during high rainfall years. During the simulation period, the groundwater storage shows a declining trend. Recharge is the main inflow to the aquifer that drives the water balance and its estimation is difficult and very uncertain. It varies both spatially and temporally. However, recharge estimation is the basis for accurate estimation of groundwater resources and for determining water allocations in water resource planning. In the present study recharge is estimated as a constant fraction of monthly rainfall. The results of transient simulation shows that the recharge rate during the simulation period ranges from 0.43 – 53.2 mm/a (a mean of 24.5 ± 14.4 mm/a, or, of 5.6 ± 1.3 % mean annual rainfall. The estimated recharge is within the range of expected recharge rates in semi-arid regions and compared well with recharge estimates using chloride mass balance approach (Baqa, 2017; GCS, 2000). To further constrain recharge estimation, independent recharge estimation was also carried out using WTF method (See annex 1). WTF method was applied at the 17 observation wells used for hydrogeological model calibration. The estimated recharge rates ranges from 3 – 14% of daily rainfall (with a mean of 10 ± 3%). The estimated specific yield with the WTF ranges from 0.013 – 0.10 (with a mean of 0.043 ± 0.023).

Results of the transient model water budget shows that approximately 80% of the recharge entering the aquifer exits as GWET. However, even if GWET accounts for the larger water balance component it was not accounted for in any of the previous modelling studies. Groundwater discharge to the river is a very small component of the overall water budget. Low groundwater discharge to the river is expected given the ephemeral nature of the river which often dry.

8. Model assumptions, simplification and limitations

Limitations and uncertainty exist in any modelling. The most common sources of uncertainty include: 1) lack of adequate data recharge process representation, 2) Groundwater extinction depth or method for improving GWET, 3) Uncertainty in the conceptual model e.g. karastic features such as conduits, sink holes, etc.), 4) conceptual model and aquifer heterogeneities (the level of details included in the conceptual model, e.g. dipping in geological formations and geological heterogeneity spatially as well as vertically), 5)Faults not represent in the model, 6) influence of dyke of groundwater flow

The following assumptions were made in the present 3D hydrogeological model:

1) The aquifer is represented by two layer model due to lack of data on lithology and degree of karstification with depth.
2) Groundwater flow through the karstic aquifer is assumed to behave similar to flow through Equivalent Porous Media and flow through individual fractures and conduits cannot be adequately represented.
3) Dikes compartmentalizing the groundwater flow are assumed to be impermeable, hence no flow occurs across these dikes even in the weathered top part.
4) Lateral boundaries at the north and some part of the eastern side are not physical boundaries but were chosen as no flow boundaries based on their low permeability or flow along the flow lines coinciding with the boundary. Hence, flow across these boundaries are assumed to be negligible.
5) The dolomite is dipping to the South but this was not accounted in the model. Model layers were assumed to be horizontal.
6) The groundwater recharge process is non-linear, however, in this study constant fraction of monthly rainfall data was assumed to recharge the aquifer.
7) Evapotranspiration from the saturated zone is assumed to be a linear function of groundwater depth below the land surface. It is maximum at land surface and decreases linearly to zero at 3 m below the land surface.
8) The model is impervious at the bottom.

9. Conclusions

To better understand the aquifer system, a transient 3D hydrogeological model was developed in MODELMUSE modelling environment using MODFLOW 2005. The model was calibrated to simulate the groundwater levels for 2000-2008, and validated using measured levels during the period of 2009-2012. Water level data from the last year was used as post-validation. There is a good correlation between observed and simulated water levels. Parameter values estimated by the calibration process are within the range of expected values. The overall results of the model calibration and validation suggest that the model is appropriate for evaluating alternative groundwater management scenarios (e.g. MAR potential assessment).

The transient model was used to assess the temporal variability in water budget in the study area over the 18 years simulation period 2000-2017. Results of the annual water budget analysis over the simulation period show that the water budget in the study are is highly variable. Recharge rate during the simulation period ranges from 0.43 – 53.2 mm/a (a mean of 24.5 ± 14.4 mm/a, or, of 5.6 ± 1.3 %

mean annual rainfall and compared well to previous estimates in the study area. About 15% of the recharge is leaving aquifer system through the GHB. Simulation results also show that groundwater supported evapotranspiration drawn from the aquifer exceeds mean annual recharge. The groundwater supported fraction of evapotranspiration is higher in drier years, when evapotranspiration exceeds rainfall. Quantifying recharge is a key component for better management of the groundwater resource but also its estimation is difficult and uncertain. As the aridity increases recharge from rainfall decreases significantly. This is because most of the water infiltrated into the soil will not reach the groundwater table, rather it may be stored in the root zone and ultimately returned back to the atmosphere through evaporation and plant transpiration. Hence, in this areas, increasing recharge though MAR is a viable solution for increasing the reliability of groundwater supply for domestic and other uses.

References

Allen, R. G., Pereira, L. S., Raes, D., and Smith, M., 1998, FAO Irrigation and drainage paper No. 56: Rome: Food and Agriculture Organization of the United Nations, v. 56, no. 97, p. e156.

Allison, G., Gee, G., and Tyler, S., 1994, Vadose-zone techniques for estimating groundwater recharge in arid and semiarid regions: Soil Science Society of America Journal, v. 58, no. 1, p. 6-14.

Altchenko, Y., Genco, A., Pierce, K., Woolf, R., Nijsten, G. J., Ansems, N., Magombeyi, M., Ebrahim, G., Lautze, J., Villholth, K., Lefore, N., Modisha, R., Baqa, S., McGill, B., and Kenabatho, P., 2017, Resilience in the Limpopo basin: The potential role of the Transboundary Ramotswa aquifer, hydrogeology report.

Anderson, M. P., Woessner, W. W., and Hunt, R. J., 2015, Applied groundwater modeling: simulation of flow and advective transport, Academic press.

ASTM Standard D5447, 2010, Standard Guide for Application of a Groundwater Flow Model to a Site-Specific Problem.

Balco, G., 2017, Is a cheap GPS OK for elevation measurements, or do you need a fancy one?,https://cosmognosis.wordpress.com/2017/03/28/is-a-cheap-gps-ok-for-elevation-measurements-or-do-you-need-a-fancy-one/ (accessed September 2, 2018).

Baqa, S. S., 2017, Groundwater Recharge Assessment in the Upper Limpopo River Basin: A Case Study in Ramotswa Dolomitic Aquifer MSC Thesis,University of the Witwatersrand, Johannesburg,.

Bredehoeft, J., 2005, The conceptualization model problem—surprise: Hydrogeology journal, v. 13, no. 1, p. 37-46.

Bromley, J., Mannström, B., Nisca, D., and Jamtlid, A., 1994, Airborne Geophysics: Application to a Ground-Water Study in Botswana: Ground Water, v. 32, no. 1, p. 79-90.

Burns, E. R., Morgan, D. S., Lee, K. K., Haynes, J. V., and Conlon, T. D., 2012, Evaluation of long-term water-level declines in basalt aquifers near Mosier, Oregon: US Geological Survey Scientific Investigations Report, v. 5002, p. 134.

Catuneanu, O., and Eriksson, P. G., 1999, The sequence stratigraphic concept and the Precambrian rock record: an example from the 2.7–2.1 Ga Transvaal Supergroup, Kaapvaal craton: Precambrian Research, v. 97, no. 3-4, p. 215-251.

Cobbing, J., 2018, An updated water balance for the Grootfontein aquifer near Mahikeng: Water SA, v. 44, no. 1, p. 54-64.

Cook, P. G., 2003, A guide to regional groundwater flow in fractured rock aquifers, Citeseer.

Cuthbert, M., 2010, An improved time series approach for estimating groundwater recharge from groundwater level fluctuations: Water Resources Research, v. 46, no. 9.

Doherty, J., 2003, Ground water model calibration using pilot points and regularization: Groundwater, v. 41, no. 2, p. 170-177.
Doherty, J., and Johnston, J. M., 2003, Methodologies for calibration and predictive analysis of a watershed model1, Wiley Online Library.
Donahue, B., Wentzel, J., and Berg, R., 2017, Guidelines for RTK/RTN GNSS surveying in Canada. Version 1.2.
Du Toit, W. H., 2001, An investigation into the occurrence of groundwater in the contact aureole of large granite intrusions (Batholiths) located West and Northwest of Pietersburg Volume 1, Department of Water Affairs and Forestry.
DWA, 2006, Ramotswa Test Pumping of Production Boreholes, Groundwater Division – Department of Water Affairs.
DWAF, 2006, Vaal River System: Large Bulk Water Supply Reconciliation Strategy: Groundwater Assessment Dolomite Aquifers, Department of Water Affairs and Forestry, South Africa, December 2006. .
Ebrahim, G. Y., Jonoski, A., Al-Maktoumi, A., Ahmed, M., and Mynett, A., 2015, Simulation-optimization approach for evaluating the feasibility of managed aquifer recharge in the Samail lower catchment, Oman: Journal of Water Resources Planning and Management, v. 142, no. 2, p. 05015007.
Eriksson, P., and Altermann, W., 1998, An overview of the geology of the Transvaal Supergroup dolomites (South Africa): Environmental geology, v. 36, no. 1-2, p. 179-188.
Eriksson, P., and Reczko, B., 1995, The sedimentary and tectonic setting of the Transvaal Supergroup floor rocks to the Bushveld Complex: Journal of African Earth Sciences, v. 21, no. 4, p. 487-504.
Faunt, C. C., Blainey, J. B., Hill, M. C., D'Agnese, F. A., and O'Brien, G. M., 2004, Transient numerical model: Death Valley regional ground-water flow system, Nevada and California—hydrologic framework and transient ground-water flow model. US Geological Survey Scientific Investigations Report, v. 5205, p. 257-352.
GCS, 2000, Groundwater Monitoring, Review of Monitoring Performed by DWA and DGS, Assessment of Water Resources and Suggestion for Improvements, Phase 1 of the National Groundwater Information System TB10/3/4/96-97, Volume 19, Ramotswa Wellfield Final Report by Geotechnical Consulting Services
Gebreyohannes, T., De Smedt, F., Walraevens, K., Gebresilassie, S., Hussien, A., Hagos, M., Amare, K., Deckers, J., and Gebrehiwot, K., 2017, Regional groundwater flow modeling of the Geba Basin, Northern Ethiopia: Hydrogeology Journal, p. 1-17.
Genco, A., and Pierce, K., 2016a, Conceptual Model, Hydraulic Properties, and Model Dataset Support Progress Report for the Development of Subsurface Mapping for the Transboundary Ramotswa Aquifer, that is part of the Limpopo River Basin, using Airborne Geophysics, XRI BLUE Report October 2016,, XRI BLUE, Midland, Texas, USA.
-, 2016b, Geophysical QA/QC Corrected, and Final Inverted AEM Data Report for the Development of Subsurface Mapping for the Transboundary Ramotswa Aquifer that is part of the Limpopo River Basin, using Airborne Geophysics ,XRI BLUE Report June 2016, XRI BLUE, Midland, Texas, USA. .
Ghasemizadeh, R., Yu, X., Butscher, C., Hellweger, F., Padilla, I., and Alshawabkeh, A., 2015, Equivalent porous media (EPM) simulation of groundwater hydraulics and contaminant transport in karst aquifers: PloS one, v. 10, no. 9, p. e0138954.
Goodrich, D. C., Williams, D. G., Unkrich, C. L., Hogan, J. F., Scott, R. L., Hultine, K. R., Pool, D., Goes, A. L., and Miller, S., 2004, Comparison of methods to estimate ephemeral channel recharge, Walnut Gulch, San Pedro River basin, Arizona: Groundwater recharge in a desert environment: the southwestern United States, p. 77-99.

Gupta, G., Erram, V. C., and Kumar, S., 2012, Temporal geoelectric behaviour of dyke aquifers in northern Deccan Volcanic Province, India: Journal of earth system science, v. 121, no. 3, p. 723-732.
Harbaugh, A., 2009, Zonebudget Version 3.01, A computer program for computing subregional water budgets for MODFLOW ground-water flow models: US Geological Survey Groundwater Software.
Harbaugh, A. W., 2005, MODFLOW-2005, the US Geological Survey modular ground-water model: the ground-water flow process, US Department of the Interior, US Geological Survey Reston.
Hargreaves, G. H., and Samani, Z. A., 1985, Reference crop evapotranspiration from temperature: Applied engineering in agriculture, v. 1, no. 2, p. 96-99.
Hassan, S. T., Lubczynski, M. W., Niswonger, R. G., and Su, Z., 2014, Surface–groundwater interactions in hard rocks in Sardon Catchment of western Spain: an integrated modeling approach: Journal of Hydrology, v. 517, p. 390-410.
Healy, R. W., and Cook, P. G., 2002, Using groundwater levels to estimate recharge: Hydrogeology Journal, v. 10, no. 1, p. 91-109.
Hsieh, P. A., and Freckleton, J. R., 1993, Documentation of a computer program to simulate horizontal-flow barriers using the US Geological Survey's modular three-dimensional finite-difference ground-water flow model, US Department of the Interior, US Geological Survey.
IoH, 1986, Ramotswa Wellfield S.E. Botswana, Digital Model Study and Storage Estimates, The Institute of Hydrology, University of Blomfontein, South Africa
Kaehler, C. A., and Hsieh, P. A., 1994, Hydraulic properties of a fractured-rock aquifer, Lee Valley, San Diego County, California: US Geological Survey.
Kinzelbach, W., Bauer, P., Siegfried, T., and Brunner, P., 2003, Sustainable groundwater management--Problems and scientific tool: Episodes-Newsmagazine of the International Union of Geological Sciences, v. 26, no. 4, p. 279-284.
Koenig, F., and Wong, D., 2010, Real-time Kinematics Global Positioning System (GPS) Operation and Setup Method for the Synchronous Impulse Reconstruction (SIRE) Radar: ARMY RESEARCH LAB ADELPHI MD SENSORS AND ELECTRON DEVICES DIRECTORATE.
Kuniansky, E. L., 2016, Simulating groundwater flow in karst aquifers with distributed parameter models—Comparison of porous-equivalent media and hybrid flow approaches: US Geological Survey, 2328-0328.
Larocque, M., Banton, O., Ackerer, P., and Razack, M., 1999, Determining karst transmissivities with inverse modeling and an equivalent porous media: Ground water, v. 37, no. 6, p. 897-903.
Lee, J., Choi, S.-U., and Cho, W., 1999, A comparative study of dual-porosity model and discrete fracture network model: KSCE Journal of Civil Engineering, v. 3, no. 2, p. 171-180.
Long, J., Remer, J., Wilson, C., and Witherspoon, P., 1982, Porous media equivalents for networks of discontinuous fractures: Water Resources Research, v. 18, no. 3, p. 645-658.
Mansouri, B. E., and Mezouary, L. E., 2015, Enhancement of groundwater potential by aquifer artificial recharge techniques: an adaptation to climate change: Proceedings of the International Association of Hydrological Sciences, v. 366, p. 155-156.
Merz, S. K., 2012, Australian groundwater modelling guidelines: Waterlines Report Series, no. 82.
Meyer, R., 2014, Hydrogeology of Groundwater Region 10: The Karst Belt, Report to the Water Research Commission, WRC Report No. TT 553/14
Morel, E., and Wikramaratna, R., 1982, Numerical modelling of groundwater flow in regional aquifers dissected by dykes: Hydrological Sciences Journal, v. 27, no. 1, p. 63-77.
Nilsen, K., Sydnes, M., Gudmundsson, A., and Larsen, B., How dykes affect groundwater transport in the northern part of the Oslo Graben, *in* Proceedings EGS-AGU-EUG Joint Assembly2003, Volume 1, p. 9684.
Niswonger, R. G., and Prudic, D. E., 2005, Documentation of the Streamflow-Routing (SFR2) Package to include unsaturated flow beneath streams--A modification to SFR1, US Department of the Interior, US Geological Survey.

Panagopoulos, G., 2012, Application of MODFLOW for simulating groundwater flow in the Trifilia karst aquifer, Greece: Environmental Earth Sciences, v. 67, no. 7, p. 1877-1889.
Petheram, C., Walker, G., Grayson, R., Thierfelder, T., and Zhang, L., 2002, Towards a framework for predicting impacts of land-use on recharge: 1. A review of recharge studies in Australia: Soil Research, v. 40, no. 3, p. 397-417.
Prudic, D. E., 1989, Documentation of a computer program to simulate stream-aquifer relations using a modular, finite-difference, ground-water flow model: US Geological Survey, 2331-1258.
Prudic, D. E., Konikow, L. F., and Banta, E. R., 2004, A new streamflow-routing (SFR1) package to simulate stream-aquifer interaction with MODFLOW-2000, 2331-1258.
Quinn, J. J., Tomasko, D., and Kuiper, J. A., 2006, Modeling complex flow in a karst aquifer: Sedimentary Geology, v. 184, no. 3-4, p. 343-351.
Ruhl, J., and Cowdery, T. K., 2004, Regional ground-water-flow models of surficial sand and gravel aquifers along the Mississippi River between Brainerd and St. Cloud, central Minnesota: US Geological Survey, 2328-0328.
Samani, Z., 2000, Estimating solar radiation and evapotranspiration using minimum climatological data: Journal of irrigation and drainage engineering, v. 126, no. 4, p. 265-267.
Scanlon, B. R., Mace, R. E., Barrett, M. E., and Smith, B., 2003, Can we simulate regional groundwater flow in a karst system using equivalent porous media models? Case study, Barton Springs Edwards aquifer, USA: Journal of hydrology, v. 276, no. 1, p. 137-158.
Selaolo, E. T., 1985, Evaluation of Aquifer Hydraulic Parameters in Ramotswa: S.E. Botswana , MSc Thesis in Hydrogeology, University College London
Shah, N., Nachabe, M., and Ross, M., 2007, Extinction depth and evapotranspiration from ground water under selected land covers: Groundwater, v. 45, no. 3, p. 329-338.
Shanafield, M., and Cook, P. G., 2014, Transmission losses, infiltration and groundwater recharge through ephemeral and intermittent streambeds: A review of applied methods: Journal of Hydrology, v. 511, p. 518-529.
Shevenell, L., 1996, Analysis of well hydrographs in a karst aquifer: estimates of specific yields and continuum transmissivities: Journal of hydrology, v. 174, no. 3-4, p. 331-355.
Singh, R., and Jamal, A., 2002, Dykes as groundwater loci in parts of Nashik District, Maharashtra: Geological Society of India, v. 59, no. 2, p. 143-146.
Singhal, B. B. S., and Gupta, R. P., 2010, Applied hydrogeology of fractured rocks, Springer Science & Business Media.
Soylu, M., Istanbulluoglu, E., Lenters, J., and Wang, T., 2011, Quantifying the impact of groundwater depth on evapotranspiration in a semi-arid grassland region: Hydrology and Earth System Sciences, v. 15, no. 3, p. 787-806.
Staudt, M., 2003, Environmental Hydrogeology of Ramotswa South East District, Republic of Botswana
Takasaki, K. J., and Mink, J. F., 1985, Evaluation of major dike-impounded ground-water reservoirs, Island of Oahu, US Government Printing Office Washington, DC.
Teutsch, G., and Sauter, M., Groundwater modeling in karst terranes: Scale effects, data acquisition and field validation, *in* Proceedings Proc. Third Conf. Hydrogeology, Ecology, Monitoring, and Management of Ground Water in Karst Terranes, Nashville, TN1991, p. 17-35.
Tucci, P., 1997, Simulated effects of horizontal anisotropy on ground-water-flow paths and discharge to streams: Ground water protection alternatives and strategies in the USA.
USGS, 2018a, https://earthexplorer.usgs.gov/ (accessed on, March 2018).
-, 2018b, https://water.usgs.gov/osw/gps/, accessed September 2, 2018.
Varalakshmi, V., Venkateswara Rao, B., SuriNaidu, L., and Tejaswini, M., 2012, Groundwater flow modeling of a hard rock aquifer: case study: Journal of Hydrologic Engineering, v. 19, no. 5, p. 877-886.

Vorster, P., and Koch, S., 2014, TrigNet, South Africa's GNSS base station network: past, present and future.
White, W. B., 1969, Conceptual models for carbonate aquifers: Groundwater, v. 7, no. 3, p. 15-21.
-, 2012, Conceptual models for carbonate aquifers: Groundwater, v. 50, no. 2, p. 180-186.
Williams, P. W., 2008, The role of the epikarst in karst and cave hydrogeology: a review: International Journal of Speleology, v. 37, no. 1, p. 1.
Winston, R. B., 2009, ModelMuse: a graphical user interface for MODFLOW-2005 and PHAST, US Geological Survey.
Woolfenden, L. R., and Koczot, K. M., 2001, Numerical simulation of ground-water flow and assessment of the effects of artificial recharge in the Rialto-Colton Basin, San Bernardino County, California, US Department of the Interior, US Geological Survey.
WUC, 1989, Ramotswa Wellfiled Operation Procedures and Resource Managment Project Phase 1 Report, Republic of Botswana Water Utility Corporation.
-, 2014, Ramotswa Wellfield Monitoring Report, Water Utilities Corporation, Botswana.
XRI BLUE, 2016, Conceptual Model, Hydraulic Properties, and Model Dataset Support Progress Report for the Development of Subsurface Mapping for the Transboundary Ramotswa Aquifer, that is part of the Limpopo River Basin, using Airborne Geophysics,OCTOBER, 2016.
Zhou, Y., and Li, W., 2011, A review of regional groundwater flow modeling: Geoscience frontiers, v. 2, no. 2, p. 205-214.

Annex 1: Recharge Estimation using Water Table fluctuation Method

1.1 Theoretical Background

The Water Table Fluctuation Method (WTF) is based on the hypothesis that a rise in groundwater levels in the unconfined aquifers is due to recharge water arriving at the water table. Recharge is calculated using Equation 9 (Healy and Cook, 2002).

$$R = Sy * \frac{dh}{dt} = Sy\frac{\Delta h}{\Delta t} \qquad (9)$$

Where Sy is specific yield, Δh is the difference between the peak of the rise and low point of the extrapolated antecedent recession curve at the time of the peak and Δt is the time between those points.

Cuthbert (2010) more recently, modified the original equation of the WTF method to account for net groundwater drainage away from a given observation point. According to the author, the change in groundwater level in an aquifer through time is not only controlled by recharge but also by the net groundwater drainage away from a given observation point and expressed using Equation 10.

$$R = Sy\frac{dh}{dt} + D \quad \ldots\ldots\ldots\ldots\ldots\ldots \quad (10)$$

Where R is recharge [LT^{-1}], Sy is the specific yield [-], and D is the net groundwater drainage away from observation point [LT^{-1}]

The advantage of this approach is its simplicity and its main limitations are difficulties of estimating specific yield and accounting for drainage term (Cuthbert, 2010). The author argue that for shallow water table conditions R may be much larger than D during a recharge event, hence the error in recharge estimation due to error in D may be negligible. Using discrete water level data for each time step Equation 10 can be written as Equation 11. After re-arranging the water level at time (t) can be calculated using Equation 12. Equation 12 is modified to account groundwater decline due to pumping and written as Equation 13.

$$R_t = Sy\frac{(h_t - h_{(t-\Delta t)})}{\Delta t} + D_t \quad \ldots\ldots\ldots\ldots\ldots\ldots \quad (11)$$

$$h_t = h_{(t-\Delta t)} + \left(\frac{R_t - D_t}{Sy}\right)\Delta t \qquad (12)$$

$$h_t = h_{(t-\Delta t)} + \left(\frac{R_t - D_t}{Sy} - S_t\right)\Delta t \qquad (13)$$

Where S_t is drawdown rate (LT^{-1}), h_t and $h_{(t-\Delta t)}$ are groundwater level (relative to the river level), and Δt is time step [T]

1.2 Estimated Recharge using the Water Table Fluctuation Method

The WTF method was used to estimate recharge at monitoring well BH4168, which is approximately 2.7 km from the river channel and for BH4371 approximately 0.12 km from the river. Recharge is assumed to be linear function of rainfall. As there is no pumping during this period the drawdown rate due to pumping was assumed to be zero. Three parameters namely, recharge fraction, Sy and Dt were

used as a calibration parameter. However, it is very difficult, if not impossible to simultaneously estimate a unique parameter values for each. The result of the model calibration for BH4168 which is located far from the river is shown in Figure 48. During the calibration Sy of 0.03, recharge fraction of 0.2 and D of 0.1 provided a Nash-Sutcliff (NSE) of 0.51. The recharge values obtained ranges from 0-41.9 mm/d. The highest recharge corresponds highest rainfall of year 2000.

The simulated and observed water level values for observation well located close to the river, BH4371 is presented in Figure 49. As can be seen in the Figure 49, the simulated and observed water levels did not produced a very good fit (NSE = 0.09). The calibrated parameter values were 0.9 for fraction of recharge, 0.2 for Sy and 0.04 for D. The calibration results provided a very high value of recharge and specific yield. Even if due to river leakage following flooding events high recharge value is expected and due to high karstification along the river section high Sy is common, the optimized parameters seems very high to be acceptable. The model performance is also poor. Hence, recharge simulated using observation well close to the river was not considered reliable.

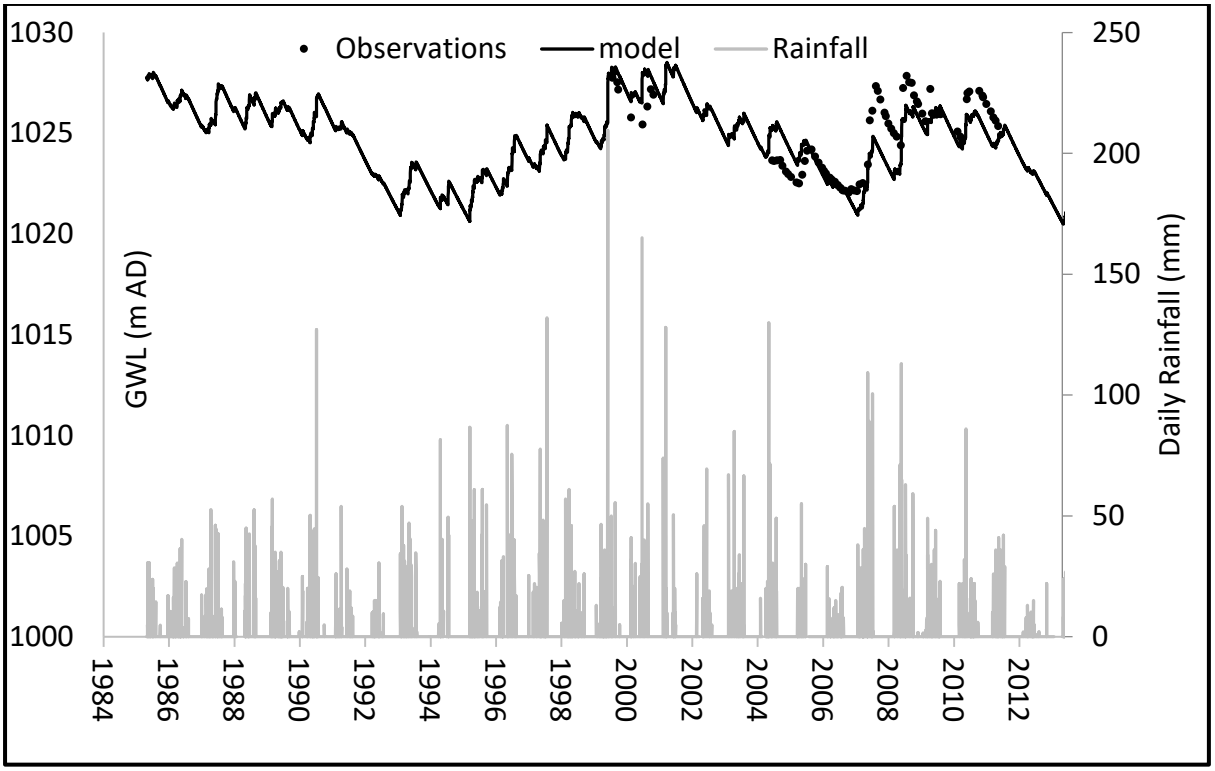

Figure 48: Observed and simulated groundwater levels using WTF for BH4168 far away from the river

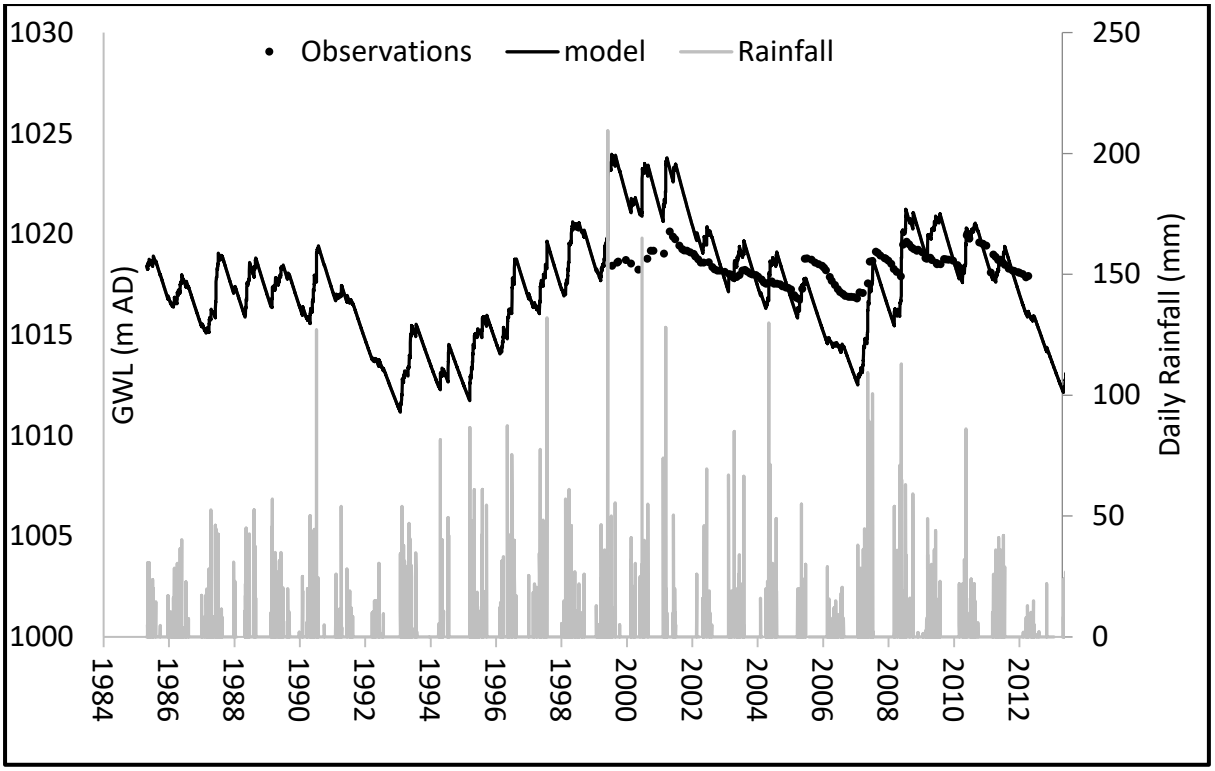

Figure 49: Observed and simulated groundwater levels using WTF for BH4371 close to the river